Imperial College London,
Department of Bioengineering

Task-based fMRI investigation of the newborn brain: sensorimotor development and learning

Sofia Dall'Orso

A thesis submitted for the degree of
Doctor of Philosophy

October 2019

I declare that the work described in this thesis is the result of my original work and it has been submitted only at the Department of Bioengineering, Imperial College London for a PhD award. The content presented that is not part of my own work has been appropriately referenced.

Sofia Dall'Orso

E-mail: s.dallorso15@imperial.ac.uk

Dedication

To my parents, who supported me whatever I wanted to do and love me whoever I will become.
I will never say enough how grateful I feel for the love and support I received throughout my life.

Abstract

Human brain development relies upon the interaction between genetic and environmental factors, and the latter plays a critical role during the perinatal period. In this period, neuronal plasticity through experience-dependent activity is enhanced in the sensory systems, and drive the maturation of the brain. While plasticity is essential for maturation, it is also a source of vulnerability as altered early experiences may interact with the normal course of development. This is particularly evident in infants born preterm, who are prematurely exposed to a sensory-rich environment, and at risk or neurodevelopmental disorders. In keeping with the somatosensory system being at a critical period for development during late gestation, sensorimotor disorders, such as cerebral palsy, are more common in preterm compared with full-term born infants. It is therefore important to understand the normal trajectory of sensorimotor development and how this may be moulded by early sensory experiences.

It is well acknowledged that the sensorimotor cortex is topographically organised so that different body parts map to a specific location within the cortex and this map is generally referred to as the "homunculus". Although the somatotopy has been well characterised in the mature brain, it remains unknown when this organisation emerges during development. Animal studies hints that functional cortical maps might emerge across the equivalent period to the third trimester of human gestation, nevertheless there is currently no evidence. Therefore, I first investigated the topography of the preterm somatosensory cortex in a group of newborn infants. In this purpose I used fMRI and automated robotic tools and measured the functional responses to different sensory simulations (delivered to the mouth, wrists and ankles). The results provide evidence that it is possible to identify distinct areas in the somatosensory cortex devoted to different body parts even in the preterm brain supporting the presence of an immature *homunculus*.

Next, I wanted to investigate how activity and development in the sensorimotor system are influenced by experience. Experience-dependent plasticity is the basis of learning (e.g. adaptive behaviour), which is observed in newborn infants. Associative learning in particular has been widely investigated in infants, however, the underlining neuronal processes have previously been poorly understood. To study the neural correlates of associative learning in newborn infants, I developed and used a classical conditioning paradigm in combination with robot-assisted fMRI. The results confirm that associative

learning can occur even at this early stage of life and with non-aversive stimuli. More importantly, I could observe learning-induced changes in brain activity within the primary sensory cortices, suggesting that such experience can shape cortical circuitry and is likely to influence early brain development.

Acknowledgements

I would like to thank my supervisors, Prof Etienne Burdet, Dr Tomoki Arichi and Prof David Edwards, for guiding me through the PhD and even more for being a living example of passionate scientists dedicated to carrying out good quality research.

I would also like to say a big thank you to all the members of the Human Robotics Group for teaching me the engineering skills I was lacking, for their inputs throughout the years on several fronts, and for the cheerful coffee breaks and lunches.

I would like to express my gratitude to the people at the Perinatal Imaging group at St Thomas' Hospital for their insights into brain development and neuroimaging, in particular, my sincere gratitude to Judit and Tanya, it has been a pleasure to work with them and I hope that the deep discussions, as well as the laughs, will continue in the coming years.

I would like to give a special word of thanks to Judit, who has been a constant companion during my PhD path from day one. Her knowledge and passion about neuroscience were an inspiration for me, but even more than a great colleague she has been a true friend and no word can express my feelings about everything we shared in the PhD roller-coaster.

I would like to sincerely express my gratitude to Millie, Jakki and the other members of the clinical team involved in the recruitment, their fantastic work and perseverance were essential for my project. Sport and good company were essential for me to survive the stress of work, therefore a word of thanks goes to my friends who sweeten my life with chats, climbing and parkour.

I am very thankful for Patric, who supported me with immense love and taught me how to disconnect from work stress outside working time.

Finally, Dr Tomoki Arichi proved to be a committed teacher, a great team leader, genuinely altruistic, always supportive, and a wonderful person. Therefore Tom deserves an immense thanks for his exceptional supervision, I will feel eternally grateful for having had him by my side.

Contents

List of Figures

List of Tables

List of Acronyms

A1 Primary auditory cortex

BET Brain extraction tool

BOLD Blood-oxygen-level-dependent

CBF Cerebral blood flow

CBV Cerebral blood volume

CP Cerebral palsy

CR Conditioned Response

CS Conditioned Stimulus

DAQ Data Aquisition Card

DOF Degrees of freedom

EBC Eyeblink conditioning

EEG electroencephalogram

EPI Echo-planar imaging

FA Flip angle

FEAT FSL's Expert Analysis Tool

FID Free induction decay

fMRI Functional Magnetic Resonance Imaging

FSL FMRIB's Software Library

FWE Family wise error

FWHM Full width at half maximum

GA Gestational age

GLM General linear model

H Hydrogen

HRF Haemodynamic response function

ICA Independent component analysis

KO Knockout

L4 Cortical layer 4

LTP Long-term potentiation

M1 Primary motor cortex

MRI Magnetic Resonance Imaging

NICU Neonatal Intensive Care Unit

NMV Net magnetisation vector

OLS Ordinary least square

P Postnatal day

PMA Postmenstrual age

PVL perventricular leukomalacia

RF Radio frequency

ROI Region of interest

RMS Root Mean Square

S1 Primary somatosensory cortex

TE Echo time

TFCE Threshold free cluster enhancement

TR Repetition time

US Unconditioned stimulus

V1 Primary visual cortex

"Progress depends on our brain. The most important part of our brain, that which is neocortical, must be used to help others and not just to make discoveries."

– Rita Levi Montalcini –

1

Introduction

Human brain development is characterised by a myriad of changes guided by a cascade of events which are shaped by both genetic and environmental factors. Knowing the timing of maturation processes in the human brain will clarify how adversities in specific time windows during development would alter the normal trajectory leading to negative outcomes, of which preterm infants are particularly vulnerable to. In the first section of this chapter, a brief description of the human brain's anatomical developmental milestones and it's functional maturation is outlined (more detailed information can be found in the review de Graaf-Peters & Hadders-Algra, 2006 and textbook Lagercrantz, 2010).

The last trimester of gestation during human brain development is particularly dynamic and vulnerable as patterns of experience-dependent neuronal activity enhance neuronal growth and guide synapses formation in the sensory regions. This time window of en-

hanced plasticity is considered a critical period as it is sensitive to environmental factors and may partially explain the higher risk of neurodevelopmental disabilities in preterm born infants. Somatosensory and motor disorders, such as cerebral palsy (CP), are one of the major negative outcomes for infants born prematurely suggesting that abnormal early experiences may lead to long lasting disabilities. In this view, the second section provides an insight into the normal sensory development that may be used to assess deviations from typical trajectory. A hallmark of the sensory cortices is the topographical organisation, of which the establishment is thought to occur during the critical period of development as sensory-driven mechanisms mould and refine its foundation. The third section describes in more detail the mechanisms underlying brain plasticity and elucidates how the period of enhanced plasticity is an asset and a hindrance at the same time. Although atypical experiences, like those of preterm birth, may lead to negative outcomes, brain plasticity might be leveraged to readjust deviations from the developmental trajectory. A better understanding of how early experiences influence brain development may provide better tools for early diagnosis and targeted intervention for infants at risk of neurodevelopmental disorders. The newborn brain is moulded by sensory experiences as adaptive brain mechanisms (like learning) are triggered in response to the rich environment newborn infants are exposed to. Associative learning in the basic form of classical conditioning has been exploited to expand our knowledge on these adaptive mechanisms. The fourth section therefore aims to describe the basic principles of associative learning and the known underlying mechanisms.

Throughout the manuscript, the age terminology used during the perinatal period is consistent with the standard definitions of the American Academy of Pediatrics Committee on Fetus and Newborn, 2004 summarised in figure 1.1, and are expressed in the format $weeks + days$. In particular, gestational age (GA) refers to the period before birth, chronological age the period after birth and post-menstrual age (PMA) comprises both periods.

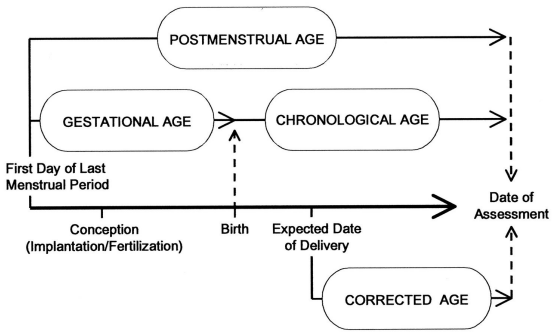

Figure 1.1: Age terminology Age terminology during the perinatal period (Committee on Fetus and Newborn, 2004)

1.1 Early brain development

Brain development results from the complex interaction between genes, which programmatically guide the formation of the initial robust architecture, and environment, which through neural plasticity moulds and refines cortical connections. Initially driven by intrinsic genetic mechanisms, the human brain starts to develop from 2-3 weeks GA in the form of the *neural tube* (Ladher & Schoenwolf, 2005), which is made of 3 portions: rhombencephalon (hindbrain), the mesencephalon (midbrain), and the prosencephalon (forebrain). The latter is further subdivided into the diencephalon, which later becomes the ventral part of the brain including structures like the thalamus, and the telencephalon which will become the cerebral cortex. Neurons of the cerebral cortex are not generated in the cortex itself, but they migrate following specific pathways driven by sequential expression of genes. The formation of the cerebral cortex, or *corticogenesis*, initiates in week 5 GA when neuroblasts (neuron precursors) migrate radially from the germinative ventricular layer of the thelencephalon to reach the cortical plate (*foetal cortex*) (Rakic, 1988; Rakic, 2007). As soon as the neuroblasts leave the germinative ventricular zone, axonal pathways begin to grow increasingly long distance organised in an array of cortical columns ("radial units"), and stop into specific position (figure 1.2). Finally, synapses are created to form the axonal and dendritic connections.

The process of *synaptogenesis* is non-linear and complex. While at an early stage it occurs slowly and at low density (first in the protocortex and later in the cortical plate), it ramps up exponentially from 20-24 weeks and continues at this rapid pace until a few months after birth (Zecevic, 1998). The cortical plate eventually differentiates into

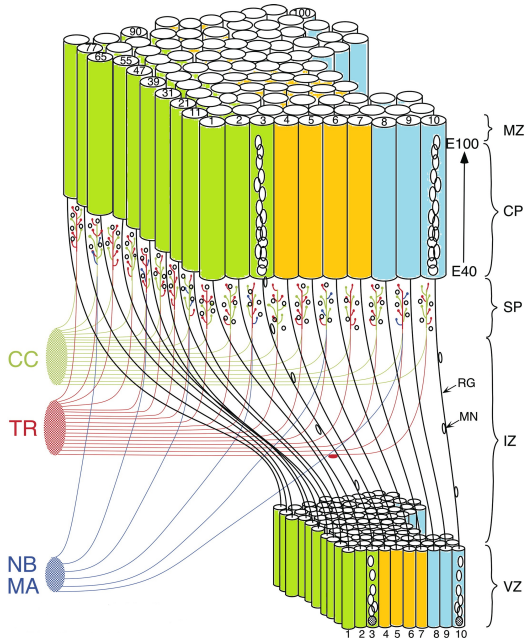

Figure 1.2: Radial unit model based on Rakic, 1988. Figure readapted from Rakic, 2007; Rakic, 2009: The cohorts of neurons generated in the ventricular zone (VZ) traverse the intermediate zone (IZ) and subplate zone (SP) containing 'waiting' afferents from several sources (cortico-cortical connections (CC), thalamic radiation (TR), nucleus basalis (NB), monoamine subcortical centers (MA)) and finally pass through the earlier generated deep layers before settling in at the interface between the cortical plate (CP) and marginal zone (MZ). The timing of neurogenesis (E40–E100) refers to the embryonic age in the macaque monkey. The positional information of the neurons in the VZ and corresponding protomap within the SP and CP is preserved during cortical expansion by transient radial glial scaffolding.

multiple layers in a deep-to-superficial fashion (with newer neurons located more superficially). Of those layers, the deepest is known as the subplate and serves as a buffer for axonal projections before they reach their ultimate destinations within the cortical plate (Kostović & Jovanov-Milošević, 2006; López-Bendito & Molnár, 2003). The subplate is the most prominent layer during mid gestation, it is thick and densely packed with cells, however, from the 35th week of gestation the cortical plate thickens as the axonal projections reach the maturing cortical plate, and the subplate thins as the neurons decline in number (Hoerder-Suabedissen & Molnár, 2015). Whilst initially synaptic architecture (radial columns and laminar layers) is guided by genetic preprogramming, later endogenous neuronal activity, and subsequently exogenous evoked activity become important to coordinate specific cortical functions during brain development. This later period overlaps with the last trimester of gestation, which encompasses the period from week 24 to full term (40th week of gestation) and is characterised by a drastic evolution.

At the early stage of the last trimester of gestation, synaptogenesis in the subplate, thalamocortical projections and grey matter growth are at a peak; endogenous activity propagates within the cortical plate; and large bundles of callosal fibres, although non-myelinated yet, start to establish inter-hemispheric connections. Then, around 33-35 weeks GA, the subplate starts to thin as the cortical plate mature, which also flourishes

with increasing cortico-cortical connections. It is at this stage, that experience-dependent mechanisms start to play a leading role in development and can modify the synaptoarchitectony both at microphysiological and morphological levels (Huttenlocher, 1990). The interaction between sensory inputs coming from the periphery (relayed by the thalamus) and the subplate neurons coordinates the formation of connections between thalamic axons and their final targets within layer 4 (L4) (López-Bendito & Molnár, 2003). Interactions with afferent inputs can also modify the final number of cortical columns, therefore, altered environmental exposure during this sensitive period might result in the pathogenesis of certain cortical regions (Rakic, 1988).

1.1.1 Critical period of development

The aforementioned period of enhanced plasticity in response to experience-dependent neuronal activity extends also in the early postnatal time. The perinatal time window is therefore particularly sensitive to the environment. Evoked neuronal activity not only can influence axonal and dendritic growth, but it is indispensable for refining synaptoarchitectony and hence optimising cortical function. It is important to note that there are multiple critical windows corresponding to the establishment of different brain functions and sensory systems are the first to undergo this process. The onset, duration and closing of each critical development window is controlled by multiple genetic and epigenetic mechanisms (Berardi *et al.,* 2000; Bartoletti *et al.,* 2004; Hooks & Chen, 2007).

Interestingly, this phase of great synaptic plasticity during cortical formation lasts longer in humans compared to other species (Berardi *et al.,* 2000) which may underlie comparitively exceptional sensorimotor and cognitive skills. This makes the human brain highly adaptable, but it may also represent a source of fragility during development. It has been shown that altered sensory experience during the specific critical window leads to aberrant sensory processing in the mature brain. This was found also in animals, indeed, monocular deprivation during the early post-natal period has been observed to permanently alter organisation in the visual cortex (for a review Hooks & Chen, 2007);

similarly, blocking afferent auditory inputs severely impairs auditory circuitry (Clause *et al.,* 2014; de Villers-Sidani *et al.,* 2007); and finally, somatosensory deprivation during the specific critical window results in abnormal cortical configuration (Fox, 1992). Although synaptogenesis is only one aspect of cerebral cortex development and maturation, altered synaptoarchitectony is always associated with sensory and cognitive dysfunction (de Graaf-Peters & Hadders-Algra, 2006).

The new formation of synapses allow neurons to communicate to each other through the passage of neurotransmitters. At this stage, the number of neurotransmitters (and also neuromodulators) undergoes a transient increase that boost neuronal communication. Neurotransmitters and neuromodulators additionally contributes to neuronal differentiation, synapse development, neuronal growth and to the formation of neuronal networks, therefore play an important role in the development of the nervous system (Herlenius & Lagercrantz, 2001; Nguyen *et al.,* 2001). Those neuroactive substances can facilitate, inhibit, block or promote neuronal signalling forming the wiring of neuronal circuits, hence the underlying foundation for larger scale neuronal networks (Herlenius & Lagercrantz, 2001). The role of some neurotansmitters and receptors (e.g. GABA, NMDA, AMPA) changes between the foetal and postnatal period (Fox *et al.,* 1999; Miles, 1999; Ganguly *et al.,* 2001), hence prenatal or neonatal insults may alter the normal sequential events leading to long-term negative consequences (Lipton & Nakanishi, 1999; Herlenius & Lagercrantz, 2001). Accordingly, the closing of the critical period for sensory cortices coincides with the switch from slow to fast glutamatergic synapses (NMDA to AMPA receptors) and results in a marked reduction of the possibilities for reorganisation of synaptoarchitectony (Rutishauser, 2008; Spolidoro *et al.,* 2009).

1.1.2 Neurodevelopmental sequelae of preterm birth

Brain development is characterised by a pivotal sequence of events that must follow the specific timing, spacing and stimulation for correct maturation. An early insult during a susceptible period can result in a deviation from the normal trajectory of development,

resulting in long lasting changes in brain structure and function. Brain injuries can occur during pregnancy, labour, delivery, transient to extrauterine life, environment or subsequent illness, and may result in lifelong negative outcomes. It is therefore important to ask which neurodevelopmental sequelae preterm infants are at risk of, and how birth before term may alter the brain's normal developmental trajectory.

In keeping with this, preterm born infants have a much higher incidence of neurodevelopmental impairments in comparison to their peers born at full term. Common pathologies in the very young population are germinal matrix-intraventricular haemorrhage, sometimes followed by periventricular haemorragic infarction, and periventricular leukomalacia (PVL), which leads to neuronal/axonal abnormalities (figure 1.3). The latter is the most common and is accompanied by a constellation of primary destructive disease and secondary developmental disturbance grouped under the name "encephalopathy of prematurity" (Volpe, 2009b; Volpe, 2009a). A major aspect of the encephalopathy of prematurity (either as primary injury or secondary effect) is neuronal/axonal disease, which includes white matter axons, premyelinating oligodendrocytes, subplate neurons, late migrating neurons, thalamus and basal ganglia (Volpe, 2009b; Volpe, 2009a). Also reduced neuronal density (of layer V) in sensory-related cortical areas has been observed in association with PVL, and thus may explain later negative outcome (Volpe, 2009b; Andiman *et al.,* 2010).

Perinatal asphyxia is a serious hazard of preterm birth, and hypoxic ischaemic injuries are one of the potential causes of PVL (other causes are inflammation and excitotoxicity). Given that the encephalopathy of prematurity occurs during a period of extraordinarily rapid and complex events in human brain development, the developmental stage at which the insult occurs yields different sequelae (Volpe, 2009b). Accordingly, hypoxic-ischaemic damage tends to be localised in the periventricular region in the case of preterm infants, whereas they are usually localised in the grey matter in full-term infants (Volpe, 2008; Volpe, 2009b). Furthermore, a cascade of neurotransmitters and transcriptional factors is triggered at birth, thus preterm birth might disrupt the correct timing of neuromodulating activity, potentially leading to abnormal development even in the absence of obvious brain

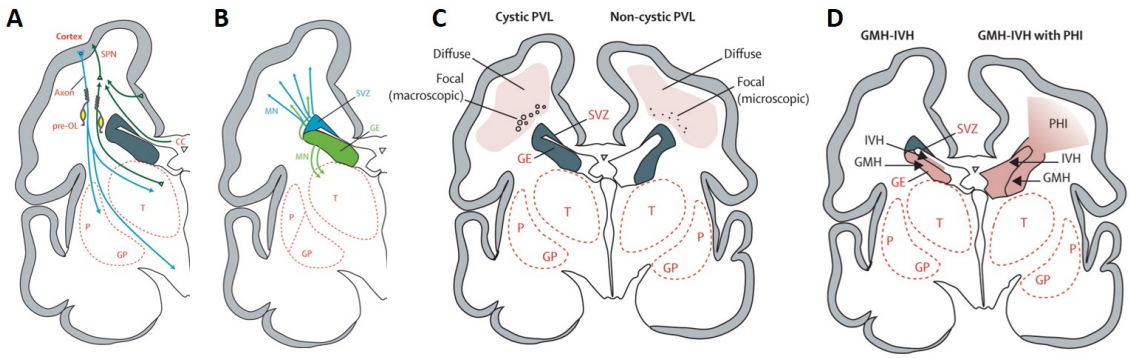

Figure 1.3: Critical events in cortical development and neuropathological correlates of the encephalopathy of prematurity **A)** Thalamo-cortical and cortico-cortical connection formation. **B)** The proliferation and migration of interneurons; **C)** Cystic and non-cystic periventricular leukomalacia (PVL). **D)** germinal matrix haemorrhage–intraventricular haemorrhage with and without periventricular haemorrhagic infarction (PHI). SVZ=subventricular zone; GE=ventral germinative epithelium of the ganglionic eminence; T=thalamus; P=putamen; GP=globus pallidus; CC=corpus callosum; SPN=subplate neurons; pre-OL=premyelinating oligodendrocytes; GE=ganglionic eminence; MN=migrating neurons. (image re-adapted from Volpe, 2009a)

lesions.

Birth comes with a drastic change of environment and although sensory stimulation is essential for cortical maturation, the exposure to such abundant sensory signals before the brain is at the corresponding developmental stage might be disruptive. Given that the preterm period is critical for sensory development, and that enhanced plasticity comes with enhanced vulnerability, infants born prematurely are thus at risk of negative clinical consequences. The most common and important disorder associated to preterms is CP (Fawke, 2007), but other sensory (visual and auditory), motor, learning, attention and cognitive impairments have also been reported (Allen, 2008). Although preterm birth does not necessarily lead to negative outcomes, the risk of developing severe disabilities increases with decreasing GA (Larroque *et al.,* 2008). Impairment of the sensory system, in particular motor and somatosensory systems, is a predominant outcome of preterm birth; thus, this thesis focus on their neurodevelopment.

1.2 Sensory systems

The cerebral cortex is of paramount importance for the neural integration of the central nervous system as it receives and sends information from and to the rest of the body. In order to optimally handle all this information, the cortex needs to be organised into functional networks. However, before these cortical networks can implement their higher level of control, they need to learn how to process the variety of sensory information coming from the surrounding environment including tactile, visual and auditory stimuli. Given that most sensory information is directed to the cerebral cortex via the thalamus (with the exception for the olfactory cortex), sensory cortex development is highly reliant upon the development of thalamocortical and corticothalamic pathways.

A hallmark of the sensory cortices is their organisation into topographic maps that hinge upon the particular patterns of thalamocortical projections. Afferent information from the periphery reaches and is processed in a specific location within the corresponding sensory cortex. The *primary auditory cortex* (A1) is spatially arranged in a tonotopy, with adjacent sites selective to specific adjacent frequencies. Likewise, the *primary visual cortex* (V1) is spatially arranged in a retinotopy, where visual inputs from the retina are mapped to specific neurons within V1. Finally, the *primary somatosensory cortex* (S1) and *primary motor cortex* (M1) are also organised such that different body parts have a correspondence within both S1 and M1.

The emergence of those topographic maps coincides with the shift from activity-independent to activity-dependent mechanisms during the foetal period in humans and during the early postnatal period in rodents. Early cortical activity during this critical developmental period becomes the propulsive force in moulding anatomical and functional cortical organisation critical for correct sensory processing (Kostović & Jovanov-Milošević, 2006; Milh *et al.,* 2007; Zhang *et al.,* 2012). Combining results from animal studies, electroencephalographic (EEG) recordings and EEG-fMRI studies from preterm infants, it is now established that in this period in sensory areas there are patterns of activity characterised by intermittent delta waves separated by periods of quiescence (Khazipov *et al.,* 2004;

Khazipov & Luhmann, 2006; Arichi *et al.,* 2017). Those patterns of neuronal activity vary with gestational age in both the spatial and temporal domains, and the early smooth delta waves evolve into delta brushes (an envelop of slow delta waves with fast alpha, beta and gamma oscillations) from the 7^{th} month of gestation to near term. Importantly, delta-brushes within the cortical plate can be elicited spontaneously as well as evoked by peripheral sensory stimulation (Whitehead *et al.,* 2017). Numerous studies provide evidence of sensory-driven delta-brushes in the auditory cortex (Chipaux *et al.,* 2013; Kaminska *et al.,* 2018), in the visual cortex (Hanganu *et al.,* 2006; Colonnese *et al.,* 2010; Zhang *et al.,* 2012) and somatosensory cortex (Khazipov & Luhmann, 2006; Milh *et al.,* 2007), suggesting that the generation of delta brushes during the critical period is ubiquitous in different sensory modalities and are localised within the corresponding sensory cortical areas.

Experience-dependent activity during the critical period is instrumental for cortical maturation and contributes to the emergence of highly adapted representations of the external world in the adult brain. As it is of particular interest to understand the mechanisms underlying the formation of cortical body maps investigated in the Chapter 3, I will now provide a more detailed description of the sensorimotor system development.

1.2.1 Sensorimotor system

The somatosensory system deals with tactile, thermal, nociceptive and proprioceptive information from the periphery. In the mature system, inputs from receptors in the skin and muscles ascend neuronal pathways via spinal cord, brainsterm, cerebellum, contralateral thalamus, and reach the somatosensory cortex localised in the postcentral gyrus. Most of what it is known about early maturation dynamics comes from animal models (especially from rodents) with the first 10 postnatal days in rats corresponding to the second half of gestation in humans. Animal models can thus provide an insight into the late foetal developmental period in humans, nevertheless, direct translation from animal findings to human brain ontogenesis should be considered with care.

In the prenatal period, thalamocortical projections do not directly target the cortical layers as in the adult brain. In contrast they rely on the transient neural layer at the boundary between white and grey matter, namely the subplate (Zhao *et al.,* 2009; Kanold & Luhmann, 2010). In rats, axonal fibres leave the thalamus to reach the cortical subplate around embryonic day 16-17, and continue their growth into cortical L4 only after birth. In contrast, human cortical L4 already begins to differentiate during the last trimester of gestation, thus, the essential anatomical substrates for transmitting somatosensory inputs from the periphery to the cerebral cortex are established prior to birth (Kostović & Jovanov-Milošević, 2006). In parallel to ascending pathways, there is also a descending flow of information important for motor control from the motor cortex (anterior to the central gyrus), however this likely matures after birth in both animals and humans (Eyre *et al.,* 2000; Eyre, 2004; Martin, 2005).

Early stages of sensorimotor development in mammals and other species are characterised by uncoordinated movement patterns. One hypothesis is that those movements are self-generated and serve to produce sensory feedback, which in turn trains immature sensorimotor circuits. In support of this hypothesis, it has been shown in rat pups that limb twitches and complex movements are generated from the motor spinal cord and that cortical activity in the sensory zones follows this motor behaviour (Inácio *et al.,* 2016). The spinal cord activity responsible for those spontaneous movements is in turn modulated by top-down mechanisms, of which the red nucleus plays an important role. The red nucleus neurons fire before the motor activity and are also triggered by the returning sensory feedback before the signal is relayed to the sensorimotor cortices (Del Rio-Bermudez *et al.,* 2015). These findings are consistent with the importance of signal arising at the sensory periphery for driving the aforementioned early cortical activity patterns.

Animal studies provide evidence that cortical activity triggered by self-generated movements in developing rats is mainly induced in S1 first in the form of a spindle burst, and later in M1 as a gamma and spindle burst (An *et al.,* 2014). Although a small fraction of M1 activity was observed to anticipate the movements instead of following it, this occurred more rarely; hence S1 directly triggers a motor response more often than M1 during

this developmental stage (An *et al.,* 2014). Interestingly, the spread of a spindle-burst to M1 is restricted to movements during sleep, whilst during wake-related movements sensory feedback to M1 is suppressed by corollary discharges (Tiriac *et al.,* 2014). In keeping with animal studies, activity in the contralateral sensorimotor cortex of human preterm newborns was elicited by both active and passive movements (Allievi *et al.,* 2016). Taken together, these findings suggest that during the early postnatal period in rats, and late foetal stage in humans, the motor cortex operates in both motor and somatosensory modalities.

After birth, endogenous mechanisms of sensory stimulation are complemented by environmental simulations, and this exogenous-generated activity also plays a pivotal role for cortical maturation during the neonatal period (Akhmetshina *et al.,* 2016). Importantly, human foetuses in utero are exposed to attenuated exogenous stimulation in contrast to neonatal rats, however this condition is seriously altered in neonates born before term. Preterm infants are exposed to passive sensorimotor stimulation due to environmental inputs in contrast to their peers inside the womb. A driving motivation of this thesis is to understand to what extent these environmental influences interfere with the normal development of the sensory system and can contribute to the neurodevelopmental disabilities that can affect preterm infants.

Somatotopy

Somatotopy describes the correspondence between each area of the body and a specific area of the central nervous system. The seminal work of Penfield & Boldrey, 1937 comprehensively characterised the effect of electrical stimulation on the adult human cortex and described somatic, motor and sensory body representations. Whilst different regions of the cortical representation preserve body continuity, body surface proportion is not preserved: as broader receptive fields within the cortex are allocated to functionally more relevant body parts. For these reasons, the sensory and motor somatotopy is generally referred to the *cortical homunculus* and can be pictorially represented by a distorted "little

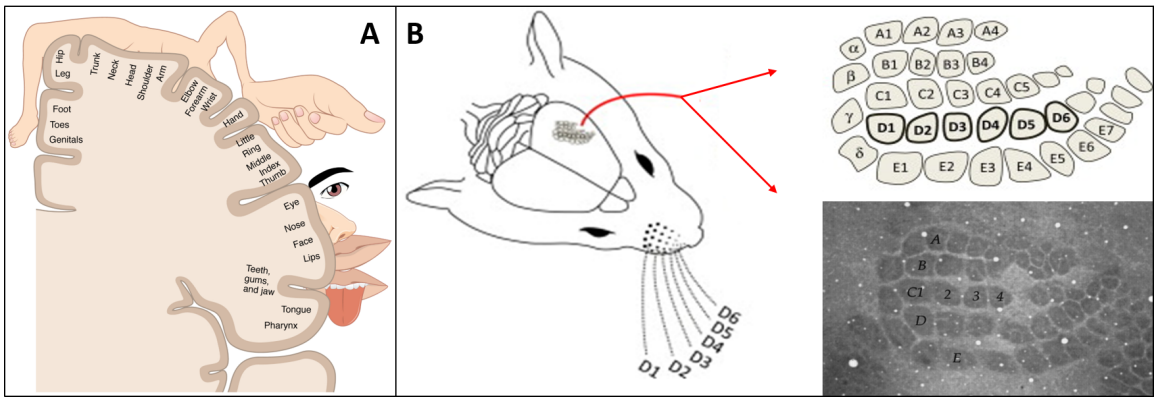

Figure 1.4: Human and rat somatotopy: A) The sensory homunculus is the physical representation of the human body located within the brain (OpenStax, 2016). The anatomical size of each body part quantitatively represents the amount of innervation in that region. B) Schematic and CO histochemistry somatotopic arrangement of wishers in the rat barrel cortex (image re-adapted from Wilson *et al.,* 2000; Diamond & Arabzadeh, 2013)

man" (figure 1.4 A). Although mature somatotopy has been extensively investigated, the developmental time-course of its formation within the cortex and the factors which drive this process are far from being fully understood in humans. In rodents, the somatosensory cortex is divided into overlapping receptive fields within anatomically segregated barrel-shaped areas. The most distinctive and well characterised area is the whisker barrels, where there is a univocal correspondence between barrels and each individual vibrissa (figure 1.4 B). Due to this remarkable clear cellular organisation, the whisker barrel cortex is an effective model to study the emergence of cortical maps and to understand somatosensory cortical processing.

In the previous section, it was explained how sensory-driven activity patterns characteristic of the critical period are instrumental to the somatosensory map formation. While at birth there is an imprecise protomap of the barrel cortex, this is soon moulded according to stimulation from individual whiskers, as the functional segregation sharpens and aligns with the anatomical barrel map (Mitrukhina *et al.,* 2015). At P0-P1 (postnatal day), sensory stimulation of the whiskers evoked delta waves which peaked in the target barrel cortex but with a widespread pattern of activation also covering neighbouring cortical territories. During P2-P7, connections between the thalamus and L4 strengthen resulting in consolidation of the maps. As the functional response becomes more localised, the barrels become more segregated. The competitive interaction of activity elicited by different

whiskers is instrumental for refinement of the cortical organisation by stabilising thalamic connections and inhibiting surrounding areas in the topography. Sensory deprivation during this critical period can therefore alter the maturation of those functional maps.

In an important study (Fox, 1992), the sensory experience of rat pups was deprived by removing the whiskers from one side of the face beginning at different developmental stages (P0, P2, P4 and P7) and maintained until cortical recordings at a mature age (P30-P90). Interestingly, the onset of deprivation had a different impact on subsequent cortical activity, with animals deprived from P4 were those with greater atypical cortical organisation in L4. While the whisker barrel cortex emerges early in postnatal life, the somatotopic representation of other body parts does not reach an adult-like form until as late as P20 (Seelke *et al.,* 2012). These animal studies suggest that the cortical topography emerges in the critical period, however, this period occurs postnatally in rats whilst in the last trimester of gestation in the human brain. Given this developmental difference it remains unclear when the cortical topography emerges in the human brain and whether a protomap is already present at birth at all. The work in chapter 3 is dedicated to addressing this question.

1.2.2 Auditory system

There are clear parallels between the development of different sensory systems, as the combination and segregation of inputs from the left and right sensory organs, the need for retinotopic, somatotopic or tonotopic maps, and the underlying activity-dependent mechanisms contributing to system development. Although various animals are born blind to sound (ear canal opening at timepoints: mice at P12, kittens at P8 and ferrets at P29), their auditory cortex responds to auditory stimulation as soon as the ear canals open, suggesting that there is an ongoing pattern of maturation in the auditory system, and this period of sound insensitivity might be a protective mechanism to isolated spontaneous activity from noisy environmental stimulation. Patterns of rhythmic bursts of high level activity separated by periods of electrical silence (similar to those found in the so-

matosensory system) are found within the auditory system prior to hearing onset (Wang & Bergles, 2015). A large body of work now supports the idea that those spontaneous bursts are essential for accurate wiring of auditory pathways and formation of a tonotopic map (Clause *et al.,* 2014; Wess *et al.,* 2017; Sun *et al.,* 2018).

In the auditory system, delta-brushes are generated in cochlear hair cells and propagate along central auditory pathways before hearing onset. Clause et al. (2014) investigated the effect of genetically altering the temporal pattern of spontaneous activity before hearing onset on the structural and functional tonotopy in mice. This subtle change drastically affected the tonotopic precision of the functional auditory map before hearing onset in KO mice. Given that functional changes due to activity-dependent mechanisms generally are reflected into structural connectivity changes, they investigated the anatomical changes as well. Aberrant spontaneous activity led to impaired axonal pruning that occurs in normal mice after hearing onset, while it had no impact on structure prior to receiving auditory input. These results hint that functional and structural refinement undergo distinct but interactive mechanisms occurring during different developmental stages. In agreement with this finding, another animal study showed that the tonotopic map emerges before ear opening (Wess *et al.,* 2017). The spatial and functional topography emerges first in the subplate and it is later transferred to the cortical plate L4, supporting that the critical period starts early in development.

The critical period for auditory system development has been identified between P11 and P13 in rat pups (de Villers-Sidani *et al.,* 2007), which implies that the equivalent critical period in the human auditory cortex occurs during late gestation. However, translation from animal models to the human is not straightforward. While rat pups are born with closed ear canals and stay closed during the first 12 postnatal days, human foetuses already receive sound stimulation throughout in-utero life, filtered by the amniotic fluid. Therefore our knowledge from animal models needs to be integrated with studies on human preterm infants. A major electrophysiological study investigated auditory-evoked activity across the preterm period (from 30 to 38 weeks PMA) and found delta-brushes patterns in the auditory cortices from the age of 30 weeks (Kaminska *et al.,* 2018). Furthermore,

this work found that the rate of induced delta-brush activity was reduced from 33 weeks PMA until it fully disappears at full-term. In agreement with maturation of the auditory cortex by full-term, several neuroimaging studies have identified activity in A1 of newborn infants in response to sound stimulation (Zaramella *et al.,* 2001; Anderson *et al.,* 2001). Behavioural evidence also supports that newborns clearly respond to sound at birth, as auditory stimuli can yield to arousal, gross body movements, orienting behaviour, cardiac reactions and motor reflexes (Eisenberg, 1976). Moreover, full-term newborn infants are already capable of detecting precise temporal intervals and reacting to the variation of auditory stimuli rate (Háden *et al.,* 2012). Taken together, these studies demonstrate that the auditory cortex is mature by the end of normal gestation, and that newborn infants are able to respond to sound stimulation.

1.3 Brain plasticity

I have used the term plasticity several times, but what does it actually mean? Synaptic plasticity is the physical shaping and changing in the connection between neurons. A seminal theory of plasticity was formulated by Hebb in Hebb, 1949 with those words: "Let us assume that the persistence or repetition of a reverberatory activity (or "trace") tends to induce lasting cellular changes that add to its stability.... When an axon of cell A is near enough to excite a cell B and repeatedly or persistently takes part in firing it, some growth process or metabolic change takes place in one or both cells such that A's efficiency, as one of the cells firing B, is increased". Hebb's hypothesis was later verified with the advance of neurophysiological techniques through observing the phenomenon of long-term potentiation (LTP) as an outcome of the increased activity between two neurons.

1.3.1 Long-term potentiation at the basis of plasticity

It has been empirically confirmed that a single pulse of electrical stimulation to a neuronal axon elicits an excitatory postsynaptic potential in the connected cell, and that a high-frequency train of stimuli induces a stronger response at the postsynaptic terminal. Importantly, if a single pulse stimulus follows a high-frequency train stimulus, this then produces an enhanced long-lasting excitatory potential, namely LTP (Lømo, 2003). When the action potential reaches the end of a presynaptic cell, it causes the release of neurotransmitters (e.g. glutamate) into the synaptic cleft and bind to receptors (e.g. AMPA) on the postsynaptic cell opening the gate to ions (e.g. Na^+) that in turn depolarise (i.e. excite) the receiving neuron. A long influx of Na^+ may unlock NMDA receptors by repelling the Mg^{2+} blockade. The opening of NMDA channels permits further entry of Na^+ and also Ca^{2+}, thus causes further depolarisation. The increase in Ca^{2+} can activate intracellular mechanisms contributing to LTP. At first, Ca^{2+} ions contribute to the insertion of additional receptors onto the postsynaptic cell membrane, hence enhancing future excitation. Later, prolonged excitation can lead to an increase in gene expression and new proteins production, such as the growth factor, involved in the formation of new synapses. Both mechanisms strengthen neuronal connection allowing even low frequency action potential to cause a greater depolarisation in the postsynaptic terminal.

In the immature brain, AMPA receptors are mainly inactive and GABA receptors play their role instead (Ben-Ari *et al.,* 1997). Although GABA is known to be an inhibitory neurotransmitter in the mature brain, it induces excitation in the developing brain (Miles, 1999). When GABA receptors open, they let Cl^- ions spurt out and the postsynaptic cell depolarise, and thus can cause LTP as previously described. The LTP has the power to alter the strength of pre-existing connections and foster dendritic growth and arborization as a consequence of patterns of neuronal activity, and therefore stands in for a universal function upon which learning and memory processes are found. Although LTP is a physiological phenomenon happening at the synaptic level, its effects extend across distributed neural networks. As a result, synaptic plasticity exerts a powerful influence on brain

network formation and shaping, this is enhanced during the critical period as it is crucial for wiring the developing brain.

1.3.2 Impacts of enhanced plasticity of the newborn brain

Plasticity is an invaluable asset of the human brain to adapt itself to environmental pressures, physiologic changes, and experiences, but at the same time a source of susceptibility. The specific vulnerability of preterm infants during the early postnatal period was introduced in section 1.1.2. As this period also represents the peak of activity-dependent synaptic plasticity, it is plausible that it is also at the highest potential to compensate for acquired brain injury. This idea was endorsed in the nineteenth century by Margaret Kennard. Her principle asserts that the capacity of recovery following brain injury is inversely proportional to the age at which the insult occurred. However, evidence about the long-term disability rate in individuals born preterm belies the Kennard principle (Bennet *et al.,* 2013). Despite the apparent potential for optimal plasticity, the immature brain fails to reorganise by itself, perhaps as it needs external support and/or guidance in the process. Scientific research should therefore focus on interpreting environment influence on the neurological mechanisms of brain development to eventually predict neurodevelopmental disorders and promptly intervene to reroute deviated developmental trajectories. In this view, it is essential to unveil the mechanisms by which experience can mould brain networks, and how the brain learns from its own environment.

The human brain is optimally adapted to learning and this occurs throughout the lifetime. Learning is however different at different time in life, hence learning processes in infants differ from those in adults. Newborn infants are suddenly exposed to a drastic change of surroundings following birth, and must learn from the experience to adapt to the new environment through brain plasticity mechanisms. Learning is therefore an essential skill for infants. Although it is acknowledged that infants are highly capable of learning, the underlying brain mechanisms of learning in early life are not clear. One of the scope of this thesis is to shade light into the neurobiology of learning to expand our knowledge

on how early experiences can mould the newborn brain responses. I will now expand on the topic of learning in the next section, and present some experimental results in the chapters 4 and 5.

1.4 Learning

The term learning can include simple habituation, long-term memory storage, as well as complex problem solving. Therefore the term can be easily misinterpreted if isolated from its context. Generally speaking, any alteration of behaviour as a result of experience is said to be learning. However, different forms of learning likely differ from each other in their process, neural correlates and also in the time at which they occur during development. For example, perceptual learning is the refinement of sensory discrimination as a response to practice of a specific sensory task, such as two-point discrimination or auditory frequency perception. While psychomotor learning is the development of fine patterns of muscular activities which improves one's performance in motor skills such as coordinated movements through repetition and practice.

In the context of this thesis, the focus will be on associative learning, and in particularly on classical conditioning. Associative learning is the process by which the representation of two events comes to be linked with another because of past experiences and lays the basis for our understanding of behaviour (Wasserman & Miller, 1997). This learning mechanism includes different subtypes such as classical conditioning, operant conditioning, observational learning and imprinting. Classical conditioning is the result of learning relationships between repeatedly paired events in the environment, and provides a simple framework to model the nature of learning, thus experience-dependent changes in the brain.

1.4.1 Classical conditioning model

Classical conditioning is also known as Pavlovian conditioning due to the seminal work of the 19th-century physiologist Ivan Petrovich Pavlov. During Pavlov's most famous experiment, food (unconditioned stimulus) was presented to a dog and it was observed that the dog started to salivate (unconditioned response). In a separate instance he presented the dog a neutral stimulus (the sound of a metronome) which did not elicit salivation in the dog. However, after the sound (now the sound becomes the conditioned stimulus) consistently anticipated the appearance of food for a few repetitions, the conditioned stimulus alone made the dog salivate even in the absence of food, and hence the dog exhibited a conditioned response. Generalising those observations, when a *conditioned stimulus* (CS) precedes an *unconditioned stimulus* (US), and this pairing is repeated multiple times, the CS will elicit a *conditioned response* (CR) like that elicited by the US. This is in keeping with Hebbian learning: "neurons that fire together wire together" (Hebb, 1949).

The two best-known typologies of conditioning are *delay* and *trace*. In both cases the CS anticipates the US, however, while in the former case the presence of the stimuli overlaps, in the latter there is an interval (trace) between the offset of the CS and the onset of the US (figure 1.5). Moreover, whilst delay conditioning is emblematic of implicit learning as it does not require awareness, trace conditioning is associated with declarative memory (Clark & Squire, 1998; Connor & Gould, 2016). Classical conditioning is far from being a stagnant field, on the contrary, it is a primary means by which organisms represent the structure of their world (Rescorla, 1988). The creation of the association does not mean the shift of the US response at the CS occurrence, as it might be simplistically interpreted, but a more sophisticated understanding of the relationships between events to which one is exposed.

Although the conditional learning phenomenon has been widely investigated since then, many variables have been found to influence conditioning and all of the studies are so different from one another that comparison is difficult and extrapolating specific rules is

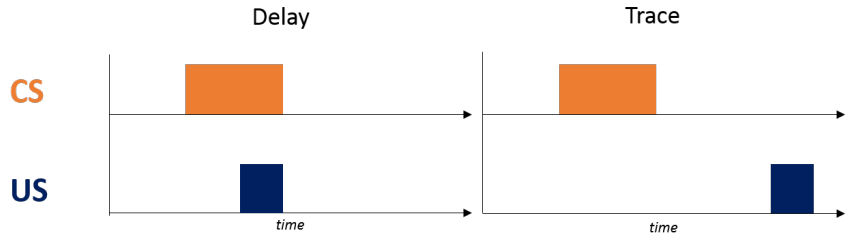

Figure 1.5: Schematic of *delay* and *trace* conditioning.

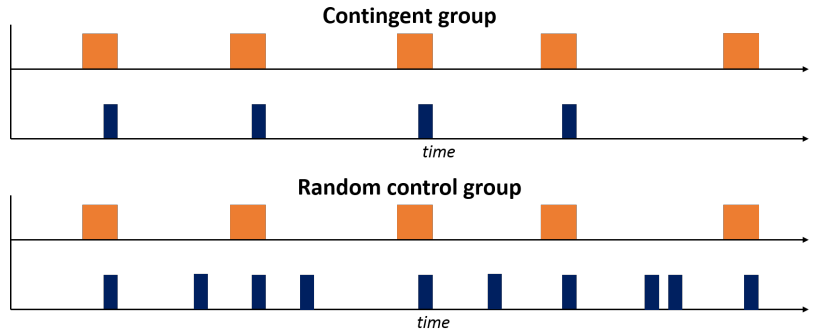

Figure 1.6: Schematic of *contingent* (top) and *random control* (bottom) groups in the conditioning of Rescorla (1968).

challenging (Fitzgerald & Brackbill, 1976). The conceptual framework of classical conditioning has been developed through the years. In the classical view of learning, temporal contiguity was necessary for associative learning, but this assumption was challenged with an important experiment (Rescorla, 1968). In that experiment, a group (contingent group) of rats underwent a conditioning protocol where a tone predicted an electric shock, while another group (truly random control) underwent a similar procedure with the addition of shocks delivered in the absence of sound in a way that the probability of a shock with the presence or absence of tone was equal (see figure 1.6). Despite the same amount of contiguous events (tone and shock together), only the first group showed evidence of learning. These results demonstrated that contingency is more important than contiguity to produce a conditioned response. After this finding, Rescorla and Wagner (1972) described conditioning with a simple, yet effective, model that interprets learning as a function of discrepancy between expectation and outcome.

Rescorla-Wagner model assumes an US of strength u and a CS that produces a conditioned response of strength v. Through repeated contingent presentations of CS and US a prediction error is updated: $\delta_n = u - v_n$ and conditioning occurs when $v \to u$ thus $\delta \to 0$. In other words, conditioning depends on mutual information between CS

and US, represented by the reduction in uncertainty about the occurrence of US given the onset of CS. In support of the idea that the CS informs about the US timing and not that the CR is transferred to the CS, a trace conditioning study showed that the behavioural conditioned response occurs at about the same time as the unconditioned stimulus (Drew *et al.,* 2005). Furthermore in an eyeblink conditioning experiment with rabbits, the animal first received a pairing with a long CS-US interval (700ms), then a second training with a shorter CS-US interval (250ms). In this case, the rabbits did not show any anticipation to the blink in the first part of the training, but they did during the second training condition. Subsequently, they performed probe trials with the CS alone and in correspondence with both the short and long CS-US interval, these subjects blinked twice suggesting that even the first pairing was learned (Ohyama & Mauk, 2001). Therefore, failures to observe anticipatory responses should not necessarily be interpreted as failures of learning (Ohyama & Mauk, 2001). All those empirical findings can now be interpreted with a more theoretical approach.

Information theory first proposed by Claude Shannon (1948) describes information in terms of the reduction of uncertainty of a random process, and is therefore well suited to the idea that a CS communicates information about the time of the next US. In this framework, the amount of uncertainty is quantified by entropy. This theory was already successfully employed to calculate the entropy of a spike train (Brillouin, 1962).If the spike train is represented as a string of zeros and ones (1s in the presence of a spike), it can be modelled with a Poisson distribution in which events occur randomly in time but with an average density distribution. The average entropy of a Poisson process is:

$$H = T\lambda \log_2 (\frac{e}{\lambda \Delta\tau})$$

where λ is the mean rate (average density) of the process, $\Delta\tau$ the temporal resolution and T the time of the process. The average interval between events is $T = 1/\lambda$, and hence entropy per one event is:

$$H = \log_2 (\frac{e}{\lambda \Delta\tau})$$

Applying this concept to conditioning, the information carried by the CS about the next US is the entropy rate. This information-theory analysis predicts many empirical results including the truly random control protocol in Rescorla (1968). In that context, the US rate in the absence or presence of CS was equal, therefore the difference of entropies between the ambience (US rate) and the pairing (simultaneous CS-US) gives zero information exchange. Mathematically:

$$H_{US} - H_{CS} = log_2(\frac{e}{\lambda_{US}\Delta\tau}) - log_2(\frac{e}{\lambda_{CS}\Delta\tau}) = log_2(\frac{\lambda_{CS}}{\lambda_{US}}) = log_2(1) = 0$$

A further example is the traditional trace conditioning protocol in which the CSs and USs occur at a fixed lag and the paired stimuli appear at a variable interval with an average rate λ_{US}. The temporal resolution $\Delta\tau$ is the subjective representation of the interval that is a Gaussian distribution with $\sigma = wT$, namely the product between the Weber fraction (measured empirically) and the time to the event (CS-US interval) (Gibbon, 1977). The uncertainty about the US onset right after CS onset is the entropy of a Gaussian distribution:

$$H_{US|CS} = log_2(\frac{\sqrt{2\pi e}\sigma}{\Delta\tau}) = \frac{1}{2}log_2(2\pi e) + log_2(wT) - log_2(\Delta\tau)$$

On the other hand, the background uncertainty is:

$$H_{US} = log_2(\frac{e}{\lambda_{US}\Delta\tau}) = log_2(e) - log_2(\lambda_{US}) - log_2(\Delta\tau)$$

The information that the CS brings is a reduction of the background entropy:

$$\Delta H = H_{US} - H_{US|CS} = \frac{1}{2}(log_2 e - log_2 2\pi) - log_2 w - log_2(\lambda_{US}) - log_2 T$$

Writing it as a function of average interval $I_{US} = 1/\lambda_{US}$, and considering that the first part is a constant (k) we obtain a more straightforward representation:

$$\Delta H = k + log_2(\frac{I_{US}}{T})$$

This theoretical result nicely explains previous empirical evidence that learning depends on the ratio between the event rate and CS-US proximity (Gibbon, 1977; Gallistel & Gibbon, 2000; Balsam & Gallistel, 2009). In keeping with this formulation, a short lag between CS and US reduces $H_{US|CS}$, while a long interval between USs increases the background entropy, making the CS more informative about the US. Taken together, a long I_{US} and a short CS-US length facilitate the anticipatory response.

1.4.2 Associative learning to date

The most well characterised descriptions to date of the basis of a learnt response has been achieved using the eyeblink conditioning (EBC) model (Christian & Thompson, 2003). In the EBC procedure, usually a sound (CS) precedes a brief (generally tens of milliseconds) puff of air to the eyelid (US), thus eliciting a eyeblink response (CR). As well as in other conditioning paradigms, the CS informs about the timing of the US.

A major player in forming a predictive temporal model is considered to be the hippocampus (Eichenbaum, 2017). Accordingly, recordings from the hippocampus during EBC have documented learning-induced increases in activity related to LTP both during delay and trace conditioning (Christian & Thompson, 2003). However, lesions in this area have relatively little effect on the acquisition and retention of the CR in a delay paradigm in contrast to trace paradigm (Clark & Squire, 1998). Further evidence from a human fMRI study demonstrated greater hippocampal activity during trace conditioning compared with delay conditioning, reinforcing the idea of the critical role of the hippocampus in declarative memory (Cheng *et al.,* 2008). An extensive collection of studies have also reported cerebellar circuitry to be active during EBC. Whilst the hippocampus has a marginal role in delay conditioning, the cerebellum is necessary for learning in both delay and trace paradigms. This was observed in electrophysiological (McCormick *et al.,*

1982; Yeo & Hesslow, 1998), lesion based (Hardiman & Yeo, 1992; Ivkovich & Stanton, 2001) and fMRI studies (Miller *et al.,* 2003; Cheng *et al.,* 2008), as well as supported by computational models (Ohyama *et al.,* 2003).

The function of the cerebellum and hippocampus during learning has widely been explored, yet the role of other involved cortical brain areas such as sensory and motor cortices is less clear. Although modern neuroimaging techniques have now made it possible to have insight into the structures engaged during classical conditioning across the whole brain, design constraints and differences across studies often give rise to conflicting evidence. Therefore, despite a vast assortment of brain regions being reported as involved in classical conditioning, the full picture of the neural correlates of associative learning is still unclear. Table 1.1 aims to display a summary of learning-related brain regions documented in EBC and other fear conditioning experiments.

Table 1.1: Learning-related brain regions

Brain regions	**References**	**Putative role**
Prefrontal cortex (PFC) Dorsolateral PFC	Molchan *et al.,* 1994; Pascual-Leone *et al.,* 1996; Passingham *et al.,* 2000; MacDonald *et al.,* 2000; Seidler *et al.,* 2002; Dunsmoor *et al.,* 2007; Dunsmoor *et al.,* 2008	Implicit procedural learning Fear conditioning Learning encoding Implementation of control
Ventral striatum	Molchan *et al.,* 1994; O'Doherty *et al.,* 2003; Linnman *et al.,* 2011	Prediction error
Orbitofrontal cortex	O'Doherty *et al.,* 2003; Dunsmoor *et al.,* 2007; Dunsmoor *et al.,* 2008	Prediction error Fear conditioning
Hippocampus	Dunsmoor *et al.,* 2007; Dunsmoor *et al.,* 2008; Albert *et al.,* 2009; Stanton, 2000; Cheng *et al.,* 2008	Fear conditioning Rapid learning Trace conditioning Extinction
Thalamus	Knight, 2004; Dunsmoor *et al.,* 2007; Dunsmoor *et al.,* 2008; Albert *et al.,* 2009; Marstaller *et al.,* 2016	Fear conditioning Rapid learning Delay conditioning Trace conditioning

Cingulate cortex	Büchel *et al.,* 1998; MacDonald *et al.,* 2000; Paus, 2001; Seidler *et al.,* 2002; Dunsmoor *et al.,* 2007; Dunsmoor *et al.,* 2008; Linnman *et al.,* 2011; Kattoor *et al.,* 2013	Fear conditioning Emotional learning Learning encoding Performance monitoring Anticipatory response Early acquisition Delay conditioning Trace condoning
Primary sensory cortices	Dunsmoor *et al.,* 2007; Dunsmoor *et al.,* 2008; Sale *et al.,* 2007; Sanes & Donoghue, 2000; Sanes, 2003; Seidler *et al.,* 2002; Paus, 2001; Kattoor *et al.,* 2013; Molchan *et al.,* 1994; Knight, 2004; Linnman *et al.,* 2011	Fear conditioning Motor skills learning Learning encoding Anticipatory response Early acquisition Delay conditioning Trace conditioning Expectation
Insula	Büchel *et al.,* 1998; Dunsmoor *et al.,* 2007; Dunsmoor *et al.,* 2008; Albert *et al.,* 2009; Marstaller *et al.,* 2016; Linnman *et al.,* 2011	Fear conditioning Rapid learning Emotional learning Expectation
Amygdala	Dunsmoor *et al.,* 2007; Dunsmoor *et al.,* 2008; Albert *et al.,* 2009; Marstaller *et al.,* 2016; Kattoor *et al.,* 2013; Stanton, 2000; Linnman *et al.,* 2011	Fear conditioning Rapid learning Late acquisition
Brainstem	Albert *et al.,* 2009; Marstaller *et al.,* 2016	Fear conditioning Rapid learning
Parietal cortex	Seidler *et al.,* 2002; Knight, 2004; Marstaller *et al.,* 2016	Extinction Learning encoding Trace conditioning
Temporal lobe (temporal pole medial temporal lobe)	Cheng *et al.,* 2008; Marstaller *et al.,* 2016	Acquisition Extinction
Frontal Operculum	Knight, 2004	Trace conditioning
Cerebellum	Molchan *et al.,* 1994; Stanton, 2000; Seidler *et al.,* 2002; Cheng *et al.,* 2008	Learning expression

Precuneus	Kattoor *et al.,* 2013	Anticipatory response Early acquisition

A limitation of the EBC model is that elicits a reflex response mediated by brainstem-cerebellar circuitry, thus leaving questions about cortical-dependent learning mechanisms unanswered. Although many adaptive movements are learnt driven by an attempt to minimise adverse consequences, adverse stimuli (as in fear conditioning) might engage different brain areas (such as the amygdala) compared to neutral stimuli. When emotions are involved, there are two independent but interactive factors: the emotional and sensorimotor forms of learning. Whilst sensorimotor learning is slow, it can be accelerated by the emotional component (Stanton, 2000; Christian & Thompson, 2003). Accordingly, it has been suggested that ecologically valid cues can ease the learning process (Reeb-Sutherland *et al.,* 2011). Although learning mechanisms are present throughout the lifespan, they might engage different areas of the brain depending on the developmental stage, hence adults findings cannot be directly translated to the immature brain. For instance, the sophisticated cerebellar circuit that is essential for the learning of discrete, precisely timed skilled movements, is likely to be not fully developed right after birth and more imprecise mechanisms might take place at that developmental stage. In conclusion, despite the extensive exploitation of classical conditioning there remain many unknowns, such as the precise role and interplay of cingulate, parietal and primary sensory cortices among others. Importantly, when those brain areas are engaged in the learning process across development is still an open question.

1.4.3 Infant learning

Learning is a progressive skill that may be expressed in different forms at different stages of life. Most of what we know about associative learning comes from studies in animals and human adults, and how these finding translate to human newborn infants is not known. Given the aforementioned dynamic developmental processes happening in the

early postnatal period, it is clear that we cannot infer the learning and memory capacity of infants from our knowledge derived from adults. For instance, implicit learning appears to function right from birth, whereas explicit memory formation is thought to require a level of awareness not present until late in the first year which further requires considerable development throughout infancy (Herbert *et al.,* 2003; Bauer, 2008; Rovee-Collier & Cuevas, 2009). This development is accompanied by maturation of the hippocampus and other memory systems. As maturation of these regions occurs at different rates, characterising the evolution of learning and memory in early human life becomes particularly challenging. Moreover, a great limitation is that the underlying process representative of a one type of learning or memory (and tested for using a particular task) cannot be generalised. In adults, awareness of learning is used to discriminate explicit from implicit learning processes, however this criterion cannot be applied in infants. An alternative hypothesis to maturation of learning through development of individual systems is the ecological theory (Rovee-Collier & Cuevas, 2009). This model assumes that every developmental stage encounters different environments and that related challenges require specific adaptive solutions (selected through evolution). In this view, infants are not imperfect adults, but on the contrary are in a different yet optimal state. Therefore an infant's capacity to learn is not weakened by their developmental stage but rather embodied in a different manner.

Behavioural evidence of early learning

The infants' learning capability is an intrinsic attribute of development that enables adjustment of their physiology and behaviour to meet the specific demands of the novel postnatal environment. A more appropriate question which has been investigated for many years is "what infants can learn", as it can provide evidence of their capacities. Conditioned rotation of the head and conditioned sucking clearly demonstrates that the adaptive mechanisms of learning are already enabled in human newborn infants (Papoušek, 1961; Siqueland & Lipsitt, 1966; Blass *et al.,* 1984). For instance, Blass *et al.* (1984) applied a gentle forehead stroke as the conditioned stimulus, followed by the delivery of some su-

crose (unconditioned stimulus) to successfully elicit a conditioned head orienting turn and sucking response. Furthermore, neonates have been described as showing classical EBC in both awake (Little *et al.,* 1984) and sleeping (Fifer *et al.,* 2010) conditions. This kind of learnt behavioural response to an adverse stimulus might be essential for survival, such as learning how to overcome respiratory challenges (Paluszynska *et al.,* 2004). However, neonates within the first day of birth are also already capable of learning a conditioned response to positive stimuli. Accordingly, the association between a neutral odour and a positive tactile stimulation was readily learnt by both awake and sleeping newborns (Sullivan *et al.,* 1991). In another experiment, a group of newborn infants had to learn how to discriminate between canonical (peat, teap) and non-canonical (pst and tsp) syllable pairs by changing their sucking behaviour when their mother's voice was used as a reinforcer (Moon *et al.,* 1992). It has also long been known that neonates can distinguish their mother voice among others and prefer it over the unfamiliar ones (DeCasper & Fifer, 1980). Moreover, emotion might play an active role in motivating behaviour, such as creating infant-parent bonding or avoidance responses to negative stimuli (Lipsitt, 1998).

EBC as a link between atypical behaviour and neurodevelopment

Classical conditioning has been exploited in the human infant population for half a century, making it a model to evaluate and discriminate aberrant behaviour. In an EBC study (Herbert *et al.,* 2004), differences in learning capabilities where found when comparing preterm and full-term born infants. This possibly reflects there is a difference in their motor abilities, in keeping with the higher risk for motor impairments in preterm infants. Moreover, an infant's ability to detect, understand and respond to socially-relevant stimuli possibly reflects their social skills, thus may help to identify infants at risk for developing a social disorder (Reeb-Sutherland *et al.,* 2011). Therefore, by comparing individual differences in the presence, rate of learning, and morphology of the response, the EBC may represent a tool with which to identify a number of neurodevelopmental disorders including foetal alcohol syndrome, genetic disorders, attention deficit/hyperactivity disorder, learning disorders, schizophrenia, and autism spectrum disorder (Reeb-Sutherland &

Fox, 2015). While an abnormal EBC may be a valid predictor of many neuropathologies, it lacks the specificity to distinguish between distinct disorders. A possible reason for this is that different pathologies may share common underlying mechanisms, but more importantly, we also have an inadequate understanding of the ontogenesis of learning brain mechanisms. Future scientific research should therefore attempt to bridge the gap in knowledge of learning behaviour in neonates and the neural correlates of learning in older individuals to better predict the link between abnormal behaviour and abnormal neurodevelopment.

1.5 Aim and hypothesis

In this chapter I have shown the dramatic changes that the brain undergoes during development. In particular, the perinatal period is characterised by the critical window for development of the sensory areas, during which activity-dependent neuronal activity and therefore experience are necessary to guide the brain's maturation and network organisation. Enhanced neural plasticity during this developmental stage represents a significant brain asset for adapting to evolutionary changes, environmental pressures, and experiences, as well as a window of vulnerability that might lead to pathological behaviour. This is particularly evident in preterm born infants who are at risk for neurodevelomental disturbances leading to life-long impairments. The sensorimotor system is particularly susceptible to deviations from the normal development, as motor disorders (e.g. CP) have an high incidence in this vulnerable population. It is therefore important to study normal development of the sensorimotor system and how early sensory experiences can influence this trajectory. In this thesis I investigate 1) the organisation of the somatosensory cortex (somatotopy) in the immature brain to identify when the somatotopy emerges in development; and 2) how experience-dependent activity can influence development in the sensorimotor system, potentially moulding cortical features.

Cortical organisation into topographic maps is a hallmark of sensory networks, and somatotopy can be used as a model to infer cortical maturation. On the basis of the *radial*

unit hypothesis the spatial arrangement of the cerebral cortex is pre-established by genetic factors that guide the neuronal migration along cortical columns. However this protomap is later refined by activity-dependent mechanisms, and therefore environmental sensory inputs might mould its maturation. Animal studies suggest that those maps may form across the equivalent period to the third trimester of human gestation and that they can be permanently affected by adverse environmental events occurring in this time window. While the high rate of sensorimotor disabilities affecting preterm born individuals suggests the vulnerability of the last trimester of gestation in sensorimotor development, there is no evidence about whether the topological organisation has already been established. I therefore assessed the somatotopy of the preterm brain as descried in chapter 3.

Although the foundation of the sensorimotor system might already be established early in development, there is general consensus that experience-dependent plasticity can influence its functions. Neuronal plasticity has an imperative role in driving brain development and enables great adaptation skills in humans. Early life experiences are therefore important to shape the developmental destiny of the individual. While perceptual processes and the learning capabilities of human newborn infants have been investigated for decades, the underling mechanisms of plasticity and how the environment can shape brain function are yet to be fully understood. In particular, associative learning is a relative simple example of an adaptive mechanism which newborn infants are capable of, although the corresponding neural correlates have not been identified. My goal was to design an associative learning paradigm to be used on neonates inside the fMRI scanner and to then explore the effect of learning on the functional brain responses (chapter 5).

"A method is more important than a discovery, since the right method will lead to new and even more important discoveries."

– Lev Landau –

2

Imaging the newborn brain using fMRI

Much of what we know about the human brain has been acquired thanks to neuroimaging techniques. Amongst these techniques, *magnetic resonance imaging* (MRI) has been particularly useful to investigate neural activity in the brain. In order to give the reader an understanding of the methodology used in this thesis, I will first describe the basic principles of MRI and the specific features and challenges associated with newborn brain images. MRI can be used to image the human brain tissue structure, while advanced techniques can be further used to investigate the brain function using e.g. functional magnetic resonance imaging (fMRI). Here I will first describe the principles underlying MRI and its application on the neonatal population. I will then describe the steps involved in fMRI data analysis including preprocessing, statistics, group analysis and measure of percent signal changes. The design of the task to perform during the fMRI experiment is of paramount importance for an effective study, and special considerations are required while

investigating the brain response of neonates. I will then outline the dedicated robotics tools I have used to create reproducible, well controlled stimuli and acquire objective quantitative movement data.

2.1 Magnetic Resonance Imaging

In contrast to X-ray and CT scans, MRI uses magnetic fields and radio frequencies rather than ionising radiation. The magnetic field of an MRI scanner is measured in Tesla (T), with the majority of clinical MRI scanners currently having a magnetic field of 1.5 or 3T. A 3T MRI scanner such as the one used for all the experiments described in this thesis, generates a strong magnetic field, up to 60 thousand times stronger than the earth's natural magnetic field (2-6 μT), and 300 times stronger than a common small bar magnet (0.01T). However to our knowledge this exceptionally strong static magnetic field does not adversely affect the human body or its functions, making MRI an invaluable non-invasive imaging tools with good spatial resolution (in the range of 3-4mm) and acceptable temporal resolution (in a 1-4 s range). MRI relies on the magnetic properties of the human tissues that are rich in water and therefore hydrogen atoms. Hydrogen atoms (^1H or simply H) are peculiar compared to other atoms because their nucleus is composed by a single proton that can interact with the powerful magnetic field of the scanner. By leveraging physical laws and the *nuclear magnetic resonance* (NMR) phenomenon, it is possible to obtain an analogue signal from the hydrogen-rich tissues and digitalise it into an image (Westbrook *et al.,* 2005). Here I will provide only simplified background necessary to understand the imaging terminology while more details are attached in the appendix 6.3.3 (which I strongly recommend reading if the reader is alien to MRI physics) or in the book (Westbrook *et al.,* 2005).

MRI active nuclei like H are susceptible to magnetic field and when they are exposed to it two main processes occur. Their "spin" align longitudinally to the main magnetic field either parallel (low energy state) or antiparallel (high energy state) with a majority in the low energy state, thus together produce a produce a *net magnetisation vector* (NMV)

parallel to the scanner magnetic field. The *spins* are not simply aligned to the main magnetic field, but they wobble around it in a circular path ("precession") at an atom-specific frequency (Larmor frequency). The Larmor frequency of H at 3T correspond to the radio-frequency (RF) band. A radio-frequency (RF) pulse is then used to excite the H nuclei. As a consequence the system gains energy reducing the longitudinal NMV and the atoms start to precess in phase creating a nonzero transverse component of the NMV. Once the RF pulse is switched off, the nuclei return to their parallel orientation, the longitudinal component recovers to the initial NMV as it loses energy, and the transverse component decays as the precession movements dephase. This change in magnetisation vector induces an electric current in a nearby coil (placed for example around the head in case of brain images). The recovery and decay processes take more or less time depending on the organisation of the atoms within surrounding tissue or material, and produce accordingly a different signal intensity. Using a specific combination of additional gradient coils, it is possible to locate the signal in the 3D space and (using an inverse Fourier transform) reconstruct a greyscale image that has tissue-specific contrasts.

The recovery of the longitudinal magnetisation and the decay of the transverse magnetisation are concurrent yet independent phenomena that are sensitive to distinct tissue properties. Choosing which phenomenon to measure determine the contrast of the image, which is named *T1-weighted image* in the case of the longitudinal recovery and *T2-weighted image* in the case of transverse magnetisation. There is an additional contrast, termed T2* that is faster and susceptible to magnetic field inhomogeneity and therefore crucial for functional MRI acquisition (more about this in section 2.2). Many intrinsic and extrinsic parameters determine the contrast of the MRI image, including the TR (*repetition time*) and TE (*echo time*). The TR corresponds to the time in between successive RF pulses, whereas the TE is the time between the RF pulse and the measure of the induced signal. The tuning of those parameters determines the image contrast like the aperture and shutter speed settings of a camera control the exposure of the photo.

2.1.1 MRI of the newborn brain

MRI has become the gold standard to study in vivo the structure and function of the human brain. It has provided an invaluable tool to identify structural brain injury, altered functional connectivity and individual differences predictive of neurological pathology. Of those neurological disorders, many are known to originate early during development shifting the neuroimaging focus on the prenatal, neonatal and very early childhood periods. In keeping with the importance of the early period of development for the later outcome, a high prevalence of neurodevelopmental disorders has been reported in those subjects who were born prematurely and or had early brain injury (Fawke, 2007; Allen, 2008; Ment *et al.,* 2009). Moreover, the spotlight has been turned on neonatal research following remarkable improvements in neonatal care which have increased the survival rates of infants born preterm but have also resulted in an overall increase in the incidence of long-term neurodevelopmental disabilities (Allen, 2008). While the behavioural features of those disabilities have been well described (Fawke, 2007; Allen, 2008; Ment *et al.,* 2009), the underlying aetiology remains poorly understood (Ment *et al.,* 2009). Improved understanding of what influences neurodevelopmental outcomes could enable physicians and scientists to develop targeted therapies to restore brain functionality. To develop better biomarkers and treatment strategies, neuroimaging research needs to characterise the normative developmental trajectory and investigate deviations that predict behavioural, cognitive and neurological functions before the clinical symptoms become evident (Ment *et al.,* 2009; Batalle *et al.,* 2018).

Although neonatal MR imaging can provide an invaluable tool for identifying such deviations, adult protocols need to be adapted to match the requirements of the immature brain (Rutherford *et al.,* 2006). With this in mind, advances in MRI techniques have aimed to address the rising need for paediatric imaging through addressing the practical aspects of scanning and preparation protocols in order to minimise subject disturbance and motion. These upgrades include extra foam cushions, vacuum immobilisers, faster or quieter scanning acquisition sequences, and suitable acoustic protection (Dean *et al.,*

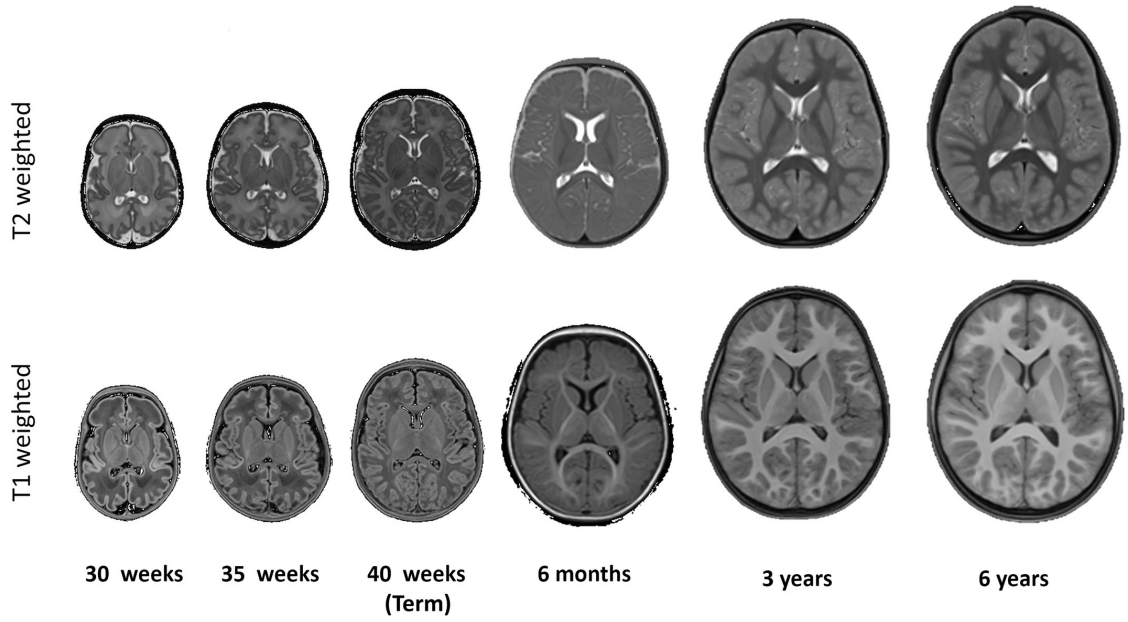

Figure 2.1: T1- and T2-weighted images at different age points throughout the perinatal and early childhood period. (Batalle *et al.,* 2018)

2014; Smith-Collins *et al.,* 2015; Solana *et al.,* 2016; Hughes *et al.,* 2017). Moreover, neonatal head coils have been developed to improve the signal-to-noise ratio and overall image quality of the newborn population (Hughes *et al.,* 2017). Thanks to the joint effort of clinical and research communities perinatal imaging is a rapidly progressing field towards understanding the developing brain (Ment *et al.,* 2009; Batalle *et al.,* 2018).

The infant's brain is not just a small adult brain (Batalle *et al.,* 2018). The MRI appearance of a newborn brain differs from that of an adult brain reflecting substantial differences in structure at distinct developmental stages. Given that the developing brain is changing rapidly, the MRI images at different weeks during the perinatal period show more differences than across longer age-ranges later in life (see figure 2.1). During the peri- and early post-natal period, the brain undergoes drastic macroscopic and microscopic changes. Morphological transformations include an increase of brain volume, gyrification patterns and cortical thickness. In addition, microstructural changes alter the tissue properties and thus the image contrast in different areas of the brain at different ages.

Looking at Figure 2.1, there is a striking dissimilarity in the signal of the white matter in the immature brain compared to that of a 3-year-old due to differences in myelination.

This appearance in the white matter arises from sheets of neuronal cells (oligodendrocytes) that wrap the axons of the neurons in a fatty myelin sheath to increase their electrical transmission efficiency. The white matter of preterm infants younger than 36 weeks PMA is almost completely (98%) unmyelinated (Hüppi *et al.,* 1998). However, after that time myelination rapidly increases and from 29 weeks to term age the proportion of myelinated white matter increases approximately fivefold (Hüppi *et al.,* 1998) and myelination continues during the first years after birth. At full term (40 weeks) it is possible to recognise hyperintensity in T1-weighted contrast and hypointensity in T2-weighted contrast within the posterior limb of the internal capsule between the basal ganglia and thalamus (Rutherford *et al.,* 2006) marking the development of corticothalamic and thalamocortical connections. It is also possible to appreciate a linear increase of grey matter volume relative to intracranial volume across the period 29-41 weeks PMA (Hüppi *et al.,* 1998). All those structural changes are accompanied by functional changes that can also be detected using functional MRI.

2.2 Functional MRI

MRI provides a powerful tool to identify brain injuries and localise them at high spatial resolution in a non-invasive way. However, the link between structural abnormalities and long-term disabilities (such as motor, sensory, and cognitive impairments) later in life is not straightforward. There is therefore a compelling need to explore the functional correlates between aberrant brain appearances and their clinical consequences in order to provide accurate prognosis and earlier intervention. In the early 1980s, in parallel to the upcoming of MRI, the Positron Emission Tomography (PET) scanner was invented. This technology provided the first glimpse into functional processes in the brain. However, PET involves very expensive equipment, is technically challenging and above all, it requires the individual of interest to be injected with a radioactive tracer. MRI in contrast involves neither ionising radiation nor radioactive injections. Therefore, researchers were motivated to obtain functional brain images similar to those obtained with PET whilst

using the safer MRI scanner. By late 1991, three different groups (Ogawa, Kwong, Bandetini) were working to develop a technique to image brain function without the need for injected contrasts and lead to the technological breakthrough of functional MRI (fMRI). Thanks to fMRI we can now investigate brain function in vivo in humans, with its intrinsic safety making it also ideal to explore the youngest population.

2.2.1 Principles of functional MRI

Neuronal activity is metabolically demanding and requires a supply of glucose, ATP and importantly oxygen. The vascular system is responsible for the transport of those substrates, as a consequence, neuronal signalling causes local changes in cerebral blood flow (CBF), cerebral blood volume (CBV), and blood oxygenation. The oxygen is carried by the haemoglobin protein that changes its structure whether it is loaded with oxygen (oxyhaemoglobin) or not (deoxyhaemoglobin). While the oxyhaemoglobin is diamagnetic, the deoxyhaemoglobin is paramagnetic and is therefore highly susceptible to a magnetic field resulting in a localised disturbance to the field. This different magnetic property can be leveraged to create an MRI contrast. An increase of oxyhaemoglobin relative to the deoxyhaemoglobin reduces field inhomogeneity and boosts the MR signal. Using a gradient-echo imaging sequence it is possible to measure the temporal evolution of the blood oxygenation and produce the BOLD (Blood Oxygen Level Dependent) contrast (Ogawa *et al.,* 1990). This technique has then been used to measure the brain functional response to visual and motor tasks at a temporal resolution of seconds (Ogawa *et al.,* 1992; Kwong *et al.,* 1992). This technique has then been used to measure the brain functional response to visual and motor tasks at the temporal resolution of seconds (Ogawa *et al.,* 1992; Kwong *et al.,* 1992). This is possible thanks to the tight relationship between neural activity and the subsequent changes in cerebral blood flow, termed neurovascular coupling, which forms the basis of fMRI. Because of the neurovascular coupling, it is possible to infer brain activity from changes in BOLD and to generate high spatial resolution functional maps using fMRI.

As fMRI became a suitable technique to investigate in vivo human brain activity, researchers around the world have endeavoured to better understand its underlying principles, potential and limitations. As the BOLD response is a secondary effect of brain activity, it is critical to describe the temporal characteristics of the haemodynamic response. The haemodynamic response to neuronal activity triggers multiple effects such as CBF and CBV increase and a change in the cerebral metabolic rate of oxygen (CMRO2) which are non-linearly dependent (Wu *et al.,* 2002; Chen & Pike, 2009a). For instance, a small increase in oxygen requires a large increase in cerebral flow and the change in CBF is exponential compared to the one in CBV (Chen & Pike, 2009a). To understand and predict the fMRI signal, there is the need for a model that describes the overall BOLD change in response to neuronal activation. A first "Balloon model" was proposed (Buxton & Frank, 1997) and then revised (Glover, 1999) providing what it is now considered the canonical haemodynamic response function (HRF). The HRF is characterised by an initial dip during the first couple of seconds from the onset of the stimulus, followed by a transient increase that peaks around 5.5 seconds, next and undershoot and finally the signal returns to its baseline level. The initial dip is thought to be an effect of the immediately after post-stimulus increase in oxygen consumption while the supply of oxygenated blood does not compensate the demand yet (Buxton, 2009). This demand in oxygen is then met by an increase in CBF followed by the capillary dilatation, hence the increase in CBV, causing the BOLD signal to rise to approximately 2-3% above the baseline level (Friston *et al.,* 1995; Buxton *et al.,* 1998; Glover, 1999). After the stimulus there is an undershoot of CBF accompanied by a slow biomechanical response of the venous CBV (prolonged elevation), which taken together contribute to the BOLD undershoot (Buxton *et al.,* 2004; Chen & Pike, 2009b).

Infants' HRF

The emerging interest in developmental neuroscience has encouraged the employment of fMRI in newborn infants and foetuses as well. This raised new challenges during the data analysis of the immature brain and the design of the experiment. Not only is the

infant's brain structurally different from the adult brain, cortical and subcortical function progressively develop (Batalle *et al.,* 2018). The perinatal period, the third trimester of gestation in particular, is a period of rapid neural growth accompanied by rapid functional maturation (Doria *et al.,* 2010). In parallel with functional network organisation, the cerebral circulation also undergoes dynamic maturation to address the metabolic demands of the developing cortex (Virgintino *et al.,* 2003). During this period of ongoing angiogenesis, the preterm brain is characterised by immaturity of vasoregulation, lower CBF and slower vasoreactivity compared to the full-term brain (van Kooij *et al.,* 2010; Brew *et al.,* 2014). While CBF in very young infants is particularly low, cerebral oxygen metabolism is high, suggesting a different interplay of factors in the haemodynamic response (Brew *et al.,* 2014). Taking into account the immature vasculature, vasoactive signalling, and brain functions in preterm infants, it is critical to consider the age-specific HRF when performing fMRI studies in newborns. Although initial fMRI studies reported poor or inconsistent results in neonates, BOLD fMRI responses can be reliably identified in both term and preterm neonates with proper considerations (Arichi *et al.,* 2010; Arichi *et al.,* 2012). Arichi et al. (2012) described the evolution of the HRF in the neonatal period, providing an invaluable tool that significantly improves BOLD fMRI data analysis throughout development. The BOLD response undergoes a systematic maturational change in the morphology characterised by an increase in peak amplitude and decrease in time to peak with increasing age (figure 2.2). These characteristics are in keeping with the changes in BOLD found in developing animals (Colonnese *et al.,* 2008). In addition to the trend toward reduction in time to peak and increase in amplitude, the term HRF is characterised by a deeper negative undershoot (with respect of the positive peak) in comparison to the canonical HRF form seen in the mature adult brain and the one identified in preterm infants (Arichi *et al.,* 2012). The age-specific HRF here described have been used for all the neonatal data collected in this thesis.

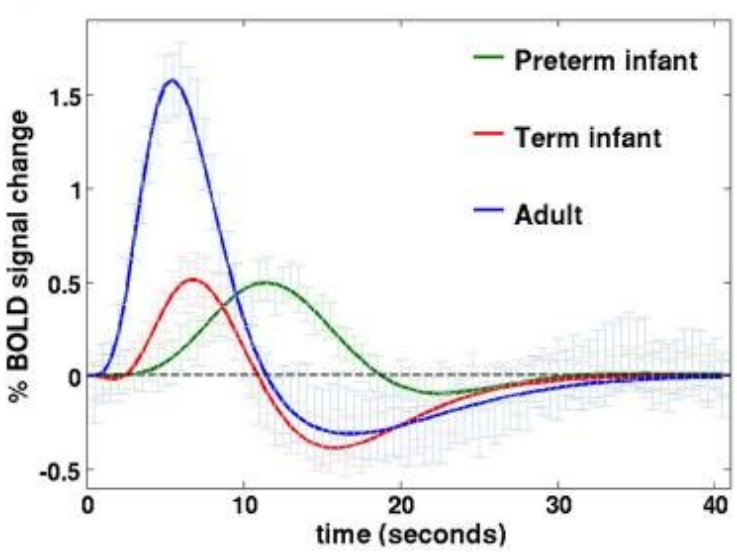

Figure 2.2: Development of HRF in the human brain. Mean % BOLD signal change relative to a somatosensory stimulus (1 sec) in adults, term equivalent infant and preterm infant (Arichi *et al.,* 2012).

2.3 fMRI data analysis

FMRI data consists of a four-dimensional data file: a sequence of 3D volumes (brain images) concatenated in time (4th dimension). Each voxel of the brain volumes contain a signal that varies in time and the time series represents the BOLD signal. The variation in BOLD can then be related to the underlying brain activity associated with a task (task fMRI) or rest (resting-state fMRI). The most commonly used approach to analyse task fMRI data is the general linear model (GLM) which measures the fit of the time series within each voxel with a temporal model of the predicted activation (Friston *et al.,* 1994; Friston *et al.,* 1995; Jenkinson *et al.,* 2012). A test statistic is then calculated for each voxel correcting for multiple comparisons to minimise false positives. The model represents a prediction of the sampled BOLD time series and is generally built as the convolution of the experimental design (timing of stimulation or task) with the HRF. The GLM then identifies those voxels that have a significant relationship with the model, thus infer which brain locations were active at the same time as the stimulus.

A major advantage of fitting with a GLM, is that it is also possible to compare different experimental conditions by calculating the contrast between the parameter estimates for one condition to than another in the GLM. Since the brain response is not instantaneous (5-7 s in adult and even slower in infants), the task design needs to be re-shaped to match BOLD response, and this is achieved by convolving the task occurrence with the HRF.

The resulting modelled time series takes the name of the explanatory variable, as they aim at explaining the variance in the measured time series data at each voxel location using statistical modelling. Importantly, there are ongoing spontaneous BOLD fluctuations in the brain which also contribute to the change in BOLD signal despite not being associated with the response to a task (stimulus), therefore the particular stimulus needs to elicit a sustained response that can stand out against the overall variability. Moreover, the fMRI signal does not reflect only the activity-coupled haemodynamic change, but is rather a complicated spatio-temporal correlation structure including multiple sources of noise that need to be disentangled (Lindquist, 2008). Therefore the data need to be pre-processed before posing any kind of statistical question.

2.3.1 Preprocessing

As mentioned, fMRI data are particularly noisy and require a series of cleaning processes to address specific known causes of non-neuronal signal change before they can actually be informative. In modern software, like FSL (Jenkinson *et al.,* 2012) and SPM, preprocessing is facilitated by a built-in series of standardised steps (or pipeline). While the preprocessing pipeline can be customised, it is important to keep the same steps for each fMRI data set within a given study as the way the data has been preprocessed to attenuate noise can significantly influence the statistical results (Bright & Murphy, 2015). The data in this thesis are analysed using the FSL library (FMRIB, Oxford, UK), therefore the focus will be on these tools for brain imaging data analysis.

A first step to clean the data is the removal of non-brain tissue from the whole head image. Brain extraction improves the robustness of registration, reduces multiple comparisons and computational load and can be accurately performed using BET (Brain Extraction Tools, Smith, 2002). The time series from each brain voxel then needs to be corrected to take into account that each slice has been acquired at slightly different times. Using Hanning-windowed sinc interpolation, the time series within in each slice is shifted in accordance with the acquisition order. Another consequence of acquiring MRI data in

time is the presence of signal drift caused by physiological and scanner-related noise. The low-frequency component of this drift is removed by applying a high-pass temporal filter. It is critical to remove this signal drift because the statistical analysis assumes the stationarity of the timecourse, although the filter threshold must be selected carefully and taking into account the timing of the experimental time course to avoid the removal of activity-related frequencies. As it will be explained later in the GLM analysis, one fundamental requirement for the unbiased estimates of the GLM parameters is that the time series are uncorrelated. The intrinsic autocorrelation of the data needs therefore to be addressed to reduce the number of false positives. A common technique that serves this purpose is prewhitening (Woolrich *et al.,* 2001) that will be better defined in the context of the GLM. An additional procedure to reduce false positives is to apply Gaussian spatial smoothing on each volume with the result of reducing noise (often appearing as sparse isolated voxels) while preserving valid activation and further reducing multiple comparisons.

An additional substantial source of noise is caused by head motion artefacts. It is likely that during acquisition the head moves causing a mismatch between voxels at different time points, and therefore each volume must be realigned. In FSL, MCFLIRT corrects this head motion by registering each brain volume with each other using rigid body realignment (Jenkinson *et al.,* 2002). MCFLIRT performs automated iterative searches of the motion parameters of each time series in reference to a template image (the middle volume by default) by means of tri-linear interpolation. The resulting motion parameters can be later used as statistical covariates in the GLM. Motion is not the only source of noise, as hardware artefacts and physiological pulsations also contribute to the mixture of signals present in the data. A promising approach to address this is to use independent component analysis (ICA), which is a hypothesis-independent technique to explore the data and has the capability to separate different sources that contribute to the signal (Beckmann & Smith, 2004; Griffanti *et al.,* 2017). This concept has been implemented in FSL as the MELODIC (Multivariate Exploratory Linear Optimised Decomposition into Independent Components) tool which decomposes the 4D data into spatial components

associated with a time series (Beckmann & Smith, 2004). The resulting independent components are then visually inspected and hand classified as noise or signal following established guidelines (figure 2.3), and then removed from the data (Griffanti *et al.*, 2017). Nevertheless, removing structured noise while retaining as much signal as possible is challenging and subject to human bias, therefore components should be kept in the data unless they are clearly artefactual (Griffanti *et al.*, 2017).

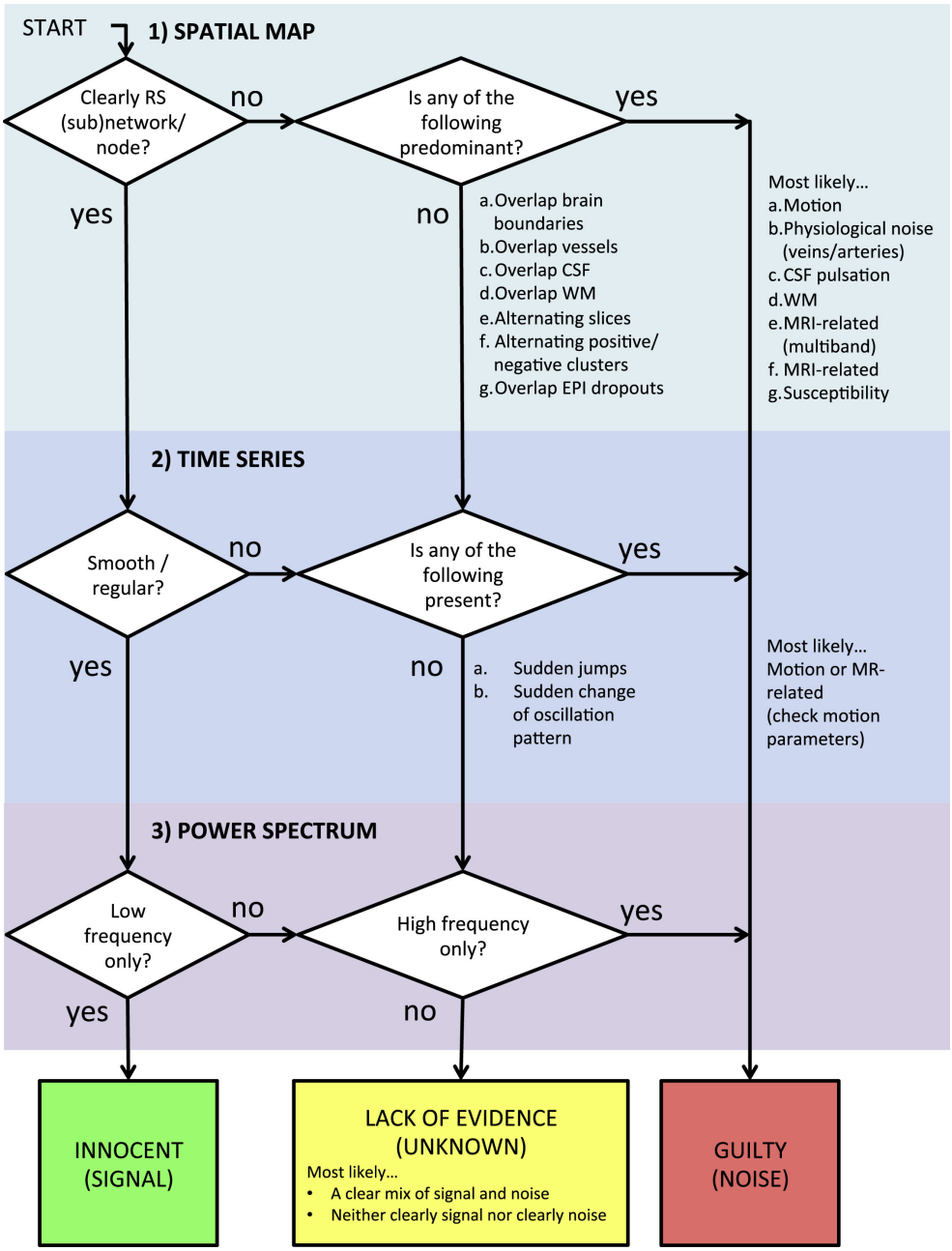

Figure 2.3: Flowchart that summarise the procedure for visual inspection and manual classification of ICs proposed by Griffanti *et al.*, 2017. Spatial maps, time series and power spectra need to be evaluated and only the "proven guilty" components should be removed.

2.3.2 The General Linear Model for fMRI

After the data have been preprocessed, the next step is to "ask questions" of the data. The GLM is the most widely used analysis technique to investigate task-based fMRI data, and provides a simple framework to implement standard statistics and answer most questions (Poline & Brett, 2012). In fMRI analysis, the GLM is implemented as a univariate analysis that tries to fit a model to each voxel's time series independently. The same tool can also be applied to more complex analysis that takes into account the interaction between voxels (e.g. multivariate analysis), nevertheless, in this thesis they are not applied and multivariate analysis is omitted.

The GLM assumes some hypothesis about the data and model them as a linear combination of parameters: $\vec{y}(t) = \beta_0 + \beta\vec{x}(t) + \vec{\epsilon}(t)$. In task-fMRI, the model represents the predicted functional activation in response to a stimulus, which is then fit into the time series at each given voxel (in the formula represented by $\vec{y}(t)$). In the equation, the β_0 represents the offset (baseline BOLD level), the $\vec{x}(t)$ is the suggested explanation of the data, for example the stimulation provided, and ϵ represents the remaining unexplained data, thus the error in the model fit. The model also assumes that the errors are independent samples of a Gaussian distribution with zero mean and constant variance $\epsilon \sim N(0, \sigma^2)$. To have more flexibility, a more accessible representation, and an easier implementation for computer coding, the equation can be expressed in matrix form: $Y = X\vec{\beta} + \vec{\epsilon}$. Where Y represents the data, X is the design matrix, $\vec{\beta}$ the parameter estimate vector, and $\vec{\epsilon}$ the error vector. The design matrix allows multiple explanatory variables (regressors) to be included in the form of different columns (X_j), whereby each regressor is multiplied by the estimated parameter β_j.

Based on the Gauss-Markov theorem, the best linear unbiased estimator of the coefficients, if it exists, is given by the ordinary least squares estimator, hence the fit then aims to find the best $\vec{\beta}$ vector that minimises the error vector. This however is true if the errors are distributed with zero mean, constant variance and not correlated. This assumption is violated for BOLD time series because the data are temporally autocorrelated and in this

case $\epsilon \sim N(0, \sigma^2 V)$, where V is the covariance matrix that describe the correlation between time points. Nevertheless it is possible to remove the autocorrelation using a prewhitening technique (Woolrich *et al.,* 2001). The idea of prewithening is to estimate the V covariance matrix and compute a K matrix such as $KVK^{-1} = I$, to then multiply the GLM equation by K. In keeping with this, data are prewhitened during the preprocessing stage so that the ordinary least squares (OLS) can be used on the whitened model having constant variance.

The error vector includes the noise intrinsic to fMRI data, however, some of the noise can be estimated and included in the model. Given that head motion can partially explain the data, it is reasonable to add the motion parameters calculated during the preprocessing step as additional nuisance regressors in the model. Although this is a simplistic solution as it assumes a linear relationship between motion and artefacted signal, it helps to remove large residual noise effects due to motion. Another confound that can be added is a matrix of zeros and ones where the ones correspond to outliers timepoints that need to be ignored completely during the analysis. This is particularly useful in case the fMRI dataset has been corrupted by large motion that cannot be recovered by the linear regression of motion parameters. There are several metrics to calculate outliers, some based on motion correction parameters, others based on intensity differences within the time series, although intensity-based metrics tend to be more accurate (Power *et al.,* 2012). In this thesis, the method used to detect the corrupted timepoints is the measure of the root mean square intensity difference between consecutive volumes (Power *et al.,* 2012).

A simple example of a model is made by alternating rest with task periods. This allows comparison of the increase in signal in response to the task (with active or passive stimulus) versus the baseline signal. The task can be presented as a single brief event of stimulation (*event-related paradigm*), or in blocks of constant stimulation (*block design paradigm*). More information about the task design can be found in the next section. As already explained in section 2.2.1, the brain response that is expected in response to a stimulus is not instantaneous but follows the profile of the HRF due to the underly-

ing brain physiology. Therefore the design paradigm alone is not representative of the predicted signal and must be convolved with the HRF. The result is a blurred and delayed waveform that now resembles the hypothetical brain response. The haemodynamic responses can vary significantly across subjects and within the same subject in different areas (Handwerker *et al.,* 2004; Henson, 2006). To overcome this limitation, it is possible to include the HRF's temporal derivative in the design matrix. The effect is equivalent to shifting the waveform slightly in time, hence adding flexibility to the model.

After the model has been fit to each voxel's time series, the design matrix results in 3D images of β values (an image for each explanatory variable). Although larger parameter estimates represent a better fit, to enable full statistical inference it needs to be converted into a t-statistic image. This is achieved by dividing the image by its standard error estimated by the ϵ of the model. The explanatory variables in the design matrix can then be considered as distinct effects both independently or via different contrasts between them. For instance, if the researcher wants to test if one variable explains the data better than another, the effect can be modelled by the difference between the two. At this point, the strength of the fit of a specific condition expressed by the t-statistic is compared against the null hypothesis that the condition does not explain the variance in the data ($\beta = 0$). If the null hypothesis is unlikely (small p-value) the voxel is considered "active". To enable inference between different voxels, the t-statistic is converted into a z-statistic by equating the probabilities under the tails of the distribution. While the t-statistics depend on the degrees of freedom (DOF), z-statistics are normally distributed and therefore allow comparisons across stimuli and subjects.

Given the large amount of voxels present in the data, the p-value needs to be corrected for multiple comparisons using methods like Gaussian Random Field theory (Worsley *et al.,* 2004). There are also some additional post-statistic considerations to limit the number of false positives, such as cluster thresholding. In this method, the z-statistic threshold is adopted to define clusters (contiguous active voxels) and if the cluster does not pass a certain significant threshold it will be masked out (Worsley, 2001). An important consideration is that the significance threshold that determines the minimum cluster size

is arbitrary. A low threshold can detect clusters with large spatial extent despite a low z value, in contrast, a high threshold enhances clusters with high z despite their small spatial extent. The trade-off chosen in this thesis was to use clusters determined by $Z > 2.3$ and a (corrected) cluster significance threshold of P=0.05 (Worsley, 2001). The voxels that exceed the threshold of the contrast of interest and post-statistic corrections represent the functional map of activation. However, single-subject inference is not typically reliable and multi-subject analysis is necessary to answer questions with more confidence. Therefore, the first level of analysis of various subjects needs to be combined into one group map. For this, the different sessions must be registered into a common space (brain template).

2.3.3 Group analysis

Registration Before a group analysis can be carried out, the individual subject statistical maps must be registered to a brain template that represents the group population. This registration is classically achieved using algorithms that aim to minimise the sum-of-squared differences between two images. Given that the temporal resolution of fMRI data is achieved at the cost of its spatial resolution, fMRI images possess a low spatial resolution and therefore registration to the standard space is challenging due to the great difference between the images. In this thesis registration has been performed in a multi-step process as follows. The first step is a rigid body (6 DOF) transformation from the higher resolution T2-weighted image to the lower resolution functional space of the same subject. This generates a matrix that can then be inverted and applied to transform the lower resolution thresholded z-statistic maps to the higher resolution space. The higher resolution space can more easily be registered to the standard space, and the best result is given by a combination of an initial linear transformation with 12 DOF followed by a non-linear transformation that optimises the previous step. The high-resolution individual subject image can finally be warped by the last transformation and be overlaid onto the template brain.

Permutation method A simple example of an fMRI group analysis is the identification of the group average. In statistical terms, this is equivalent to asking if the group activates on average and has a non-zero mean. The GLM can be applied in the form $Y_k = X_k\vec{\beta}_k + \vec{\epsilon}_k$ where k stands for each subject. There are different tools to compute this statistical question, but most of them require assumptions about the data distribution. There are however cases in which the null distribution is unknown and these assumptions fall short, especially for small groups, as is often the case in infant studies. In this situation, permutation methods (also known as randomisation methods) favour inference when the null distribution is unknown. In FSL, nonparametric permutation inference tool is implemented in *Randomise* (Winkler *et al.,* 2014). Instead of assuming a priori knowledge of the null distribution, *Randomise* permutes the data to obtain the null distribution, hence identify the threshold associated with the 5% upper tail probability. The user can generate a design matrix in accordance with the question (this can include confounds such as the age distribution), and s/he is given the options to perform variance smoothing and Threshold-Free Cluster Enhancement. Finally, Randomise produces a test statistic image in p-values that represent the group result.

2.3.4 Percent BOLD change calculation

Group analysis provides the means to study inferences about the average response of a population or the difference between populations. However, one may want to investigate the difference between individual responses, by means of comparing the amplitude of the response to the same stimulus across different subjects or the response to different stimuli within the same subject. To compare the percentage of signal change provides a means to compare brain responses across individuals and/or tasks. However, the parameter estimate from an fMRI model does not convert to the percentage signal change directly, and researchers should be careful with their interpretation. The parameter estimate depends on the design matrix and the HRF model used, therefore comparing different β values obtained from the GLM fitting is inaccurate (Mumford, n.d.). With the right

re-scaling it is however possible to translate the parameter estimate to the %BOLD and to perform correct comparisons.

Firstly, the effective regressor height of an isolated event must be computed for each contrast. The FSL GLM design tool provides the value of the height but it corresponds to the peak-to-peak difference, therefore it is not representative of the amplitude of the response as it includes the post-stimulus undershoot. The baseline to peak should be taken instead as a reference for the amplitude of the response, especially considering that the term-age HRF has a deeper undershoot compared to the canonical adult HRF or preterm-age HRF (Arichi *et al.,* 2012). The best way to identify the baseline to peak height is to create a high temporal resolution ($\Delta t = 0.1$ instead of the real TR time) dummy model of the event and take its maximum value (Mumford, n.d.), where the model is the convolution between the task and the relevant basis function of the HRF. In the case of negative contrasts, the undershoot trough would fit as the amplitude, therefore the minimum value should be considered as the height of the HRF in those specific cases. Secondly, the baseline-to-max range should be multiplied by 100 in order to compensate for the grand mean scaling carried out by FSL preprocessing and obtain a proper scale factor. Finally, the percentage signal values within a region of interest (ROI) for all subjects for each parameter estimate can be computed from the preprocessed data masked with the ROI, multiplied by the scale factor and divided by the mean values. The average of those values within the ROI corresponds to the average %BOLD change and can be used to compare the intensity of the responses to a task.

2.4 Task-based fMRI experiments with newborns

Now that the principles of fMRI acquisition and data analysis have been clarified, the next consideration is what can be actually measured with this technique. Brain activity is not limited to the response of a specific task, in contrast, there are ongoing low frequency fluctuations organised in hubs that overlap between functional networks (Biswal *et al.,* 1995; De Luca *et al.,* 2006). In a task-free experiment, namely resting-state fMRI, a

subject can lay inside the MRI scanner and despite the absence of stimulation, informative BOLD fluctuations can be identified that correlate with the underlying maturation of brain networks (Doria *et al.,* 2010; Fransson *et al.,* 2011). Resting-state fMRI allows investigation of functional connectivity in patients unable to perform a task, and therefore is particularly appealing for neonatal imaging (Rosazza *et al.,* 2014; Batalle *et al.,* 2018). However, the underlying biology of such resting-state activity is still not fully understood, and resting-state networks miss detailed information relative to process specific sensory inputs. Therefore whilst resting-state fMRI is very interesting due in particular to its simplicity of application, this protocol can only compliment but not replace task-based fMRI (Rosazza *et al.,* 2014). The work in this thesis makes use of task-based fMRI to elucidate the neural correlates of sensory processing in neonates. Looking at the literature of task-based fMRI, a variety of task designs can be found, with the choice of the design depending mainly on the question of interest of the study. When designing a task for fMRI there are many considerations to take into account as the optimal design results from a trade-off between statistical efficiency and practical constraints, both of which are more stringent in the case of imaging newborn infants.

2.4.1 Experimental design and challenges

The power of statistical inference is very dependent on the degrees of freedom that corresponds to the number of data points. Therefore the longer the scan, the more volumes that can be acquired, and the stronger the statistical inference. In practice, scanning time is limited as it is advisable to keep a subject within the MRI environment for at most one hour (Henson, 2006). In the case of adult scans, the time is set by the participant's comfort and attention to the task, whilst infants require additional care. Newborn babies spend most of their time asleep, although not continuously and require feeding approximately every 1.5-3 hours. The scanning session should therefore be done in between feeds and during their natural sleep period to avoid sedation that might compromise the infant's response to the task. A scanning session comprises a long preparation time (e.g.

metal check, positioning the subject in the scanner, equipment testing etc.), the acquisition planning and a series of image acquisitions collected for clinical purposes, all before actually starting with the research task-fMRI. With all of this in mind, fMRI scans with neonates should be designed to last not more than 30 minutes.

Infant care has the foremost priority at all time. Therefore vital signs (heart rate, oxygen saturations, temperature) are monitored throughout the session to supervise the well-being of the baby and a microphone inside the scanner allows listening from the control room if the baby cries. The scanner is stopped whenever the baby manifests signs of discomfort, and the clinical team assesses the situation. Sometimes the baby is fussy for short intervals and settles down soon after, and in these cases the acquisition protocol is carried on. As interrupting the scanner disrupts the spin equilibrium, data no longer constitutes a single time series and additionally the head position might have changed. Therefore once the scanner is paused the session cannot be resumed. It is therefore suggested that breaking up the experiment into separate sessions where possible is optimal so that the session can be more easily repeated (Henson, 2006).

With these practical considerations in mind, the experimental paradigm can then be designed. The basic idea behind maximising the efficiency of a design is to maximise the information content of the signal produced. The simplest designs are *event-related paradigms*, consisting of a train of brief (less than 2 seconds) "events" of stimulation or task sufficiently spaced apart. Events are approximated by a delta function, and the activation model is identical to a single HRF. Given that the BOLD response is slow compared to the stimulus, events should be spaced out with a sufficient interstimulus interval (12-15 seconds) (Henson, 2006). However, as the HRF of preterm infants is considerably slower than the adult one, double the time should be given in between stimuli (Arichi *et al.,* 2010). An additional challenge related to the infant HRF is the lower maximum amplitude compared to the canonical adult HRF. Accordingly, the signal to noise ratio in neonatal fMRI is relatively low. Therefore, sensitivity and efficiency of event-related design tend to be poor and alternative designs should be considered when possible. When a stimulus is presented for a longer time, it elicits a larger amplitude

response as overlapping responses add up linearly, hence a *block paradigm* increases the signal to noise ratio and is a more efficient design. Block designs consist of alternated periods of rest ("off") and periods of continuous stimulation ("on") in a boxcar fashion. The "on" periods can also be constituted as blocks of short stimuli with a short interval (less than the peak time), as they elicit a sustained response as in a square-wave stimulus (Henson, 2006). However, block designs are more efficient only if the active period is not too long (less than 50 seconds) due to the reduction of variability in the signal (the response would look as an offset baseline) and the risk of removing the meaningful slow fluctuation after the high-pass filter applied in the preprocessing stage (Henson, 2006).

fMRI data quality is susceptile to head motion, and thus the design should discourage unnecessary movements. Although healthy adults are capable of voluntarily minimising motion during the acquisition and can move in between scans if they feel uncomfortable, this does not apply for newborn infants. Head motion therefore remains a major challenge in neonatal fMRI studies although it can be partially tackled by careful preparation aiming to maximise the infant's comfort (Hughes *et al.,* 2017). Infants are best imaged during their natural sleep using a "feed and wrap" technique. This has been found to achieve desirable results with success rates similar to as if they had been sedated, yet without the drawbacks associated with sedative medication (Edwards & Arthurs, 2011). Infants are placed into the MRI scanner after feeding, with warmth and comfort, then gently placed wrapped in a sheet, immobilised by an apposite vacuum bag, and allowed to settle before starting any acquisition (Hughes *et al.,* 2017). Additional padding should be placed between the head and the receiver coil to reduce space for head motion, yet without putting pressure around the head. In addition, hearing protection and active noise cancelling headphones are used to attenuate the noise produced by the scanner sequences, further contributing to the infant's relaxation and sleep. Finally, it is critical that the stimulus itself does not disturb the infant while being effectively capable to elicit a brain response (Arichi *et al.,* 2012). Therefore, a paramount requirement for the adequate task fMRI implementation is the choice of an optimal stimulus.

2.4.2 Technology for task-fMRI in neonates

One major constraint for neonatal task-dependent neuroimaging studies is given by the lack of cooperation of the young population, nevertheless, different passive stimulations have been successfully employed in combination with fMRI (Seghier & Hüppi, 2010). In particular, successful tasks in newborn infants have included auditory, visual, somatosensorial and olfactory stimuli (Born *et al.,* 2000; Anderson *et al.,* 2001; Arichi *et al.,* 2010; Arichi *et al.,* 2013; Allievi *et al.,* 2014). Technological aids are decisive to produce satisfactory results. Novel robotic techniques have been employed to develop MR-compatible devices that enable controlled delivery of stimuli within the scanner environment (Gassert *et al.,* 2008; Su *et al.,* 2017). However, having a robotic system within the MR scanner environment leads to hard constraints. The robotic system should contain no ferrous materials due to the strong magnetic field of the MRI scanner, except for small components securely anchored at a sufficient distance from the scanner bore (Gassert *et al.,* 2008). However, as infants subjects are positioned with their full body inside the scanner bore, any system cannot contain any ferromagnetic component in order to be fully MRI/fMRI compatible. Stimulating the infant inside the scanner requires therefore non-standard engineering solutions (Allievi *et al.,* 2013; Allievi *et al.,* 2014).

Additionally, infants are smaller and more delicate than adults, which therefore requires an appropriate design that matches these differences. Some requirements for an infant-friendly fMRI compatible system have been suggested (Allievi *et al.,* 2014), and are here summarised and integrated. Suitable devices should be lightweight, comfortable, have the appropriate size, and fit the infant without constraining their spontaneous movement. The robotic device needs to provide a pattern of stimulation suitable to the young population without exceeding the infant's capability to avoid potential harm or distress. Not only must it be mechanically safe, but also safe from spreading infections, thus either easily cleanable or even single-use. To safeguard the baby and to ensure a consistent presentation of the task, the stimulus patterns should be monitored and recorded throughout the acquisition. The stimulation pattern should be able to be induced with controlled

amplitude, frequency and time-locked with the image acquisition to ensure consistency, a robust response and high quality data. Finally, the interface should have an easy fit to minimise the preparation time, in order to avoid waking up the baby and to be effectively used by the clinical staff.

This thesis includes task-based fMRI studies with preterm and term newborn infants. In particular, the study described in chapter 3 has the goal to identify the somatotopic mapping of the preterm brain, therefore requiring stimulation of different body parts. A safe system able to produce a highly reproducible pattern of stimulation synchronised with the fMRI acquisition is of paramount importance to achieve robust results in fMRI studies. In keeping with this, reliable robotic systems have been employed to provide tactile stimulation of the hands, feet, and mouth. Furthermore, the same system has been used in combination with commercial MR-compatible headphones to investigate the neural processes of learning in neonates by means of an auditory-motor classical conditioning paradigm (chapter 5). The fMRI tasks exploited for investigating early brain responses to environmental stimuli were possible thanks to the technological support here presented.

Robotic interfaces for limb passive movement stimulation

A desirable system to passively move the limbs (wrist and ankle) of infants has been previously developed and tested (Allievi *et al.,* 2013; Allievi *et al.,* 2014), and has been exploited for the studies described in this thesis. Furthermore, the fMRI compatible wrist robotic interface has been employed in a developmental study with infants from 30 to 43 weeks PMA, demonstrating that it is a robust tool to probe patterns of functional activity in neonates at different ages (Allievi *et al.,* 2016). The custom-made robotic stimulation device is a modular system consisting of a control unit and interchangeable interfaces that can fit the hand or the foot of the newborn. The system is connected to a laptop where tailored software written in the LabVIEW environment controls the device and the researcher can monitor the ongoing task from the same laptop. The device works on a

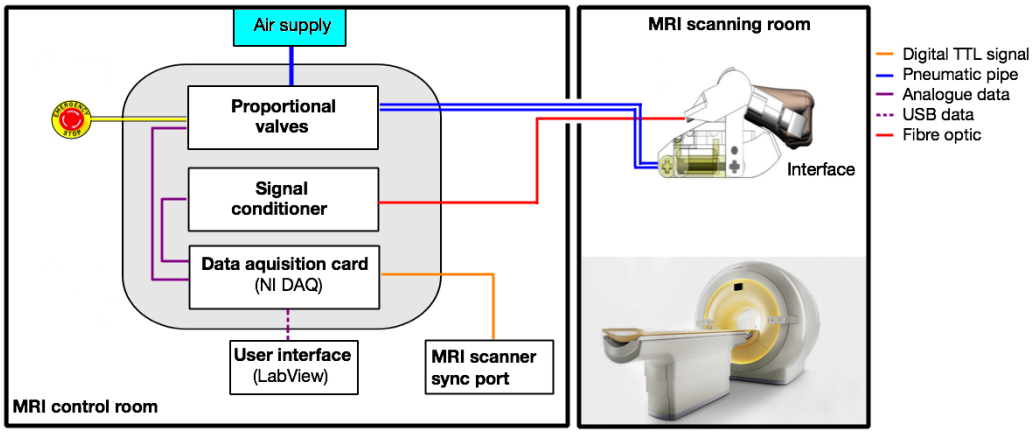

Figure 2.4: Diagram of the fMRI experimental setup. The control unit is located in the MRI control room, while the haptic interface in the shielded MRI scanning room. The interface is remotely controlled in sync. with the MRI acquisition and is actuated via a pneumatic system.

master-slave configuration: the control box is located in the MRI control room protected from the magnetic field and the plastic haptic interface attached to the infant inside the scanner (figure 2.4). Transmission from the control unit to the interface is obtained through pressurised air coming from the hospital air supply and regulated by proportional valves within the control box. The control unit contains a NI Data Acquisition Card (DAQ) that reads the TR of the image acquisition fed via the MRI scanner sync TTL pulse. Then, according to the TR and the preset custom task paradigm, the pneumatic valves open to deliver air at a precise pressure (controlled via a PID loop), which in turn actuates the haptic interface causing flexion and extension movements of the joint. The system incorporates a smart non-traditional method to provide a measure of the angle as feedback of the movement. From the control unit, there is a a thin fibre optic cable which is attached to the interface creating a loop and return to the signal conditioner. Importantly, the fibre optic has a cut at the pivot point of the interface allowing the light to escape; therefore the analogue signal measured varies depending on the bending angle. The DAQ finally transforms the voltage in angle and displays the position on the GUI of the laptop. For safety reasons, the air supply can be cut off at any time using an emergency stop button.

The interfaces developed by Allievi *et al.*, 2013; Allievi *et al.*, 2014 are designed to fit the hand or the foot, with the same rationale so as to provide a similar pattern of stim-

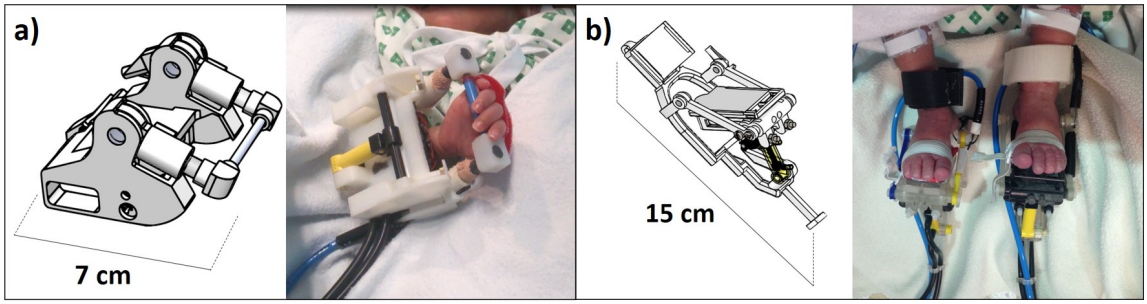

Figure 2.5: FMRI-compatible robotic interfaces for somatosensory stimulation: a) wrist and b) ankle. The devices can fit the small hand/feet of the newborn and produce the passive flexion and extension of the joint (wrist/ankle)

ulation and to be easily interchangable (figure 2.5). The devices have been carefully designed to be compatible with the anatomy and biomechanics of newborn limbs so that the range of motion is within the infant's capability. A combination of elastic bands and VELCRO®straps ensure that the device would stay in position throughout the experiment duration. Moreover, washable or single-use padding sits between the lib and the interface to improve the comfort of the subject. The motion is driven by a pneumatic piston which is expanded and compressed by two out of phase airwaves. The interfaces are fully made of plastic, with the body of the interface 3D printed and the driving piston a plastic piece produced by LEGO®.

Tactile stimulation of the lips

The mouth is an important body part as it covers a crucial role for eating and speaking. Whilst vocalisation is a skill that appears only after few months after birth, the newborn already possesses the sucking behaviour necessary for feeding immediately following birth. In keeping with the time-window of sensorimotor development in humans, the maturation process of oral-motor skills emerges in the perinatal period and preterm infants often have difficulties in oral feeding (Lau *et al.,* 2000). Oral-feeding performance is associated with the motor abilities of an infant and via sensory feedback coming from the mouth. Assessment of the functional processing of mouth stimulation in preterm infants is therefore particularly interesting in addition to the stimulation of other body parts. For this reason, the custom-made robotic stimulation device previously described was modified to

integrate mouth stimulation. To ease the multi-part stimulation of the infant, the mouth interface should be an additional interchangeable interface compatible with same control unit and pneumatic system.

Different computer-controlled systems for somatosensory stimulation of the lips have been used in adults fMRI studies using a balloon diaphragm attached to the lips (Schulz *et al.,* 2004) or air-puff delivered via nozzles mounted on the head coil of the scanner (Huang & Sereno, 2007). However, to attach a balloon diaphragm directly onto a baby's skin might be unsafe and cause distress to such a delicate body part. The air puff stimulation therefore seems to be a better option for the very young population, although there is a risk that the airflow is not consistently delivered at the right location if fixed to the scanner. During the fMRI session, there is little visibility of the infant's face and therefore any stimulus might be delivered at different locations if an infant moves during the image acquisition period. Another option suggested for neonates was to use an instrumented MR-compatible pacifier (Allievi *et al.,* 2014). Despite the targeted development of this technology and its great potential for infant fMRI, the robotic pacifier had two major drawbacks: the difficulty to keep the pacifier within the infant's mouth, and the induction of additional motion as a result of sucking behaviour. In keeping with this (which would require an elastic band which is inappropriate for ethical reasons), an alternative solution has been adopted here to deliver an air stimulus. A nasal cannula was identified as a suitable interface to deliver the desired stimulus (figure 2.6). The nasal cannula is a clinical device consisting of a lightweight tube that can fit around the baby's head and is used to deliver oxygen to the patient. The nasal cannula has two prongs that are normally inserted into the nostrils for breathing support, however if reoriented downwards, they can instead stimulate the mouth. Moreover, nasal cannula are commonly used in the hospital and therefore the clinical staff feels comfortable with its use. The mouth interface aims at delivering a gentle air puff precisely to the lips of the sleeping infant and ensuring that the device remains at the same location throughout the session without causing any distress.

The airflow was programmed to deliver blocks of a sinusoidal pattern of puffs, whilst avoiding habituation and preventing the lips to dry under constant flux. The mouth

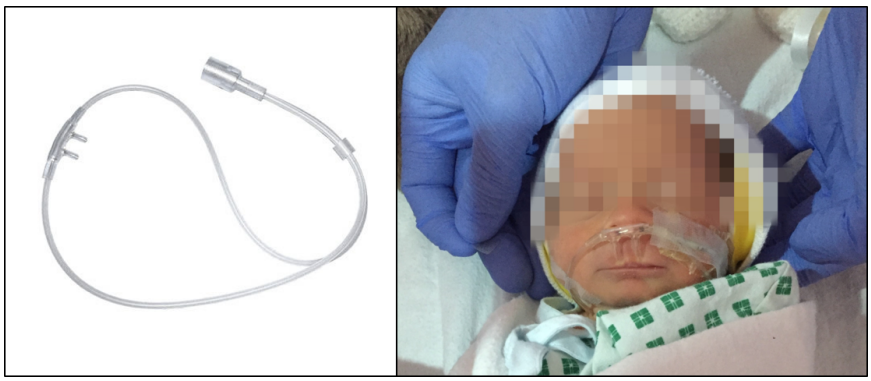

Figure 2.6: Clinical nasal cannula fitted around the baby's head and having the prongs directed towards the lips.

stimulator has been tested on adult subjects prior to any use on infant subjects. Importantly, different air pressure (0.4atm, 0.8atm, 1.2atm) and frequencies (0.2Hz, 0.5Hz) of delivery have been investigated to determine a stimulus strong enough to elicit a brain response yet gentle enough to limit distress. All the different combinations tested elicited a robust brain activation identifiable with the fMRI, however, the higher amplitude puffs were associated with more motion suggesting greater discomfort. This was confirmed by adult subjects who were able to detect an increase in pressure, whilst increases in frequency were almost imperceptible. Given that all stimulation parameters elicited a robust response, the lower pressure (0.4atm) was considered the best suited for the use of the stimulus with the newborn population.

In practice, the interfaces can all be fitted onto the subject and only the connecting pneumatic pipes and fibre optic are swapped in between sessions to stimulate the body part of interest. For the purpose of the topographic mapping of the preterm somatosensory cortex described in chapter 3, an identical block design was used for each stimulus type and consisted of a boxcar of 24 seconds "off" and 24 seconds "on", where the active period consisted of a sinusoidal pattern of movement or airflow directly to the lips (figure 2.7). The system can produce different paradigms by simply providing the required design as input matrix into the software.

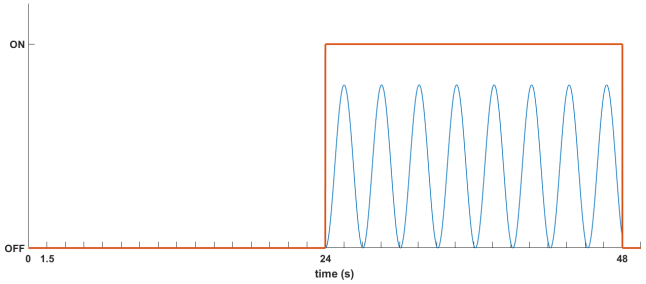

Figure 2.7: Block design selected for the task-fMRI experiment involving the different body parts stimulation. The TR=1.5s beats the time of periods task and rest 24 (both seconds long).

2.4.3 Auditory tasks inside the scanner

In chapter 5 I describe a study using an audio-motor classical conditioning paradigm to investigate learning mechanisms in newborn infants. In this experiment, an auditory cue was played in combination with the somatosensory stimulation provided by the previously described wrist device. A key feature of the study was therefore to identify a proper auditory stimulus to perform the task. Nowadays there are industrial solutions to deliver sound inside the scanner using MRI compatible headphones. The OptoActive^{TM}headphones used in the experiments have as an additional feature of actively attenuating most of the echo-planar imaging (EPI) gradient noise of the MRI scanner, thus improving the subject's experience (figure 2.8). Although playing the sounds through these headphones facilitates fMRI auditory studies, it remains a major challenge to identify the proper kind of stimuli given the loud environment. Information about the work invested in testing different sounds as a possible auditory cue is found in section 4.2.1.

Figure 2.8: OptoActive^{TM}active noise cancelling headphones http://www.optoacoustics.com

2.5 Conclusions

The development of novel technology has opened new windows of possibility for the investigation of brain function, by enabling task-based fMRI studies even in the youngest and most fragile populations like neonates. While resting-state fMRI is appealing to most for its ease and is often employed to study functional maturation in the developing brain, task-fMRI can address unique research questions. Given that early postnatal sensory experiences play a critical role in shaping brain development, it is imperative that we unveil the neurological mechanisms underlying sensory inputs processing. In this context, there is a compelling need to identify the normative sensory responses to environmental simulation in order to provide better care to newborns. Preterm infants in particular are exposed to an abnormal environment that might undermine their normal trajectory of development, as suggested by the higher prevalence of disabilities in those children born prematurely. It is therefore critical to assess preterm brain maturation from an early stage to better understand the risks they are exposed to, and potentially to identify neurodevelopmental pathology from as early as possible. In this view, I employed the techniques described in this chapter to assess the normative organisation of the somatosensory cortex in a group of preterm infants. In the next chapter, I describe an experiment **somatotopic mapping of the developing sensorimotor cortex in the preterm human brain** performed using the aforementioned technology-assisted fMRI methods.

"Understanding the complex structure of the brain and its intricate function is a daunting task. [...] Should we abandon the search for unlocking the mystery of the brain, or do we accept the challenge of searching for the truth with all the imagination that we can master?"

– Jayant P. Shenai –

3

Somatotopic mapping of the developing sensorimotor cortex in the preterm human brain

The work described in this chapter has been published in *Cerebral Cortex*, Volume 28, Issue 7, July 2018, Pages 2507–2515, https://doi.org/10.1093/cercor/bhy050 (Dall'Orso *et al.,* 2018)

Abstract

In the mature mammalian brain, the primary somatosensory and motor cortices are known to be spatially organised such that neural activity relating to specific body parts can be somatopically mapped onto an anatomical "homunculus". This organisation creates an internal body representation which is fundamental for precise motor control, spatial awareness and social interaction. Although it is unknown when this organisation develops in humans, animal studies suggest that it may emerge even before the time of normal birth. We therefore characterised the somatotopic organisation of the primary sensorimotor cortices using functional MRI and a set of custom-made robotic tools in 35 healthy preterm infants aged from 31 + 6 to 36 + 3 weeks postmenstrual age. Functional responses induced by somatosensory stimulation of the wrists, ankles, and mouth had a distinct spatial organisation as seen in the characteristic mature homunculus map. In comparison to the ankle, activation related to wrist stimulation was significantly larger and more commonly involved additional areas including the supplementary motor area and ipsilateral sensorimotor cortex. These results are in keeping with early intrinsic determination of a somatotopic map within the primary sensorimotor cortices. This may explain why acquired brain injury in this region during the preterm period cannot be compensated for by cortical reorganisation and therefore can lead to long-lasting motor and sensory impairment.

Acknowledgements and contributions

Dr. Tomoki Arichi and I were involved in all aspects of the study including study design, data collection, data analysis and interpretation, and manuscript preparation. Dr. Johannes Steinweg was involved in data collection and interpretation. Dr. Alessandro G. Allievi, Prof. A. David Edwards and Prof. Etienne Burdet were involved in study design and data interpretation. All authors reviewed and contributed to manuscript preparation.

I thank the patients and families who kindly agreed to participate in this work and our clinical colleagues in the Evelina Newborn Imaging Centre and the Neonatal Intensive Care Unit at St Thomas' Hospital London.

3.1 Introduction

In the mammalian brain, the anatomical connections and neural activity of the primary sensorimotor cortices (comprising the primary motor (M1) and somatosensory cortices (S1)) are known to be functionally organised, such that information relating to a specific body part is processed in a distinct area within the contralateral cerebral hemisphere (Penfield & Boldrey, 1937). Whilst there are subtle differences between M1 and S1, the general principles of this organisation can be applied to both and are often pictorially represented in the classic cortical "homunculus" map; in which inferior body parts such as the feet are represented superiorly in the sensorimotor cortices (adjacent to the brain's midline), whilst more superior body parts such as the hands and mouth are represented lower and more laterally. Body parts are also known to be disproportionately represented within the somatotopic map relative to their anatomical size, with highly innervated structures such as the mouth or fingers taking up a larger cortical area in comparison to other body regions like the trunk and legs. The resulting cortical map is thought to provide the framework for the brain's internal body representation, thus allowing it to encode position, accurately perform motor tasks, and socially process the motor behaviour and body position of others (Marshall & Meltzoff, 2015).

Small animal studies suggest that a whole body topographical map emerges within the sensorimotor cortices during the equivalent period to the human late third trimester and early infancy (Seelke *et al.,* 2012). This process is thought to be initially driven by genetic factors and feedback from spontaneously generated peripheral neural activity which activates both the primary motor and somatosensory cortices, with later experience-dependent mechanisms refining the cortical map and moulding the local cortical network (Florence *et al.,* 1996; Khazipov *et al.,* 2004). The critical importance of this specific period can be readily seen in studies of sensory deprivation which result in permanent alterations of S1 organisation and function (Fox, 1992). It is possible that this period may be similarly crucial in human infancy for the long-term development and organisation of the sensorimotor cortex. This may partly explain why preterm birth (delivery less than

37 weeks gestation) engenders a significant increase in the risk of developing motor and somatosensory dysfunction, even in the absence of overt brain injury (Larroque *et al.,* 2008; Williams *et al.,* 2010; Setänen *et al.,* 2016).

In recent years, Blood Oxygen Level Dependent (BOLD) contrast functional Magnetic Resonance Imaging (fMRI) has been successfully used to noninvasively characterise the cortical homunculus map of the mature human brain (Stippich *et al.,* 1999; Moore *et al.,* 2000; Blatow *et al.,* 2007). These studies have confirmed that the topographical organisation is highly reproducible and stable across adult populations, and have also demonstrated that fMRI has high enough sensitivity and specificity to even characterise the somatotopic map of each individual finger (Schweizer & Frahm, 2009; Martuzzi *et al.,* 2014). We have also previously shown that the combination of fMRI and custom-made robotic stimulation devices can be used to precisely map somatosensory responses in the developing sensorimotor cortex across the human preterm period (Arichi *et al.,* 2010; Arichi *et al.,* 2012; Allievi *et al.,* 2016). These studies have further highlighted the importance of this juncture for the developing sensorimotor system, as somatosensory functional responses were found to rapidly mature in preterm infants up to term equivalent age with increasing integration of activity in distinct structures such as the ipsilateral sensorimotor cortex and supplementary motor area (SMA) (Allievi *et al.,* 2016). In addition, this maturation was found to be experience dependent with increased inter-hemispheric functional connectivity significantly correlated to greater post-natal age.

In this study, we aimed to use fMRI and a set of robotic tools for stimulating the wrists, ankles, and mouth to see whether functional responses could be somatotopically mapped in a cohort of healthy preterm infants. As our previous work has shown that functional responses in preterm infants increase their spatial specificity with maturity and occur concurrently in the primary motor and somatosensory cortices (Allievi *et al.,* 2016), and recent evidence suggests that activity patterns in the mature sensorimotor cortex are flexibly arranged by exposure to everyday motor behaviour (Ejaz *et al.,* 2015); one possible hypothesis was that functional responses in our population would not be topographically organised. In contrast, in the context of animal studies, the alternative hypothesis

was that induced responses would already be topographically organised into a cortical homunculus map even before the time of normal birth.

3.2 Methods

The study was approved by the NHS research ethics committee and written parental consent was obtained prior to MRI/fMRI data acquisition.

3.2.1 Study population

The study population consisted of 35 preterm infants (GA at birth range: 26+0 to 36+1 weeks+days; PMA at the time of study range: 31+6 to 36+3 weeks+days) recruited from the Neonatal Intensive Care Unit (NICU) or postnatal wards of St Thomas' Hospital, London, UK (demographic details of each infant can be found in table 3.1). All of the infants were healthy at the time of scanning and did not require any respiratory support during data acquisition. Infants were excluded from the study group if they were known to have a neurological disease or injury such as focal brain injury, a diagnosed congenital brain abnormality, and/or a clinical history of birth asphyxia or neonatal encephalopathy.

Body part group	n	GA at birth in weeks median (range)	Birth weight in grams median (range)	PMA at scan in weeks median (range)
Left ankle	10	34+2 (28+3 – 36+1)	1850 (1120 – 3110)	35+2 (33+6 – 36+3)
Left wrist	10	32+3 (26+3 – 34+5)	1930 (840 – 2330)	34+2 (33+0 – 35+3)
Right ankle	9	33+3 (28+5 – 35+4)	2100 (1340 – 3110)	34+4 (31+6 – 36+3)
Right wrist	10	32+4 (29+1 – 35+6)	1680 (1330-2100)	34+2 (33+3 – 36+1)
Mouth	10	34+1 (30+4 – 35+4)	1980 (1440 – 3110)	35+1 (32+3 – 36+3)

Table 3.1: Demographic information of the final study population for each stimulus type. GA= gestational age at birth in weeks; PMA= Post Menstrual Age at scan in weeks

.

3.2.2 Data acquisition

All infants were studied during natural sleep immediately following feeding, were swaddled in a blanket and then immobilised using a vacuum evacuated bag (*Med-Vac, CFI Medical Solutions, Fenton, MI USA*). Moulded dental putty was placed in the external auditory meatus (*President Putty, Coltene Whaledent, Mahwah, NJ USA*) and adhesive earmuffs (*MiniMuffs, Natus Medical Inc., San Carlos, CA USA*) were applied in all infants to attenuate MR scanner noise. All data collection sessions were attended by a clinician (doctor or nurse) trained in neonatal resuscitation and physiological parameters (oxygen saturations, heart rate and axillary temperature) were monitored throughout. All infants studied tolerated the study protocol well and there were no adverse events during the entire study period.

Data acquisition was performed using a 3-Tesla MRI scanner (*Philips Achieva, Best, Netherlands*) located on the NICU at St Thomas Hospital. BOLD contrast fMRI images were acquired with a 32 channel head coil and an EPI sequence using the following parameters: TR/TE/FA=1500 ms/45 ms/90; resolution(x/y/z) = 2.5/2.5/3.25 mm; slice gap = 0.75 mm; non-interleaved ascending slice acquisition order; 22 slices; 256 total volumes (total time: 6 min and 34 s). For clinical reporting and image registration purposes, high resolution structural T1-weighted and T2-weighted images were also acquired for all infants studied.

A set of dedicated MR compatible robotic devices were used to induce a safe and reproducible pattern of somatosensory stimulation to different body parts across our study population (Allievi *et al.,* 2013; Allievi *et al.,* 2014). These devices were custom designed and made using 3D printing to specifically fit the ankles and wrists of preterm infants (figure 3.1). Joint flexion/extension at a frequency of 0.3Hz was achieved via a pneumatically piston driven by the hospital pressurised air supply, which was computer-controlled from the MR scanner control room and synchronised with image acquisition. For detailed description of the wrist and ankle robotic devices please refer to (Arichi *et al.,* 2010; Allievi *et al.,* 2013). To provide a somatosensory stimulus to the mouth, we repurposed clinical

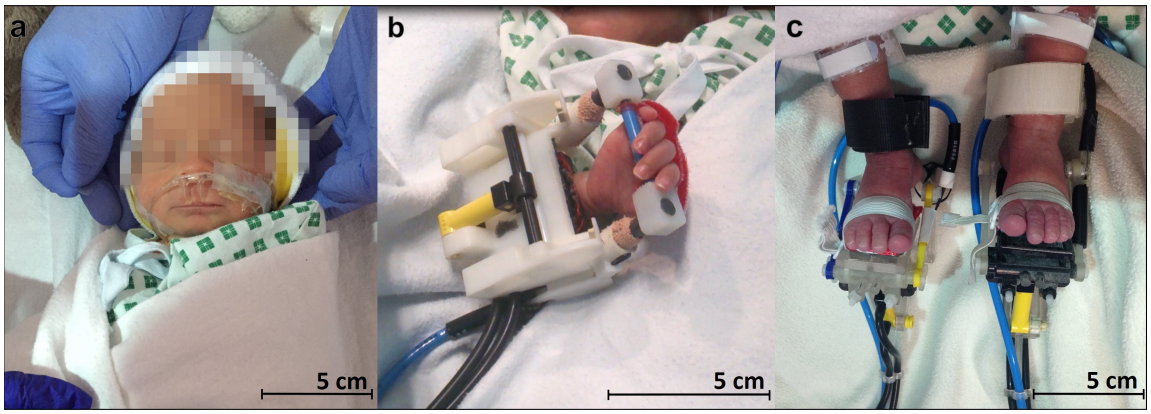

Figure 3.1: MRI-compatible automated devices used for sensory stimulation. A soft puff of air was delivered to the mouth via inverted clinical nasal cannula (a), while pressurised air was used to actuate the yellow piston in the robotic devices resulting in controlled flexion and extension movements of the wrist (b) and ankle (c).

nasal cannulae which are usually used to provide supplemental oxygen therapy. Nasal cannulae were chosen so as to minimise the amount of equipment attached to the infant's face (and thus prevent discomfort) and to ensure that clinical infection control measures were followed with single-use equipment. The cannulae were fit around the baby's head but with the prongs orientated downwards so that a gentle puff of air (0.4 atm at 0.3Hz) could be delivered to the area between the nose and lips. The pattern of stimulation, timing and amplitude of all patterns of stimulation were constantly monitored on a user interface displayed on a PC connected to the control box (*Labview, National Instruments, Austin, TX USA*). Every experiment consisted of an identical "on-off" block paradigm in which a single stimulus type was presented (i.e., only one joint was stimulated at a time across the entire run). Each of the five experiments (stimulating either the left or right wrist, the left or right ankle, or mouth) consisted of a total of 8 blocks containing 24s of stimulation interleaved with 24s of rest. A given infant in the study population was involved in a maximum of four experiments with a different type of stimulation, which were chosen at random prior to data collection inside the MRI scanner (full details of each infant can be seen in table 3.2).

3.2.3 Data analysis

fMRI data analysis was performed using tools implemented in FMRIB's Software Library (FSL, www.fmrib.ox.ac.uk/fsl) (Smith *et al.,* 2004). The raw images were first visually assessed for evidence of severe image artefacts or a large amount of head motion which would not be amenable to correction and data was discarded accordingly. Head motion was quantified from displacement parameters derived from rigid body head realignment to the reference (centre) volume and the calculation of the Root Mean Square (RMS) intensity difference of volume N to the reference. Corrupted data points were dealt with by deleting contiguous blocks of data if the absolute displacement during a volume exceeded 1.25mm (equal to half the in-plane resolution); and by using the RMS intensity difference metric to define a binary confound regressor for the later general linear model (GLM) analysis (akin to "motion scrubbing" (Power *et al.,* 2012)). Raw data were then pre-processed using an optimised pipeline for neonatal subjects implemented in FEAT (FSL's Expert Analysis Tool v5.98), consisting of slice time correction, high pass filtering (cut-off 50s), non-brain tissue removal using BET (brain extraction tool), global intensity normalisation and spatial smoothing (Gaussian filter of 5mm FWHM) (Arichi *et al.,* 2010). Additional data denoising was performed using independent component analysis (ICA) to remove signal artefacts related to the non-linear effects of head motion and physiological effects such as cardiovascular pulsation and respiratory movements (Beckmann *et al.,* 2005). A univariate (voxel-wise) analysis was then performed using the GLM, with the stimulation paradigm convolved with an optimised set of basis functions derived from an age-specific haemodynamic response function (HRF) (Arichi *et al.,* 2012)). To further deal with the possible confounding effects of head motion, additional confound regressors were also included in the GLM analysis including extended head motion parameters (head translation and rotation, their squares, the derivatives, and the square of the derivatives) and the binary regressors derived from the first stage of pre-processing. The resulting t-statistical images were converted to a normally distributed z-statistical image and a threshold of 2.3 (with a corrected cluster significance level of $p<0.05$) was defined to generate individual subject activation maps.

Lower level functional activation maps were then registered to the subject's own high resolution T2-image using rigid-body registration and then to an age-specific template brain (Serag *et al.,* 2012) using a non-linear registration. Group analysis (controlling for gestational age at birth and PMA at scan) was then performed separately for each of the body areas stimulated using a nonparametric one-sample t-test implemented with permutation methods and threshold free cluster enhancement (TFCE) (family wise error (FWE) corrected $p<0.05$) using Randomise (v2.0)(Nichols & Hayasaka, 2003; Smith & Nichols, 2009). For the final characterisation of the somatotopic map of functional responses, only the main cluster within the sensorimotor cortices was considered, therefore additional areas of activation such as within the insulae following mouth stimulation were not included. Group response maps were thresholded ($p=0.05$) and combined together using a "winner-takes-all" approach, so that voxels containing overlapping functional responses were assigned to the dominant cluster. The final results of these group analyses were then projected for visualisation onto the inflated cortical surface of an age-appropriate template brain using MIRTK (`mirtk.github.io`).

3.3 Results

Data was successfully collected in 49/68 experimental sessions following discard of data corrupted by excessive head motion or image artefact. Successful data was collected in 10 of 17 subjects with left ankle somatosensory stimulation (median PMA: 35+2 weeks; range: 33+6 - 36+3 weeks); 9 of 14 subjects with right ankle stimulation (median PMA: 34+4 weeks; range: 31+6 - 36+3 weeks); 10 of 12 subjects with left wrist stimulation (mean PMA: 34+2 weeks; range: 33+0 - 35+3 weeks); 10 of 12 subjects with right wrist stimulation (median PMA: 34+2 weeks; range: 33+3 - 36+1 weeks); and 10 of 13 subjects who received stimulation of the mouth (median PMA: 35+1 weeks; range: 32+3 to 36+3 weeks) (demographic information of the included study population is reported in table 3.1). All of the infants were reported as having a normal brain appearance on their structural images. All of the infants were reported as having appropriate brain appearances

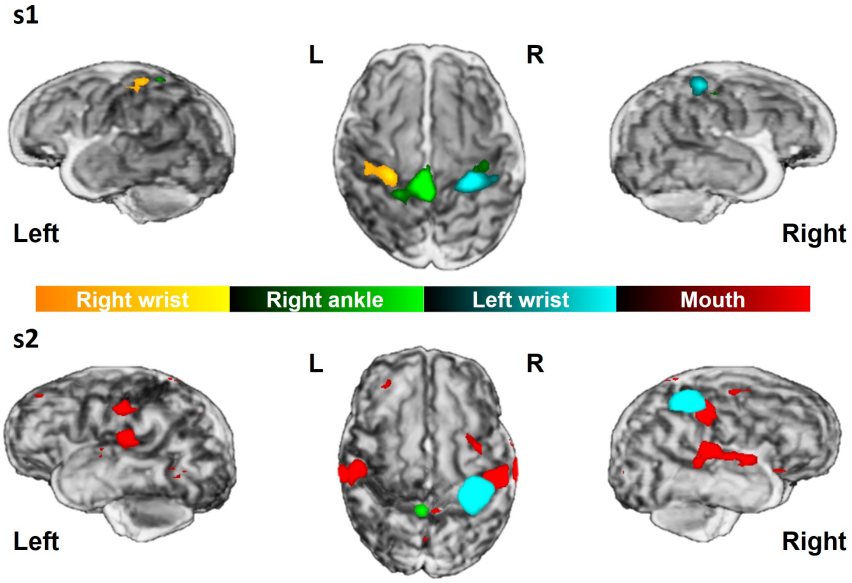

Figure 3.2: Representative functional responses in two subjects scanned at 33+6 weeks PMA (s1) and 35+3 weeks (s2). Single subject results show distinct significant clusters of functional activation (thresholded at z=2.3) following stimulation of different body parts overlaid on the subject's own 3D rendered T2-weigthed image.

on their structural images. Four of the infants had unilateral grade 1 intraventricular haemorrhage (IVH) and 3 of the infants had a small number of punctate white matter lesions (see table 3.2 in supplementary information).

In all subjects, passive movement of a single joint resulted in a significant cluster of positive BOLD response in a localised area within the sensorimotor cortex spanning both S1 and M1 across the central sulcus contralateral to the body part stimulated (figure 3.2). As seen in the mature somatotopic "homunculus" map, clusters of functional activation relating to ankle movement were located superiorly to those of the wrist which were located on the superior medial portion of the central sulcus "hand-knob" (Yousry *et al.,* 1997; Hlustik *et al.,* 2001). In addition, wrist stimulation induced significantly larger clusters of functional activation (median volume: $2737.33mm^3$; range: 478.54 – $11306.65mm^3$) in comparison to those following ankle stimulation (median volume: $1208.41mm^3$; range:

$252.6 - 17209.08mm^3$) (Wilcoxon rank sum test, p=0.0151). Somatosensory stimulation of the mouth induced a bilateral pattern of functional activity which was situated inferiorly and laterally to the wrist response within the sensorimotor cortex.

Activation following wrist stimulation was also seen in some infants within the ipsilateral sensorimotor cortex (8/20, 5 subjects in the right wrist group and 3 in the left wrist group) and supplementary motor area (SMA) (10/20, half of the subjects in each group). In contrast, SMA activation following ankle stimulation was seen in less subjects (5/19) compared to wrist. Clusters of identified activity for a given side of stimulation (i.e. the right wrist) appeared to be symmetrical with those seen following stimulation of the opposite side (i.e. the left wrist). Of interest, when clusters of ipsilateral activity were seen, they were located in an overlapping region to that of the primary response cluster to stimulation of the same limb on the opposite side, suggesting that this activity was occurring in its functional homologous within the ipsilateral hemisphere. However at a group level, functional clusters in the ipsilateral hemisphere and supplementary motor area did not reach significance for any of the individual limb stimulation groups (figure 3.3). Mouth stimulation was also associated with additional clusters of activity in the insular cortices and SMA (figure 3.4).

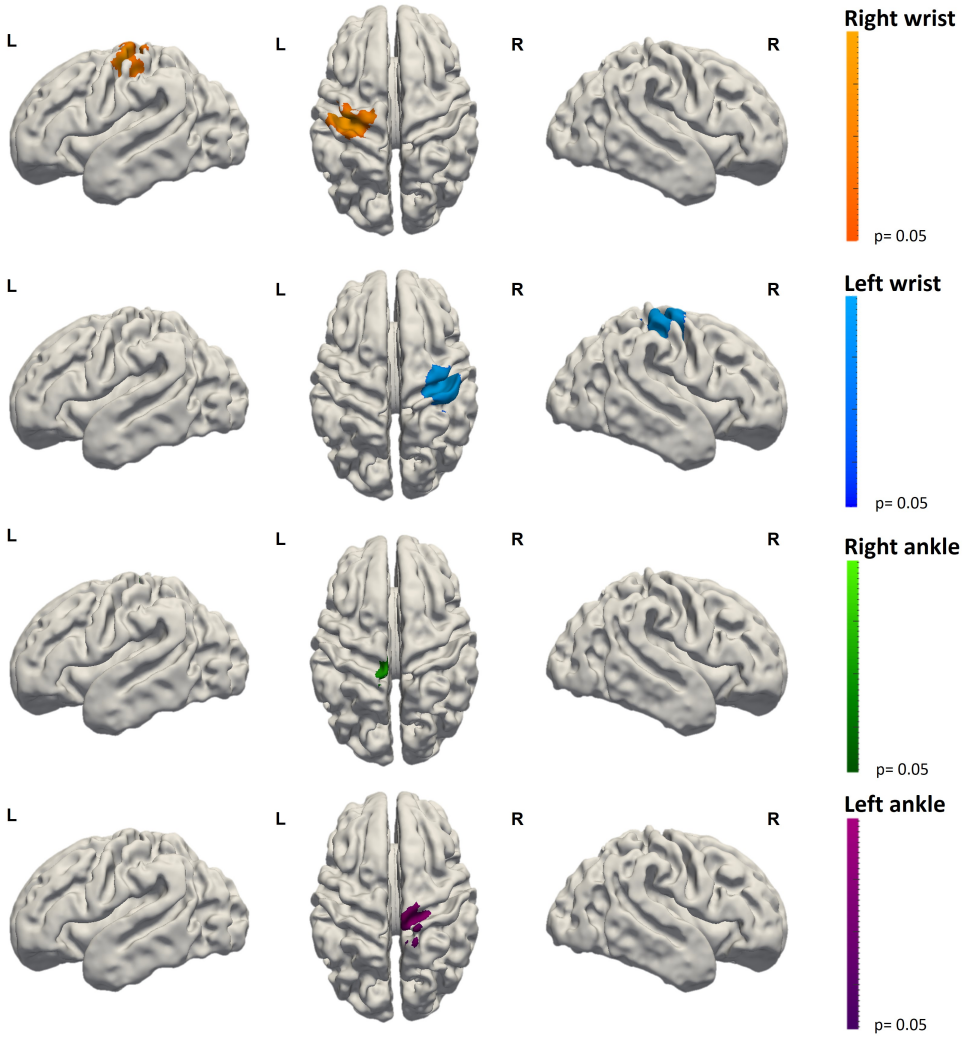

Figure 3.3: Functional responses resulting from the group analysis following somatosensory stimulation of the left ankle (n=10), left wrist (n=10), right wrist (n=10), and right ankle (n=9). Well localised distinct clusters of activation can be seen within the contralateral sensorimotor cortex across the central sulcus. Images show the results of one-sample non-parametric t-tests ($p<0.05$ corrected for family wise error) projected onto the grey-white matter boundary of a 34 week PMA template brain.

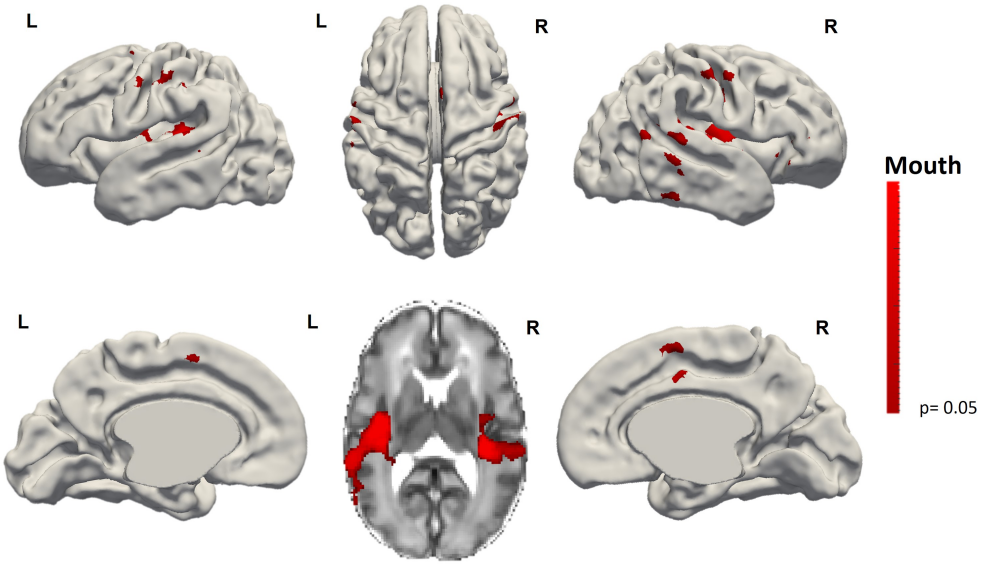

Figure 3.4: Result of the group analysis of functional responses following mouth stimulation (n=10). Clusters of activation can be seen within the bilateral sensorimotor cortices. Additional clusters of activation were also seen in the midline Supplementary Motor Area (SMA) (lower row left and right figures) and bilaterally within the insulae (lower row, center image). Images show the results of one-sample non-parametric t-test ($p<0.05$ corrected for family wise error) projected onto the grey-white matter boundary of a 34 week PMA template brain.

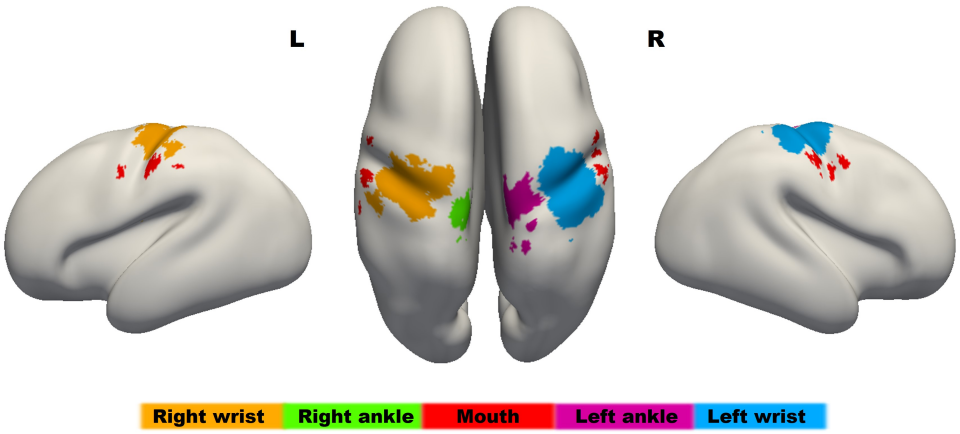

Figure 3.5: The sensorimotor homunculus in the preterm human brain at 34 weeks PMA. The map has been overlaid onto an age-specific inflated brain template using a "winner-takes-all" approach after combing the significant results of the group level activation maps from each stimulated body part. In agreement with the well characterised adult somatotopic map, functional activity relating to the ankles (green and purple) is located superiorly to those of the wrist (orange and blue) and mouth (red). This map is publically available for download from brain-development.org.

Distinct localisation of functional responses following stimulation of different body parts into a somatotopic representation could be clearly appreciated when combined into a single "homunculus" map (figure 3.5). As has been characteristically described in the adult topography, clusters of activation corresponding to the somatosensory stimulation of the ankle were identified superiorly and adjacent to the midline within the sensorimotor cortices; clusters corresponding to stimulation of the wrist were located infero-laterally to those of the ankle; and clusters relating to mouth stimulation were located inferior and lateral to those of the wrist.

3.4 Discussion

Using fMRI and specific patterns of precisely controlled somatosensory stimulation, we have been able to carry out the most detailed characterisation to date of cortical somatotopy in the preterm human brain. Our results demonstrate that there is a clear correspondence between sensory information related to distinct body parts and specific areas within the developing sensorimotor cortex even before term equivalent age. The

topography of the identified cortical representation closely resembles that of the well described "homunculus" map of the mature brain, with inferior body parts mapping to the superior cortex and highly innervated body regions disproportionately mapping to larger area of cortex relative to their physical size (Penfield & Boldrey, 1937).

Functional specialisation has long been recognised as a hallmark feature of the brain ever since it was first identified that the cortex could be histologically parcellated on the basis of its cytoarchitectonic features (Brodmann, 1909). Within this framework, function within a given cortical region is tightly constrained by its anatomical microstructure and the underlying pattern of its structural connections (Passingham *et al.,* 2002). Imaging methods have since made it possible to confirm the specific roles of the primary sensory cortices and have enabled precise mapping of their receptive fields thus enabling a new understanding of their functional organisation (Blankenburg *et al.,* 2003; Wandell *et al.,* 2007). This has included several studies which have characterised a topographical map in both S1 and M1 which is largely in agreement with Penfield's classical homunculus, including its two areas of major discontinuity (between the hands and the feet in both S1 and M1; and the feet and the genitalia in S1 only) (Nakamura *et al.,* 1998; Kocak *et al.,* 2009; Heed & Röder, 2010; Parpia, 2011). This kind of topographical organisation is thought to have evolved to provide an optimal substrate for efficient neural processing within the geometric, biophysical, and energy constraints of the brain (Laughlin, 2003) and facilitates social interaction by enabling registration of correspondence in body position and behaviour between self and others (Marshall & Meltzoff, 2015).

Whilst a relatively precise correspondence between functional and architectonic parcellation of areas such as S1 can be readily seen in a mature brain, the factors which underlie its ontogeny remains unclear (Parpia, 2011). One possibility is that of a cortical "protomap" whereby the location and function of neurons are controlled initially by genetic factors which mediate spatially specific molecular signalling within neural progenitor cells (Rakic, 1988). In contrast, it has also been suggested that neuronal function within an initially homogeneous cortex is defined by afferent thalamic inputs and activity-dependent mechanisms through early environmental influences (Sur & Rubenstein, 2005). Our results

and those of developmental animal studies suggest that both factors contribute together at different but overlapping times, as architectonic maps (including a putative barrel cortex) appear to emerge within S1 as early as the embryonic stage, whilst topographic functional maps do not develop until much later in postnatal life (Seelke *et al.,* 2012). Distinct but not topographically organised body part representation can be seen in the S1 of rats as early as P5-10, before more precise organisation emerges during the subsequent period leading up to P15, and an adult-like pattern is eventually established by P20 (Seelke *et al.,* 2012). This initial mismatch between cytoarchitecture and function therefore supports a switch from genetically driven mechanisms to a subsequent activity driven cortical refinement process which is influenced by the establishment of thalamic connectivity as suggested by the radial-unit hypothesis (Rakic, 1988). In agreement with this, very early genetic alteration during gestation yields an aberrant architectonic map (Fukuchi-Shimogori & Grove, 2001; Ragsdale & Grove, 2001), whilst later abnormal afferent information significantly alters functional maps but not the anatomical location of S1 (Fox, 1992; Feldman & Brecht, 2005).

In the last trimester of human gestation ascending thalamo-cortical axonal pathways and cortico-cortical axons grow through the transient subplate layer and establish the cortex's lifelong framework of connectivity (Florence *et al.,* 1996; Pallas, 2001; López-Bendito & Molnár, 2003). By the latter stages of the preterm period (>33 weeks PMA), the subplate decreases in thickness particularly in the parietal lobes (more so than in the temporal or frontal lobes) as these longer afferent pathways connect into the cortical plate allowing activity-dependent elaboration and refinement of the initial topographical map (López-Bendito & Molnár, 2003; Kostović & Jovanov-Milošević, 2006; Perkins *et al.,* 2008). Therefore whilst the underlying cytoarchitecture and functional role of the sensorimotor cortices is already established, ex-utero experience during the preterm period could potentially influence the further development of precise cortical topographical maps (Allievi *et al.,* 2016). This may explain in part why preterm birth and specifically perinatal sensorimotor network injury markedly increases the risk of developing conditions such as cerebral palsy which are associated with long term sensory and motor impairment

(Fawke, 2007; Larroque *et al.,* 2008; Williams *et al.,* 2010; Arichi *et al.,* 2014). Whilst previous work has found that afferent thalamo-cortical pathways can grow around areas of brain injury acquired in the preterm period (Staudt *et al.,* 2004; Arichi *et al.,* 2014), our results provide essential neonatal validation of studies in older children and young adults which have found that perinatal damage to the primary somatosensory cortex cannot be compensated for through neuroplasticity or cerebral reorganisation (Juenger *et al.,* 2011).

In keeping with previous studies in both preterm infants and equivalent animal models, we saw that peripheral somatosensory stimulation induced clear patterns of functional activity across the contralateral peri-rolandic region encompassing both M1 and S1 (Khazipov *et al.,* 2004; An *et al.,* 2014; Allievi *et al.,* 2016). This seemingly concurrent activity is thought to occur through numerous direct cortico-cortical connections between M1 and S1 (Farkas *et al.,* 1999; Ghosh *et al.,* 2010; An *et al.,* 2014). During early life, this connectivity pathway is of particular importance as sensory feedback from peripherally generated spontaneous limb movements are thought to play a crucial role in the early development and refinement of the immature motor cortex (Khazipov *et al.,* 2004; Yang *et al.,* 2009; An *et al.,* 2014). Additional functional activity in the ipsilateral sensorimotor cortex and SMA were also seen in a subset of patients, predominately following stimulation of the wrist and mouth. This is in agreement with our previous work which found a wider pattern of functional response with increasing age (Wang *et al.,* 2007; Allievi *et al.,* 2016). Our finding that ankle stimulation responses occur predominately in the contralateral sensorimotor cortex and without involvement of the SMA suggest that maturation of this dispersed network response may occur with different trajectories for distinct body parts, perhaps corresponding to different levels of sensory experience or an intrinsic mechanism which predisposes these regions to allow complex motor behaviour such as sucking or grasping soon after birth.

In addition to localisation of functional responses following limb stimulation, we were also able to identify further inferior and lateral clusters of bilateral functional activity within the primary sensorimotor cortices and insulae, as well as the SMA following somatosensory stimulation of the mouth. These findings are in keeping with adult fMRI studies which

have demonstrated that the human oral area is densely innervated with a wide network of functional connections to other distinct areas across the cortex (Stippich *et al.,* 1999; Miyamoto *et al.,* 2005). The insula is involved in the elaboration of a wide variety of sensory processes (Penfield & Faulk, 1955) including pain, thermal coding, gustatory sensation, and intraoral somatosensory processing (Zald & Pardo, 2000). Whilst there were differences in our study with respect to the type of stimulus presented to the mouth (predominately tactile) and limbs (both tactile and proprioceptive), this distinction is likely to be of less significance as both types of stimuli are communicated within a final common thalamo-cortical pathway to the primary sensorimotor cortex where processing is not modality-specific during the preterm period (Fabrizi *et al.,* 2011). SMA activation may also be partly explained by the essential role of tactile sensation in and around the mouth in early human life to elicit sucking activity.

Taken together, our results suggest that in the late preterm period, maturing patterns of connectivity acting on a genetically determined sensorimotor "protomap" are shaping the size of the pre-determined somatotopic functional areas and establishing their wider patterns of network activity. It will therefore be crucial to next study how this connectivity is maturing in both a functional and structural sense using measures such as those derived from other complementary methods such as diffusion MRI. With this in mind, we will make the homunculus map publically available for download (`http://brain-development.org/`). It is also important to consider that we cannot definitively extrapolate our findings to the foetal sensorimotor system development and therefore it will be vital to study how this putative homunculus topographic map compares to that of infants delivered at full term gestation, how it evolves throughout later infancy and how it may be altered by specific patterns of brain injury.

3.5 Conclusions

In the human preterm period, functional activity within the sensorimotor cortices is already somatotopically organised in a pattern similar to the classic mature "homunculus"

representation. This result suggests that as described in animal models, the establishment of this organisation is first driven by genetic factors ready for later elaboration through experience-driven changes in connectivity. Given that preterm infants are constantly exposed to entirely different sensory experiences in the ex-utero environment, our findings further emphasize that the human preterm period may represent a critical window of vulnerability for altered sensorimotor cortex development, which may explain the high incidence of functional motor and sensory difficulties in this population.

Funding

The authors acknowledge support from the Department of Health via the National Institute for Health Research (NIHR) comprehensive Biomedical Research Centre award to Guy's St Thomas' NHS Foundation Trust in partnership with King's College London and King's College Hospital NHS Foundation Trust, and the Wellcome Engineering and Physical Sciences Research Council (EPSRC) Centre for Medical Engineering at King's College London [WT 203148/Z/16/Z]. SD was supported in part by the Engineering and Physical Sciences Research Council [grant number EP/L016737/1]. TA was supported by a NIHR Clinical lectureship and a Medical Research Council (MRC) Clinician Scientist Fellowship [MR/P008712/1]. EB and device development were supported in part by the EU-FP7 grants PEOPLE-ITN-317488-CONTEST, ICT-601003 BALANCE, ICT-611626 SYMBITRON, H2020 ICT-644727 COGIMON and UK EPSRC MOTION grant EP/NO29003/1.

Supplementary information

Subj.	GA	PMA	HC	W (g)	Stimuli received	Clinical MRI appearance
1	34+0	35+4	28.7	1550	RW	27 normal
2	31+3	33+3	31.1	1410	RW	normal
3	29+1	34+1	30	1570	RW	grade 1 IVH
4	33+3	34+4	29.5	1960	RA,RW	6 sunctate lepions
5	32+0	33+0	30.0	1930	RA,RW	normal
6	28+5	31+6	26.0	1280	RA	normal
7	32+2	34+1	31.0	2010	RA,RW	grade 1 IVH
8	34+1	35+4	32.0	1950	LA	normal
9	26+0	33+6	31.0	1580	LW	normal
10	32+6	33+3	32.0	1870	RW	normal
11	31+4	34+1	29.2	1670	RW	normal
12	32+2	34+4	28.0	1645	RW	normal
13	35+3	36+1	31.0	1890	RW	2 punctate lesions & grade 1IVH
14	35+6	36+1	30.5	1700	RW	normal
15	33+4	34+3	29.5	1684	RW	normal
16	36+1	36+3	30.0	2380	LA,LW	normal
17	28+3	34+4	30.5	2260	LA,RW,LW	normal
18	28+3	34+4	30.0	1840	LW	Grade 1 IVH, mild eaetral vlntricular asymmetry
19	32+4	33+6	29.4	1690	RA,RW,LW	normal
20	32+4	33+6	28.0	1590	LA,LW	normal
21	33+2	34+5	31.5	2250	LA,LW	normal
22	34+4	35+0	31.0	2000	LA,RA,RW	normal
23	34+5	35+3	30.0	1840	LA,RA,LW,M	normal
24	32+5	33+6	30.0	1710	LA,RA,LW,M	normal
25	35+1	35+4	30.0	2170	LA,RA,M	normal
26	34+3	35+1	29.5	1600	LA,RA,M	normal
27	34+3	35+2	29.0	1500	LA,RA,M	normal
28	35+4	36+3	35.0	2715	LA,RA,M	normal
29	30+4	32+3	28.0	1345	LA,RA,M	5 punctate lesions
30	35+3	35+5	32.5	2680	LA,RA,M	normal
31	35+1	35+3	34.0	2550	LA,M	normal
32	33+2	33+6	31.7	1910	LA,M	normal
33	33+4	35+1	32.0	2400	M	normal
34	33+1	34+4	28.0	1450	LA,M	normal
35	33+6	34+2	31.0	1860	M	normal

Table 3.2: Supplementary table: Demographic information of the recruited study population and the stimulus type received. GA= gestational age at birth in weeks + days; PMA= Post Menstrual Age at scan in weeks + days; HC= Head circumference at scan in cm; W= Weight at scan in grams; RW= right wrist, RA= right ankle, LA= left ankle; LW= left wrist; M=mouth; IVH= intraventricular haemorrhage

"Science is a refinement of everyday thinking"

– Albert Einstein –

4

Optimisation of an associative learning paradigm task for fMRI

The previous chapter presented evidence suggesting that the brain's fundamental sensorimotor functional organisation is already in place in infants born preterm and by the time of normal birth. This knowledge is in keeping with the idea that preterm infants are in a vulnerable period and might explain why neuroplasticity cannot compensate for perinatal brain injury which therefore results in motor impairment. While the foundation of somatotopy is already established early in development, activity-dependent mechanisms during this period are believed to drive functional maturation and potentially refine the "protomap" through sensory feedback. It is therefore important that we understand how functional maturation can be manipulated by ex-utero sensory experience. In this context, a key step will be to identify the adaptive brain mechanisms characteristic to early

postnatal life that are triggered by the dynamic and stimuli-rich environment. Associative learning is a basic adaptive process that newborn infants have been shown to use in classical conditioning experiments. While there is numerous behavioural evidence showing that newborn infants are capable of learning the association between multi-sensory stimuli, little is known about the underlying brain processes. Thanks to task-fMRI it is possible to shed light into the neural activity corresponding to specific sensory experiences, though translating the current adult experimental protocols to neonates is challenging. To investigate the neural correlates of associative learning in the newborn brain, I therefore developed a classical conditioning task suitable for fMRI experiments with neonates.

4.1 Classical conditioning paradigm characteristics

Classical conditioning paradigms have been used for over fifty years as a model to investigate the newborn's capability to learn and the underlying neural process (Siqueland & Lipsitt, 1966; Reeb-Sutherland & Fox, 2015). Typically, an *unconditioned stimulus* (US) is presented several times associated with a *conditioned stimulus* (CS) that acts as a predictive cue for the occurrence of the US. Learning studies aim to study the emergence of a *conditioned response* (CR) following the CS which thus represents the learnt association between this and the US. Depending on the specific research question, different methodological considerations and decisions may apply, resulting in a daunting number of possible experimental designs. The majority of published studies have adopted different types of CSs, such as visual, auditory, tactile, taste or olfactory cues, as well as different types of stimuli for the US, including tactile, auditory, visual, taste and odour. Depending on the specific questions and/or type of learning, these stimuli have been employed as a pleasant stimulus (e.g. a caress, mother's voice) or painful stimulus (e.g. puff of air on the eye, loud noise), therefore producing a different CR, and possibly engaging different processes. Moreover, there are other factors that may influence the learnt response, such as the timing and frequency of the presentation, the total duration, the rate of reinforcement, individual differences and the environmental context (Lonsdorf *et al.,* 2017). Although

there is no consensus about the standard procedure for conditioning experiments, a common terminology framework and guidelines have been proposed in the context of fear conditioning, which can be adapted to other conditioning experiments (Lonsdorf *et al.,* 2017). Such guidelines are important to enable interpretation of the methodology and results across the field; and suggest that the following experimental factors are described (Lonsdorf *et al.,* 2017):

1. CS and US stimuli type, duration and intensity;
2. *Inter-stimulus interval* (delay between CS and US) and time of overlap if present;
3. *Inter-trial interval* (elapsed time between US offset and next CS onset);
4. Number of trials of each stimulus;
5. Reinforcement rate (probability of US occurrence in the presence of the CS);
6. Trials order of presentation (e.g. pseudo-randomised) and restrictions;
7. Context and transition between experimental phases;
8. Criteria to identify a conditioned response.

The duration of CS and US stimuli are arbitrary, and typically depend on their sampling modality and physiological measurement that will be recorded. In the case of EEG studies for instance, they are generally set to be in the milliseconds range, whilst for fMRI a longer stimulus is required due to the lower temporal resolution and slower physiological response. It is still unclear what extent the inter-trial and inter-stimulus times impact the process of learning, and an optimal interval length has not been identified (Lonsdorf *et al.,* 2017). Although precise guidelines are missing, it is suggested that the lag between stimuli should be shorter than the lag between trials in order to observe the predictive role of the CS. It is also suggested, when possible, to introduce a jittered (i.e. variable) inter-trial interval in order to exclude the possibility that the conditioned response is learnt simply from a predictable pattern of US, rather than from association with the CS (Balsam *et al.,*

2010; Emberson *et al.,* 2015; Lonsdorf *et al.,* 2017). Although, a long inter-trial interval is considered to facilitate learning, learning also depends on the number of trials, therefore a fine balance between the two parameters is required to induce learning within the time of the session. The reinforce rate, defined as the probability of US in the presence of CS, is an additional trade-off to be considered. While a 100% reinforcement rate (continuous pairing) strengthens the development of a conditioned response, a partial reinforcement schedule is often employed for pragmatic reasons, for instance the addition of unpaired CS allow to measure the conditioned response during fMRI experiments (Büchel *et al.,* 1998). Conditioning protocols can be comprised of different stages, for example pre-learning and learning training phases. A typical pre-learning phase is *familiarisation*, which allows establishment of the baseline response to the stimuli and can be used as a comparison with the conditioned response. The transition between those phases should be documented and described since changes in the context potentially induce changes in responses. These context-changes include the experiment taking place inside vs. outside of the MRI scanner, as well as the passing of time. Finally, the conditioned response measure can take different forms, such as behavioural, physiological or neurobiological. The focus here will be on the detection of a cortical functional response observable with fMRI.

Although fMRI provides an invaluable tool to identify the underlying neural correlates of learning, it is associated with particular experimental limitations. fMRI analysis is typically based on a GLM which requires independent regressors, which causes a potential problem in conditioning protocols as the two events (CS and US) are intrinsically correlated. Therefore the learning paradigm design needs to be carefully manipulated in order to increase the variance between those regressors. The collinearity between regressors can be reduced by a combination of different stimulus duration between CS and US and partial reinforcement rate (Henson, 2007; Mumford *et al.,* 2015). The introduction of a jittered inter-trial interval would also contribute to the decorrelation of events, however it also introduces a sampling bias because the image acquisition is not always at the same time with respect with the response timecourse, and thus it is discouraged. An alternative is to

collapse the CS and US regressors as if they were one event rather than two disconnected ones, and use the CS-alone events as a distinct event (Lonsdorf *et al.,* 2017). In this case, it will not be possible to disentangle the discrete activation of the two stimuli, but it will be possible to test the difference between paired and test events. One possibility to disentangle the two different sensory modalities while maintaining the time contingency is to introduce a second stimulus on the same modality which is not associated with the other. For example, there could be two visual cues of different shape and colour, one of which always followed by the US while the other is never paired with the US and therefore the visual response can be isolated from the predicted response (Büchel *et al.,* 1998; Lindner *et al.,* 2015). However, a major limitation is that this method doubles the number of trials and thus also the total time. Another critical consideration is that the stimuli might cause head motion correlated to the task and therefore this needs to be controlled in order to prevent false activation in the fMRI analysis (Hajnal *et al.,* 1994; Friston *et al.,* 1996; Lonsdorf *et al.,* 2017). With these considerations in mind, I designed and tested different auditory-motor conditioning paradigms in an iterative process for specific use with newborn subjects.

4.2 Methods

An auditory-motor paradigm was selected to perform an fMRI associative learning study with neonates. The motor task consisted of passive flexion/extension of the right wrist using the MRI-compatible wrist device described in section 2.4.2. The auditory stimulus was delivered using commercial MRI-compatible headphones (OptoActive, Optoacoutsics Ltd, Moshav Mazor, IL) with active noise cancelling of the background scanner gradient noise. While the wrist device has already been employed and validated for task-fMRI in the newborn population (Allievi *et al.,* 2016; Dall'Orso *et al.,* 2018), a preliminary auditory experiment was essential to establish its suitability for the group of interest. After the auditory task test, three different learning paradigms were designed and tested sequentially. In all different learning paradigms, the auditory stimulus was employed

as the conditioned stimulus (CS) that predicted the passive sensorimotor unconditioned stimulus (US). The two stimuli types were presented in a time-locked and paired fashion most of the time, while a few additional events consisting of the auditory stimulus alone were also included as a measure of the conditioned response (CR). A short familiarisation phase, during which the two stimuli were presented separately, was acquired before the learning paradigm took place. This initial fMRI session was for the baby to familiarise with the stimuli, and to collect the baseline responses of the independent events. The subjects were recruited at St Thomas' Hospital London and parental written consent was obtained after written information about the study was provided prior to participation. All infants were studied following the "feed and wrap" technique and with hearing protection applied (moulded dental putty to cover the ears canal (President Putty, Coltene Whaledent, Mahwah, NJ, USA) with adhesive earmuffs applied on top (MiniMuffs, Natus Medical Inc., San Carlos, CA, USA)). Data were acquired using a 3-Tesla MRI scanner (Philips Achieva, Best, NL) located on the NICU at St Thomas Hospital with a 32-channel receive head coil. High resolution structural T1-weighted and T2-weighted images were acquired prior to the fMRI images for all subjects studied. BOLD contrast fMRI images were acquired using an EPI sequence with TR 1500 ms, TE 45 ms, FA 90°, resolution x;y;z=2.5;2.5;3.25mm with 0.75 mm slice gap. MRI data were processed with the FMRIB Software Library tools.

4.2.1 Preliminary auditory task test

Although the vast collection of evidence in support of newborn infants being able to process auditory information, to detect cortical auditory processing by fMRI is challenging given that the loud environment of the MRI scanner might confound the task. Nevertheless, auditory task-fMRI studies were able to detect BOLD signal localised in the temporal lobe of few months old infants (Altman & Bernal, 2001; Dehaene-Lambertz *et al.,* 2002), newborn infants (Anderson *et al.,* 2001; Perani *et al.,* 2010; Perani *et al.,* 2011; Baldoli *et al.,* 2015) and in few cases also in foetuses (Moore *et al.,* 2001). In Anderson *et al.*

(2001), the BOLD signal in response to a frequency-modulated pure tone was identified in 14 out of 20 non-sedated neonates younger than 14 days old and PMA ranging from 37 and 42 weeks. However, the BOLD response was not consistent across subjects, most of which showed a negative response. A negative BOLD signal in newborn infants could be possibly explained by the inappropriate use of the HRF model as neonatal responses have been characterised only later (Arichi *et al.,* 2012). Regardless, Anderson *et al.,* 2001 demonstrated that fMRI can measure auditory cortical activation as a response to sound despite some difficulties. Similar results have been confirmed in a Near-Infrared Spectroscopy study in 13 out of 19 neonates younger than 49 days and PMA ranging from 28 to 41 weeks (Zaramella *et al.,* 2001). The auditory stimuli used in those two studies were a frequency-modulated tone (range 0.3-2.3kHz and rate 8Hz, intensity 60-80 dB) lasting 35 seconds (Anderson *et al.,* 2001), and an increasing tonal sweep (range 2-4kHz, intensity 90dB), thus providing a range of possible auditory stimulation which could be used for an auditory task. While more sophisticated stimuli, such as music or speech with prosodic features, elicited a robust activation in the temporal lobe, they also engage higher associative brain regions (Perani *et al.,* 2010; Perani *et al.,* 2011) and might confound the associative learning areas of activation. For simplicity and consistency I therefore preferred the use of a simple sound as a CS.

Different aspects of the auditory cue may contribute to the success of the auditory task-fMRI. The sound delivered at the headphones needs to audible (and distinguishable) within the loud MRI scanner environment, thus the volume must be high enough while being hearing safe. Tuning the frequency of the tone can potentially improve the perception of the auditory cue as it becomes more distinct from the background noise, although higher frequencies are less pleasant to hear. In addition to the volume and frequency, the duration of the cue may also influence the subject response. A brief tone may be more likely to elicit a startle reflex, which would produce a motion artefact at the time of interest, whilst a prolonged and modulated sound would be less disturbing and produce a more sustained and robust response. Considering that motion is a major limitation in fMRI studies, it is critical to select a stimulus that does not wake up or cause any distress

to the infant subject. In this view, the auditory cue should be tested on adult subjects to receive feedback about the quality of perception and importantly the level of disturbance.

Three different auditory tasks were designed and tested with a healthy adult volunteer inside the MRI scanner. All of the tasks consisted of six blocks of stimulation and rest distributed over a period of 4 minutes and 24 seconds (TR=1.5s, 174 volumes). In each task, one of the following types of sound were presented in all six blocks:

a) 1kHz tone pulses repeated 7 times in a block of 10.5s;

b) 1kHz tone presented constantly in a block of 12s;

c) 2kHz tone pulses repeated 7 times in a block of 10.5s.

Tasks a) and b) enabled comparison between a constant block of sound and a pulsed sound, whereas tasks a) and c) allowed comparison between a lower or higher frequency tone. The initial experiments with adult subjects found that a pulsed stimulus produced a more robust response compared to the long constant sound, however there was not a striking difference between the two frequencies tested (figure 4.1). Nevertheless, those results cannot be translated directly to the newborn hypothetical response as a different developmental stage may produce a different sensitivity range. Although auditory experience begins during the third trimester of gestation, the response to sound early in development is qualitatively different than the adult's response (Werner, 2007). It is suggested that infants younger than 6 months are less sensitive to sound and that a higher volume of sound compared to adults is required for a behavioural response (Tharpe & Ashmead, 2001; Werner, 2007). Moreover, newborn infants (until 6 months old) have poor frequency discrimination and might struggle to distinguish different sounds when played simultaneously (Werner, 2007). For these reasons, it may be challenging to elicit a robust auditory response from within the scanner.

Pilot tests were performed in two newborn subjects (GA: 40+1 and 37+4; PMA: 40+2 and 38+0). The experiment consisted of three different auditory cues repeated in an

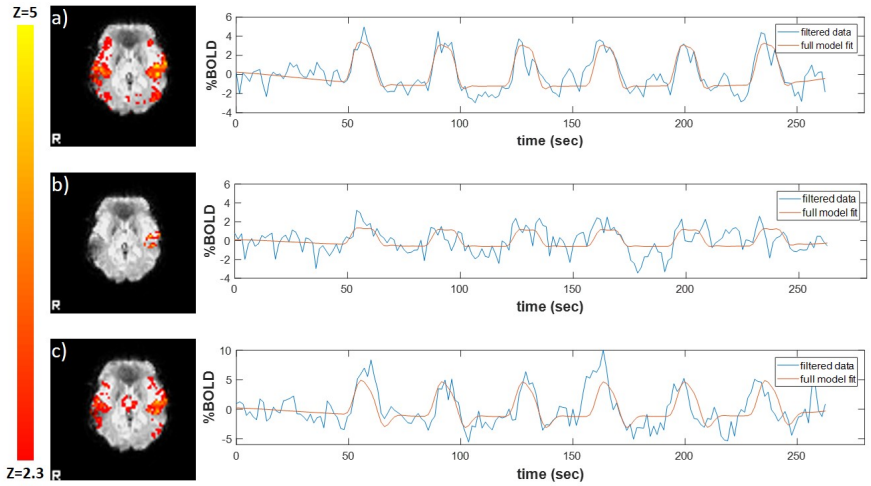

Figure 4.1: Functional activation map in response to 3 auditory stimuli: a) 1kHz tone pulses repeated 7 times in 10.5s; b) 1kHz tone for a block of 12s; c) 2kHz tone pulses repeated 7 times in 10.5s. Next to each map, the data and GLM model fit of the most significant voxel.

alternating fashion 10 times each, for a total of 30 auditory stimuli in 13 minutes and 15 seconds. The sounds tested were a 1s tone at 1kHz, followed by the same tone but repeated twice with a 0.5s gap, and a 1s tone at 1.5kHz; with 24s of rest preceding each event. Overall, significant clusters of activation in response to the sound were identified within the primary auditory cortex (A1) in both infants (figure 4.2). Only a short interval of the experiment (around 200 volumes) was used for the analysis due to intermittent motion artefacts, which limited a direct comparison between stimuli types. Although head motion often occurred in conjunction with the stimulus time, there was no clear prominence of startle in response to a specific sound type suggesting that there is no clear difference in stimulus-related movement between the auditory cues tested. Nevertheless, those were only few trials, thus more variations of sound have been tested during the process of optimisation of the learning paradigm described next.

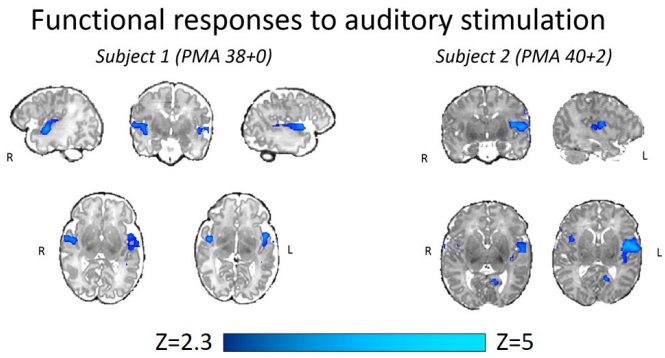

Figure 4.2: Functional responses to auditory stimuli tested in two infants subjects. In blue the significant clusters (z>2.3) of activation.

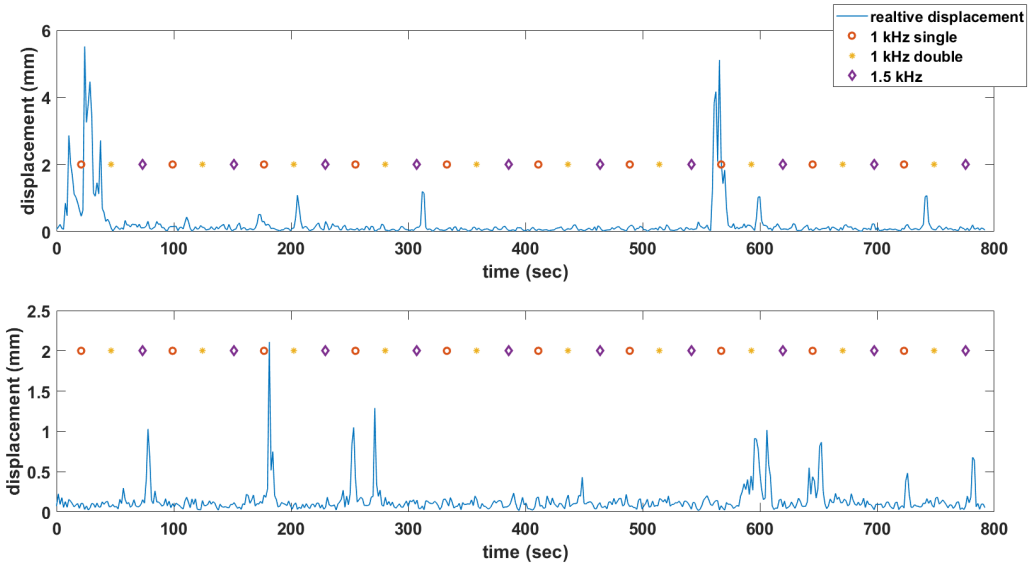

Figure 4.3: Head displacement in relation to different auditory cues. Displacement (blue line) is calculated relative to a reference volume (middle volume). Onset of each auditory cue is represented in different symbols for different sound type.

4.2.2 Paradigm 1

The first paradigm design (figure 4.4) consisted of a block of passive wrist movement (5.5 seconds), anticipated by a short auditory cue (1 second, 1kHz pure tone). The two stimuli were time-locked with an overlap period of 0.5 seconds. The inter-trial interval was predefined in a range of 24-27 seconds and was varied in a pseudo-random fashion. The auditory stimuli were presented a total of 51 times of which 43 were paired with sensorimotor stimulation, with the remaining 8 times functioning as a test for the conditioned response. Additionally, there were 5 empty trials that could be used to test the difference in response between the general task pattern and a deviant condition with a missing

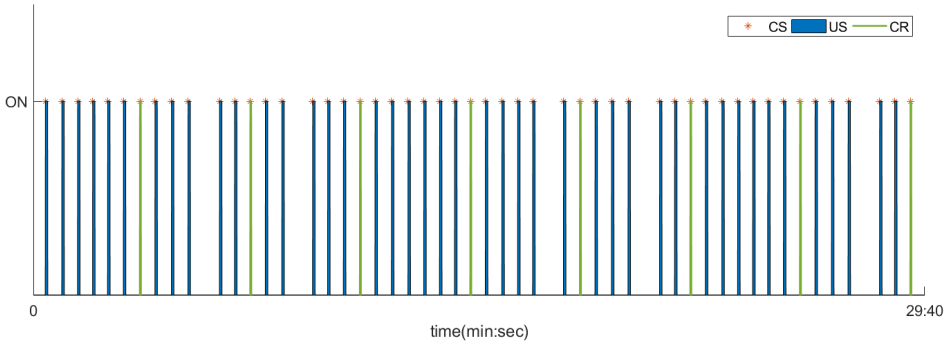

Figure 4.4: *Paradigm 1*: a 1s tone at 1kHz (orange $*$) anticipates a 5.5s of passive wrist movement (blue blocks). In green are highlighted the tone alone trials. CS=conditioned stimulus; US=unconditioned stimulus; CR=conditioned response.

association. Although this design had the potential to address multiple questions, the total duration of the learning paradigm was almost 30 minutes, preventing the addition of a familiarisation phase and potentially undermining the success of the full acquisition. The paradigm was first tested with two adult subjects, and then data was collected from three infants (GA: 39+2, 38+6, 39+1; PMA: 39+4, 45+2, 39+2). Motion outliers were then calculated using the RMS intensity difference of volume N to volume N+1 (Power *et al.,* 2012) and evaluated considering the percentage of outliers, the maximum number of consecutives corrupted volumes, and the maximum number of consecutive uncorrupted volumes. One subject had 12.63%, with up to 32 corrupted and only 77 uncorrupted consecutives volumes. Another subject had 17.85%, with up to 23 corrupted and only 98 uncorrupted consecutives volumes. Therefore, motion artefacts were too severe to allow the data to be analysed in two of the data sets (figure 4.5), suggesting that the length and protocol type would not be effective and encouraged a design variation.

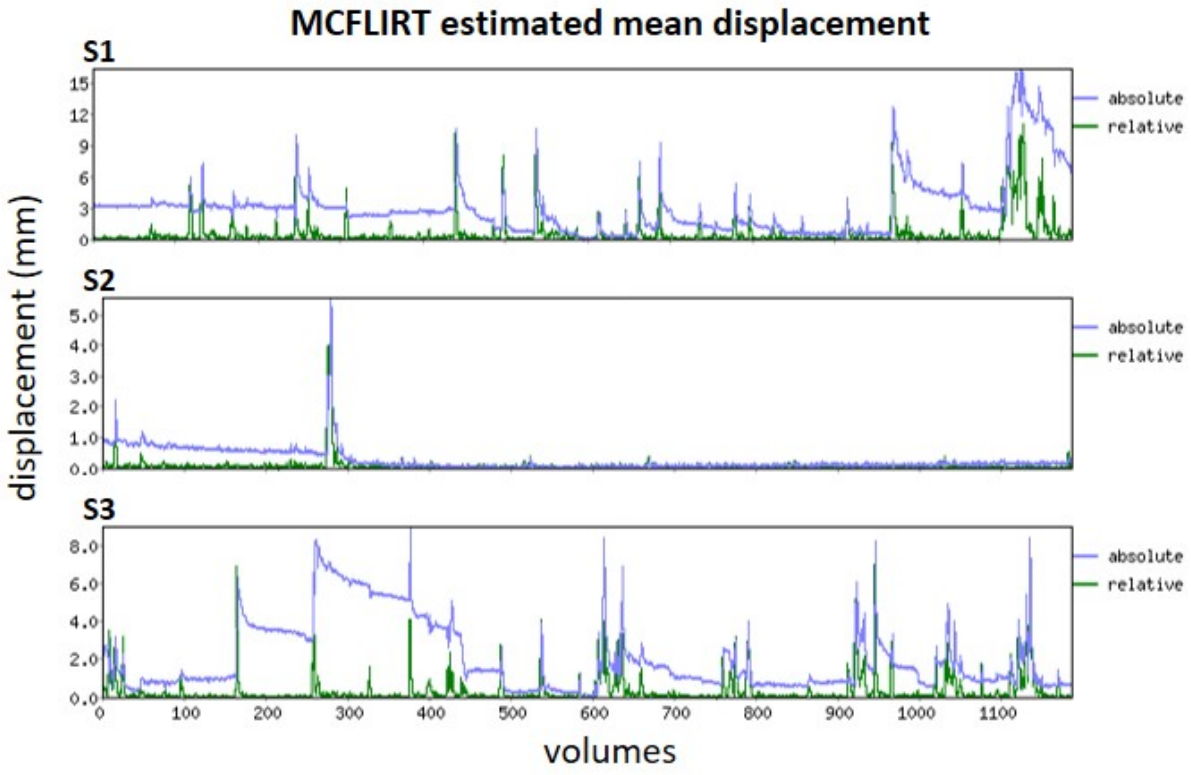

Figure 4.5: Head displacement of three different infants subjects (S1, S2, S3) during the learning *paradigm 1*. Absolute displacement relative to the reference volume (blue) and relative displacement relative to adjacent volumes (green).

4.2.3 Paradigm 2

The second paradigm design (figure 4.6) consisted of a block of passive wrist movement (9 seconds) anticipated by and co-ending with a longer auditory cue (12 second, amplitude-modulated tone) and repeated in series. As in the first paradigm, the inter-trial interval was pseudo-randomised in a range of 24-28.5s in order to avoid temporal prediction. The paradigm was split into two sections: "learning encoding" and "learning test". During the encoding phase, the stimuli were presented 12 times together on every occasion, whereas in the following phase there were some test trials in which the sound was presented alone. During the test phase, the auditory stimuli occurred a total of 24 times of which 18 were paired with sensorimotor stimulation, with the remaining 6 times in which the auditory stimulus was presented alone functioning as a test for the conditioned response. The total duration of the learning paradigm was around 23 minutes (7:34 + 15:43). To reduce the total experiment duration, the number of total trials and number of sound alone trials were

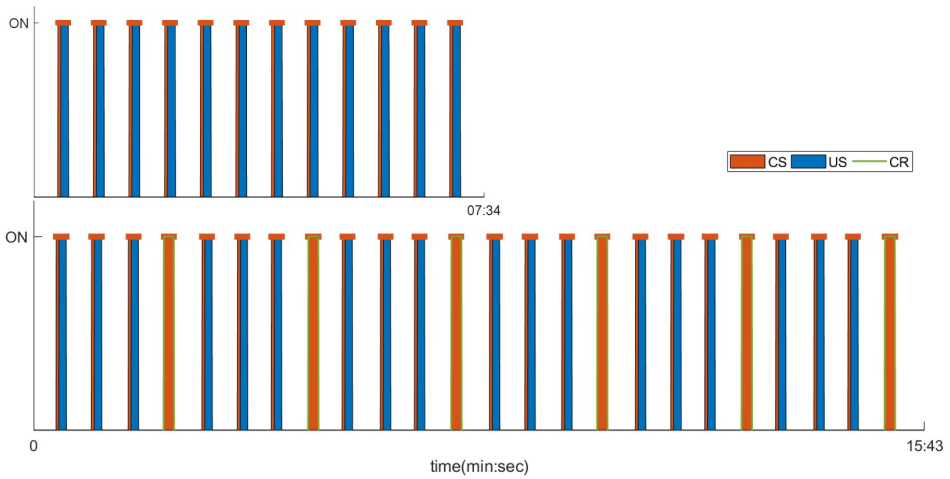

Figure 4.6: *Paradigm 2*: a 12s tone (orange blocks) anticipates a 9s of passive wrist movement (blue blocks). On top is the "learning encoding" session, on the bottom the "learning test" session. In green are highlighted the tone alone trials. CS=conditioned stimulus; US=unconditioned stimulus; CR=conditioned response.

also reduced. The latter is necessary for testing the conditioned response, hence reducing test trials decreased the efficiency of the experiment. However, compared to *paradigm 1*, this design comprised longer task blocks with the aim of increasing the signal-to-noise ratio and reducing startle responses to the brief and sudden tone.

Data were collected from 4 adults and 8 infants (demographic information is reported in table 4.1), although there were slight variations in the auditory cue across subjects. The tone was selected to be either 1kHz, 2kHz or 2.5kHz, and modulated at a rate of 0.2Hz, 0.25Hz or 0.3Hz. Although we were able to collect data from all of these subjects, in many cases the data did not meet the quality required for analysis. The commonest reason for data to be discarded was due to severe head motion artefact limiting further analysis (figure 4.7). Despite the hypothesis that a block design would disturb the infant less and reduce head motion, the results were not as desired and motivated a third alternative learning paradigm design.

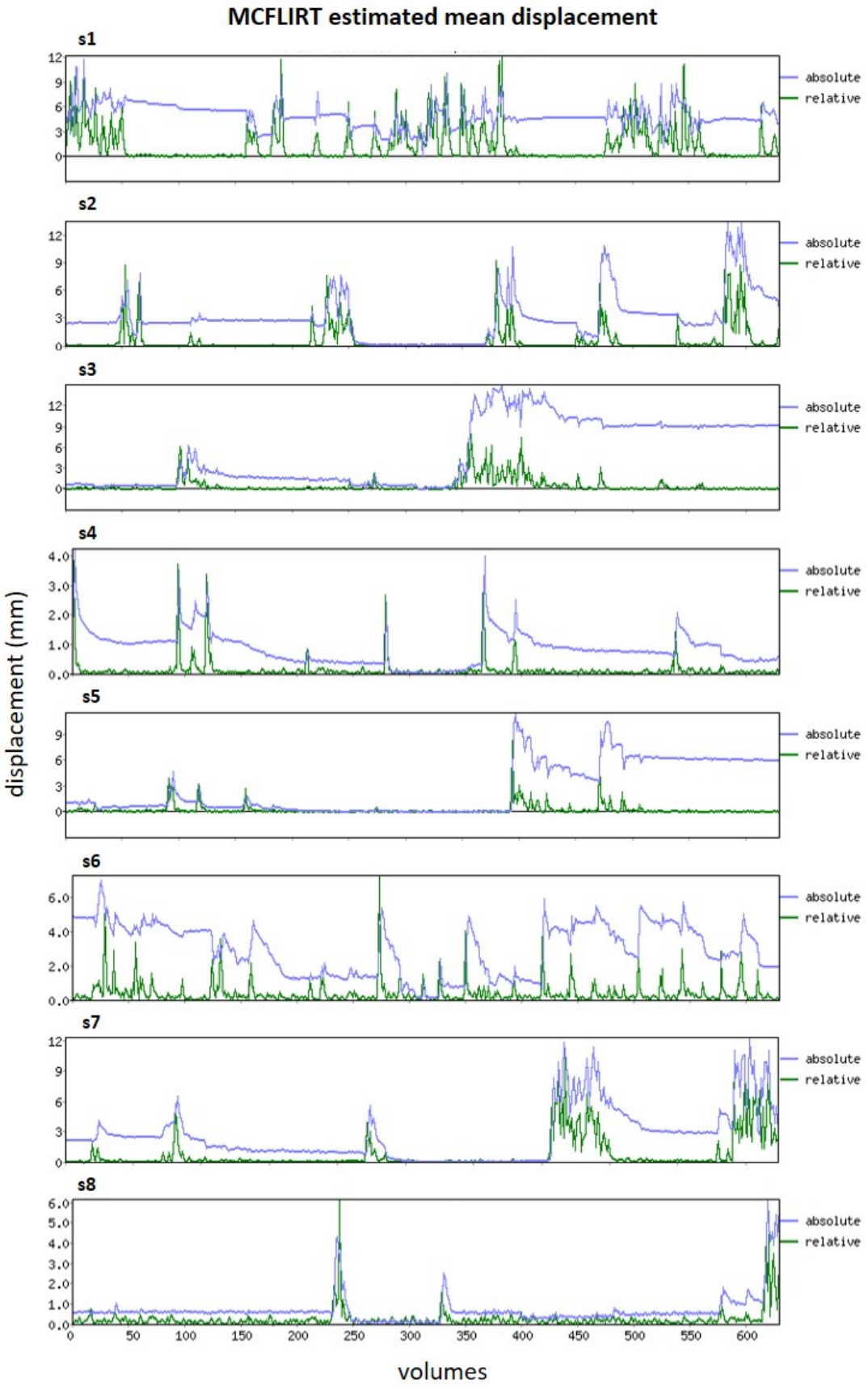

Figure 4.7: Head displacement of eight different infants subjects (s1-s8) during the learning test phase of *paradigm 2*. Absolute displacement relative to the reference volume (blue) and relative displacement relative to adjacent volumes (green).

subject	GA	PMA
s1	40+5	41+0
s2	38+4	39+0
s3	41+6	42+1
s4	41+6	42+4
s5	39+0	39+3
s6	38+5	38+6
s7	33+5	40+6
s8	33+5	40+6

Table 4.1: Demographic information of infant group underwent the learning experiment with paradigm 2. GA=gestational age; PMA=post-menstrual age.

4.2.4 Paradigm 3

A third paradigm was designed, which was inspired by an audio-visual learning paradigm employed with young children (Emberson *et al.,* 2015). In that study, a novel sound predicted a neutral visual stimulus except in some trials of visual omission, and near-infrared spectroscopy was used to record the haemodynamic responses in the infant cortex following paired and omitted trials. Compared to the previous paradigms, it was characterised by groups of paired-trials presented close together, and more isolated trials which consisted of either paired or sound alone conditions. The major benefit of this design is that the groups of trials act as an intensive learning session that maximises the number of associations. However a drawback is that it does not allow comparison of the response to the tone alone given the difference in length of the sound conditions. On the other hand, the individual trials act as a probe to compare the paired events with the sound alone event, and hence test for a conditioned response. This kind of design aims to maximise the overall number of paired and test trials while constraining the paradigm time. Therefore, this approach was re-adapted to generate the third paradigm. The first version of *paradigm 3* (figure 4.8) consisted of a 1kHz pure tone lasting 1 second and block of passive flexion/extension of the wrist lasting 5.5 seconds, thus the CS and US were the same as in paradigm 1. The events were organised in 9 groups made of 4, 5 or 6 (pseudo-randomised) paired CS-US trials, with inter-trial interval of 1.5 seconds and inter-stimulus 0.5 seconds. Each group was followed by two events, either the sound alone or the paired events pre-

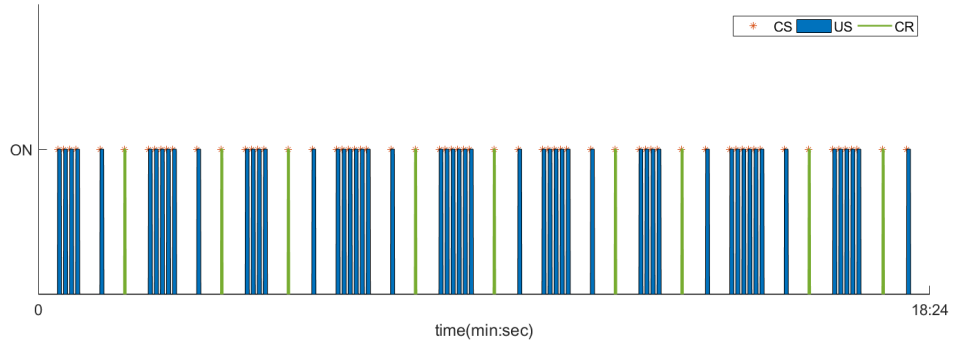

Figure 4.8: *Paradigm 3a.* A 1s tone (orange $*$) anticipates and overlaps for 0.5s with the passive wrist movement lasting 5.5s (blue blocks). Trials were grouped in a block with a 1.5 inter-trial interval, with two individual events separated by 24s of rest. The two individual events were either paired stimuli or sound alone (highlighted in green). CS=conditioned stimulus; US=unconditioned stimulus; CR=conditioned response.

sented in a random order. Between the grouped and individual events, there was a 24 second interval to allow the BOLD signal to recover to baseline. The auditory stimuli was presented a total of 63 times of which 54 were paired with the US, hence there were 9 events used to test for the conditioned response. All these trials were presented in only 18 minutes, making this learning paradigm the shortest total duration, whilst having the highest number of trials.

The paradigm has been tested in 5 newborn infants. The results with this paradigm were more positive as in 3 of the subjects it was possible to identify the functional response to the auditory and somatosensory stimuli (figure 4.9). However, head motion was still a major limiting factor and necessitated that data was severely cropped leaving only a few individual events. For this reason, the paradigm was modified to include even more trials. A second version of the paradigm was therefore designed with the same criteria (figure 4.10). The learning *paradigm 3b* consisted of 64 auditory-motor paired trials and 11 auditory alone trials for a total duration of 22 minutes. Additional modifications were made to the auditory stimulus to make it a longer duration (6 seconds) in order to have the CS and US stimuli co-ending, in accordance with the definition of a delay conditioning paradigm. In keeping with a lack of precise frequency discrimination due to the developmental stage of the auditory system (Werner, 2007) (and as supported by the previous auditory tasks), it is unlikely that a tone of a specific frequency outperforms

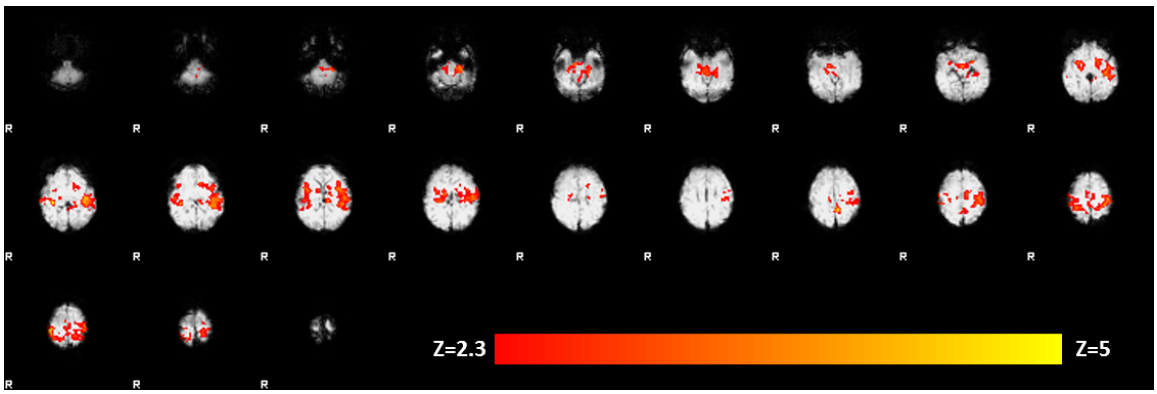

Figure 4.9: Representative functional map in response of learning paradigm 3. Significant clusters (z>2.3) of activation in response to the learning *paradigm 3* were found bilaterally in the auditory cortex and in the sensorimotor cortex.

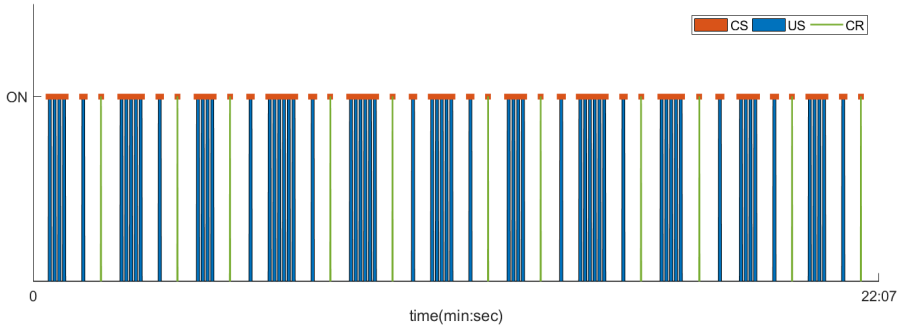

Figure 4.10: *Paradigm 3b.* A 6s sound (orange block) anticipates and overlaps for 0.5s with the passive wrist movement lasting 5.5s (blue blocks). Trials were grouped in block with 1.5 inter-trial interval, and two individual events separated by 24s of rest. The two individual events were either paired stimuli or sound alone (highlighted in green). CS=conditioned stimulus; US=unconditioned stimulus; CR=conditioned response.

any others in terms of neuronal response. While different tones are equally processed by the developing auditory cortex, specific sound features might have an effect on an infant subject's engagement: level of attention and disturbance. In contrast to the first version that used a 1kHz pure tone, the newer version used different sounds. In some cases a mixture of 2kHz and 2.5kHz tones modulated in amplitude, in later subjects a sound even more rich in frequency content corresponding to a jingle bells melody previously used for a similar purpose (Emberson *et al.,* 2015). Demographic information of the infants and the corresponding auditory cues used for each subject are reported in table 4.2. There was not a clear difference in head motion relative to the different sounds tested, however the jingle bells sound produced a more robust auditory response and was therefore chosen as the conditioned stimulus.

Subject	GA	PMA	Auditory cue	
			duration	frequency
a1	39+2	39+4	1s	1kHz
a2	42+1	42+3	1s	1kHz
a3	37+6	38+1	1s	1kHz
a4	41+6	42+3	1s	1kHz
a5	39+0	39+2	1s	1kHz
b6	40+4	40+5	6s	2kHz+2.5kHz
b7	33+3	41+2	6s	2kHz+2.5kHz
b8	33+3	41+2	6s	2kHz+2.5kHz
b9	39+3	39+5	6s	2kHz+2.5kHz
b10	40+5	40+6	6s	2kHz+2.5kHz
b11	38+3	39+6	6s	2kHz+2.5kHz
b12	39+0	39+1	6s	2kHz+2.5kHz
b13	39+0	41+1	6s	jingle
b14	41+6	42+1	6s	jingle
b15	39+6	40+2	6s	jingle
b16	34+1	40+1	6s	jingle
b17	38+5	39+4	6s	jingle
b18	41+5	42+0	6s	jingle
b19	30+4	41+5	6s	jingle
b20	32+2	40+5	6s	jingle
b21	30+4	42+3	6s	jingle
b22	36+4	38+3	6s	jingle
b23	40+0	40+4	6s	jingle

Table 4.2: Demographic information of infant group underwent the learning experiment with paradigm 3. The double line divides the subjects who received paradigm *a* or *b* and information about the different auditory cues are also provided. GA=gestational age; PMA=post-menstrual age.

4.3 Conclusions

The optimisation of a learning paradigm for a fMRI study with neonates is a complex process that involves multiple factors. The paradigm needs to be rich in information for the subjects who are learning the relationship between the two stimuli, with the CS informative about the US and sufficient time to reinforce their association. Moreover, the task design must possess enough information for the fMRI analysis such that the regressors have enough variance for statistical inference. On top of these factors, the learning task needs to be suitable for sleeping neonates, and hence the stimulation needs to be perceptible yet not wake up or disturb the infants and minimise head motion. Although expecting an infant never to move while constantly stimulated is far from realistic, it is possible to discard only the corrupted part of the fMRI data images acquired and thus perform the desired statistical analysis on the preserved subset of data. In keeping with this, an effective design should contain as many trials as possible in order to increase the chance of having enough test trials to investigate the conditioned response in a partial data set. Three main kinds of paradigm for fMRI classical conditioning have been designed and tested. While the tuning of parameters and features of the learning task is an interesting route to explore, it might lead to a large amount of tests and data discard, and therefore a pragmatic decision must be taken accepting their limitations as a trade-off. In general for statistical group inference it is better to have more subjects with shorter scans rather than few subjects with a very long scan (Henson, 2006; Monti, 2011). The estimated group variance is in fact a mixture of both "within" and "across" subjects variances, and while both are scaled by the number of subjects, the number of volumes improves only the "within" subject variability (Monti, 2011). The second version of *paradigm 3* provides a means of inducing an association between two stimuli via multiple repetitions of paired trials and to test for it in a relative short experiment. Different types of tones have been investigated with the intent of minimising head motion and measure a robust functional response. While data discard due to the head motion was a sustained problem, this paradigm provides a sufficient number of test conditions which allows the investigation

of a conditioned response even in a partial data set. For this reason this paradigm is favourable compared to the others. The sound of a jingling bell was selected as it carried a broad spectrum of frequencies and made it more distinguishable inside the MRI scanner. This final design was selected to perform an associative learning experiment in a group of newborn infants, the results of which are presented in the next chapter.

"Every expert was once beginner."

– Helen Hayes MacArthur –

5

Cortical processing of auditory-motor associative learning in human newborn infants

Following birth, newborn infants are exposed to a dramatic change in environment and must rapidly adapt their behaviour to the external world. An important basic adaptive mechanism for human infants is associative learning, which enables rapid understanding of the multi-modal sensory complexity of new environments. Although studies have provided ample behavioural evidence of associative learning in infants, the neural processes involved in this fundamental early life ability are not known. Here, I describe a study we carried out to investigate the underlying brain processing of associative learning using Blood Oxygen Level Dependent (BOLD) functional MRI (fMRI) and the classical conditioning

paradigm described in the previous chapter (4).

Acknowledgements and contributions

Substantial parts of this chapter have been prepared for submission to a peer-reviewed journal. Dall'Orso S., Fifer W.P., Balsam P.D., Brandon J., O'Keefe C., Vecchiato K., Edwards A.D., Burdet E., Arichi T. are authors of the manuscript and they contributed to its preparation and revision.

The study design and interpretation were performed in collaboration with Dr. Tomoki Arichi, Dr. Etienne Burdet, Dr. David Edwards, Dr. William Fifer and Dr. Peter Balsam. Subjects recruitment and data collection was performed in collaboration with Dr. Tomoki Arichi, Dr. Katy Vecchiato, Jacqueline Brandon, Camille O'Keefe, Emer Hughes, Elaine Green, Joanna Allsop, Katie Colford, Louise Dillon, and the clinical staff on the neonatal intensive care unit at St Thomas Hospital London.

The work here presented was performed in collaboration with the research and clinical team at the Perinatal Imaging and Health department at King's College London, Columbia University New York, and St Thomas' Hospital London

I thank the patients and families who kindly agreed to participate in this study

5.1 Introduction

Immediately after birth, newborn infants are exposed to a dramatic change in environment and must rapidly adapt their behaviour to the external world. As a part of this process, it is essential that they can associate the temporal, spatial and contextual features of the new and vast ex-utero sensory experience. This associative learning process allows them to understand environmental contingencies and use this information for behavioural and emotional-self-regulation (Lipsitt, 1998). It also has a clear role in early life survival, such as anticipating and overcoming respiratory and thermal challenges during sleep (Paluszynska *et al.,* 2004) and facilitating parent-child bonding (DeCasper & Fifer,

1980). The basic principles of associative learning can be investigated using classical conditioning, in which a *conditioned response* (CR) to a specific *conditioning stimulus* (CS) is learnt through repeated pairing of the CS and another distinct *unconditioned stimulus* (US). This approach has been successfully employed to model the nature of associative learning by studying experience-dependent changes of behaviour and brain activity in animals (Li *et al.,* 2003) and adult humans (Ramnani *et al.,* 2000). Human infants have also been shown to be capable of learning the association between odour and tactile stimuli (Sullivan *et al.,* 1991) and between an auditory tone and a mild puff of air to the eyelid (Fifer *et al.,* 2010) within the first few days after birth. However, whilst behavioural changes learnt through classical conditioning can be readily identified in infants, the challenges inherent to performing neuroimaging studies in this population have previously limited understanding of the neural processes that underlie this fundamental ability. As described in chapter 4, a classical conditioning paradigm has been designed to characterise the underlying brain activity during learning using Blood Oxygen Level Dependent (BOLD) functional MRI (fMRI) in a group of newborn infants during presumed natural sleep. Data collection from the paradigm optimisation study (chapter 4) was enlarged to include additional infants. Furthermore, to interpret these results in the context of what is known about associative learning from the adult literature and to understand if the induced patterns of activity identified were specific to the infant brain, we used the same classical conditioning protocol on a group of 10 healthy adult volunteers.

5.2 Methods

The study was approved by the NHS research ethics committee (REC code: 12/LO/1247) and informed written consent was obtained from each subject or one parent prior to participation.

	Base move	Base Sound	Learning	GA	PMA	W (kg)	HC (cm)	Sex
1	x	x	✓	40+4	40+5	3	34	F
2	✓	✓	✓	33+3	41+2	3.9	37.5	M
3	x	x	✓	33+3	41+2	3.88	38	M
4	✓	✓	x	40+5	40+6	4	35	M
5	✓	x	✓	38+3	39+6	2.7	34	M
6	✓	✓	✓	39+0	39+1	3.47	37	M
7	x	x	✓	39+0	41+1	2.79	36	M
8	x	x	✓	41+6	42+1	3.77	35	M
9	x	✓	✓	34+1	40+1	4.07	37	F
10	x	✓	✓	38+5	39+4	2.85	33	M
11	x	x	✓	41+5	42+0	3.625	33	M
12	✓	x	✓	32+2	40+5	3.09	35.2	M
13	✓	✓	-	30+4	42+3	3.95	37.5	M
14	✓	✓	✓	36+4	38+3	2.56	34	M
15	✓	✓	x	38+0	38+2	3.535	34	M
16	✓	✓	x	28+3	41+0	3.62	37	M
17	✓	✓	✓	40+0	40+4	3.99	36	M
18	✓	✓	-	39+2	39+3	2.98	32	M
19	✓	x	-	39+0	39+6	3.6	36	M
20	✓	x	-	38+1	41+6	3.4	36.2	F

Table 5.1: Demographic information of the study group and the scan session successfully used. Data collection was attempted in all conditions for every infant. Data used in the final analysis are highlighted in green. GA= gestational age at birth in weeks + days; PMA= Post Menstrual Age at scan in weeks + days; HC= Head circumference at scan in cm; W= Weight at scan in kilograms; F= female; M= male.

5.2.1 Participants

The study population consisted of 24 healthy infants studied at term equivalent age who were recruited from the Neonatal Intensive Care Unit (NICU) or postnatal wards of St Thomas' Hospital, London, UK. Data from 4 infants were discarded due to severe head motion throughout data collection, unexpected brain injuries identified on anatomical images or equipment failure. Learning dataset were discarded or not collected in additional 7 infants. Information about infants and scans are reported in table 5.1. The final infant learning study group consisted of 13 infants (median gestational age at birth: 38w+4d, range: 32w+2d – 41w+6d) scanned at term equivalent age (median post menstrual age 40w+5d, range: 38w+3d – 42w+3d), all of whom were healthy at the time of scanning. The adult study group consisted of 10 healthy volunteers (6 females, 4 males, age range: 25-39 years old).

5.2.2 Paradigm

The classical conditioning paradigm consisted of an auditory-sensorimotor task where the sound functioning as CS was presented in association with a passive movement functioning as US. The auditory stimulus consisted of a jingling bell sound (previously used in a young children study (Emberson *et al.,* 2015) and tested in a group of infants as described in chapter 4) played for 6 seconds at 90-100dB through MRI compatible headphones (Optoacoutsics Ltd). The sensorimotor stimulation consisted of the right wrist flexion/extension performed using a pneumatically actuated MRI compatible custom-made robotic device (Allievi *et al.,* 2013). In the case of adult subjects, the same device was also fitted on the right hand but provided the flexion/extension of the second and third digit given the small size of the wrist interface.

Subjects were first presented with a *familiarisation* session during which the passive motor stimulus and the auditory stimulus where presented separately, so that the spatial distribution of the functional response to each individual stimulus type could be first characterised in this baseline condition. The baseline condition consisted of 5-6 blocks of 5.5 seconds of passive movement task followed by 5-9 blocks of 6 seconds of auditory task; all blocks were alternated with 24 seconds of rest.

Immediately after the *familiarisation* session, the classical conditioning paradigm (figure 5.1) was presented to induce associative learning. During the classical conditioning paradigm, the two stimulus types were presented together in epochs of 4-6 paired trials presented every 1.5 seconds. The auditory stimulus anticipated the passive movement that was initiated after 0.5 seconds from the auditory onset, to then co-terminated in a time-locked fashion. The learning epochs were followed by a period of rest (24 seconds) and then two randomly ordered test trials (separated by a further 24 seconds): one consisting of the two stimuli presented together and the other consisting of the auditory stimulus alone (figure 5.1). In total there were 11 epochs, thus 11 auditory stimulus alone which were used to assess the CR. The total fMRI experiment including *familiarisation* and learning lasted around 30 minutes ($\sim$ 8 minutes + 22 minutes).

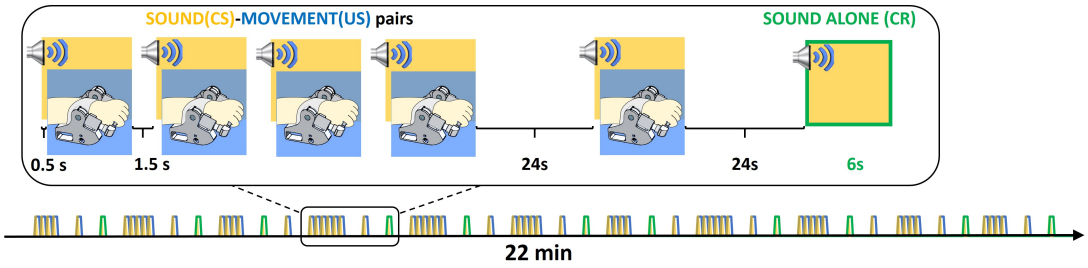

Figure 5.1: Schematic of the associative learning paradigm. Yellow areas depict the occurrence of the sound (6sec), blue the occurrence of the passive movement, and green are highlighted those sounds played alone. Blocks of sound and passive movement (starting with 500ms lag and co-ending) are repeated a variable number of times (4-6) following two trials: one coupled and one sound alone (CR). The paradigm comprised 11 CR trials lasting 22 minutes in total.

Stimulus control, monitoring and synchronisation between stimuli presentation and image acquisition was achieved though custom code developed in the LabVIEW software environment (National Instruments, Austin, TX, USA).

5.2.3 Data acquisition

All infants were studied following feeding, by swaddling in a blanket and then immobilising using a vacuum evacuated bag (Med-Vac, CFI Medical Solutions, Fenton, MI, USA). Hearing protection using moulded dental putty in the external auditory meatus (President Putty, Coltene Whaledent, Mahwah, NJ, USA) and adhesive earmuffs (MiniMuffs, Natus Medical Inc., San Carlos, CA, USA) was applied in infants. MRI compatible headphones with active gradient noise cancellation (OptoActive II, Optoacoutsics Ltd) were used to provide additional gradient noise cancellation and to present the auditory stimulus. All infant data collection was supervised by a clinician (doctor or nurse) and physiological parameters (oxygen saturations, heart and respiratory rate and axillary temperature) were monitored throughout. Infants were presumed to be asleep throughout data collation based on behavioural observations. Adult subjects were studied when awake with suitable hearing protection and the same headphones. These adults were informed about the stimuli types before data collection, but received minimal instruction about the protocol to minimise bias. Magnetic resonance images were acquired using a 3-Tesla MRI scanner

(Philips Achieva, Best, NL) located on the NICU at St Thomas Hospital with a 32-channel receive head coil. High resolution structural T1-weighted and T2-weighted images were acquired for all subjects studied for image registration purposes. BOLD contrast fMRI data was acquired using an EPI sequence with TR 1500 ms, TE 45 ms, FA 90 degrees, resolution 2.5x2.5x3.25 mm^3 with 0.75 mm slice gap. Adult data was collected with identical parameters except a resolution of 3.5x3.5x4.5 mm^3 (1.45 mm slice gap).

5.2.4 Data analysis

MRI data was processed using tools implemented in FSL (www.fmrib.ox.ac.uk/fsl) (Woolrich *et al.,* 2009). fMRI images were preprocessed using a pipeline for infant subjects consisting high pass filtering (with 0.01 Hz cut-off frequency), MCFLIRT rigid body motion correction, slice timing correction, brain extraction using BET, and spatial smoothing (Gaussian of FWHM 5mm)(Dall'Orso *et al.,* 2018). Due to the significant confounding effects of head motion, data sets were then cropped to exclude prolonged or excessive motion estimated from the RMS intensity difference of volume N to volume N+1 (Power *et al.,* 2012). Data were discarded in case of more than 13% or more than 12 consecutive images corrupted (18 s). Residual high signal artefacts due to motion were then further corrected using AFNI 3dDespike (http://afni.nimh.nih.gov/). Residual artefacts due to effects such as cardiorespiratory noise and residual head motion were then regressed from the data after identification using independent component analysis (ICA). Lower level functional activation maps were obtained by analysing the fMRI data using a voxel-wise general linear model (GLM) as implemented in FEAT v6.00, consisting of the experimental paradigm convolved with a neonatal-specific haemodynamic response function (HRF) basis function set (Arichi *et al.,* 2012) and six motion parameters (translation and rotation) derived from the initial rigid body motion correction. Significant areas of activity were identified at a corrected cluster significance level of p=0.05 and z-statistical threshold of 2.3. Lower level functional activation maps were then registered to the subject's own high resolution T2-weighted image and then into a 40 week PMA

template brain (Serag *et al.,* 2012) (infants) or the MNI152 space (adults) using non-linear registration as implemented in FSL FNIRT. Group level effects were then identified using a non-parametric one-sample t-test implemented with permutation methods (FSL randomise v2.0) with threshold-free cluster enhancement (TFCE) (family-wise error (FWE) corrected $p < 0.05$) (Nichols & Hayasaka, 2003). The percentage signal change (relative to the baseline calculated from the 6sec preceding stimulus onset) associated with different conditions was calculated from a common region of interest (ROI) identified by the overlapping clusters of the group results for the baseline sensorimotor and CR responses (SM1-CR), and following the procedure described in 2.3.4. The mean β value within the ROI was divided by the baseline value, multiplied by 100 and scaled by the modelled baseline-to-peak value specific of the HRF used. Differences in the amplitude of the BOLD response within the identified SM1-CR cluster were then tested at a group level using a Kruskal-Wallis test as implemented in the statistical toolbox of Matlab R2017b (The Mathworks Inc, Natick MA, USA).

5.3 Results

In the baseline condition, significant clusters of positive BOLD functional activity were identified in the primary auditory cortices following the auditory stimulus; and in the contralateral (left) primary sensorimotor cortex (SM1) in response to passive motor stimulation. As expected, when both stimulus types were presented concurrently during the learning condition, functional activation was detected within both the primary auditory cortices and contralateral SM1 corresponding to the baseline condition, with additional activity observed within the ipsilateral SM1 and supplementary motor area (SMA). Most importantly however, and consistent with associative learning having taken place, newborn infants were found to exhibit a significant CR to the auditory alone test condition in the contralateral SM1 and anteriorly in the pre-motor cortex (PMC) (figure 5.2 top row).

The results have then been compared with those of a group of 10 adult healthy volunteer who underwent the same task-fMRI experiment. As with the infant subjects, the adult

response during learning could be localised to the bilateral auditory cortices, contralateral SM1 and SMA, all of which were engaged during the respective auditory and passive movement baseline conditions (Fig.2 bottom row). Furthermore, and consistent with associative learning also having taken place in the adult brain, a significant CR was identified within the contralateral SM1 in response to the auditory alone test condition (figure 5.2 bottom row, green).

We then compared the amplitude of the BOLD responses within the identified somatosensory functional network identified during the baseline auditory and baseline passive movement stimulations, paired auditory-motor learning stimulations, and conditioned response. The amplitude of the BOLD response within the identified SM1-CR cluster was significantly higher when the wrist was actually moved during the baseline passive movement in comparison to the baseline auditory condition when sound was played alone ($p<0.01$, Kruskal–Wallis test, figure 5.3 top row left). Importantly and consistent with our finding of a learnt conditioned response, the amplitude of the BOLD response within the same cluster was significantly higher in response to the auditory alone test condition following learning, in comparison to the baseline (pre-learning) auditory alone condition ($p < 0.01$, Kruskal–Wallis test, figure 5.3 top row right). The above results were calculated from data of infants from whom data was successfully collected for some of the conditions. However in the majority of infants, it was not possible to collect data for all of the conditions, as data in some conditions often had to be discarded due to excessive movement. Therefore, infant groups were not identical for all conditions. To confirm the difference between baseline sound and sound test trials during learning, I carried out an additional paired-t test on the 6 subjects with data in both of these conditions. A paired t-test of the absolute change in BOLD (two infant subjects had a negative BOLD conditioned response) in these 6 subjects confirmed a significant difference in amplitude of SM1 response to the auditory only stimulation in the two conditions ($p=0.0029$, 5.4).

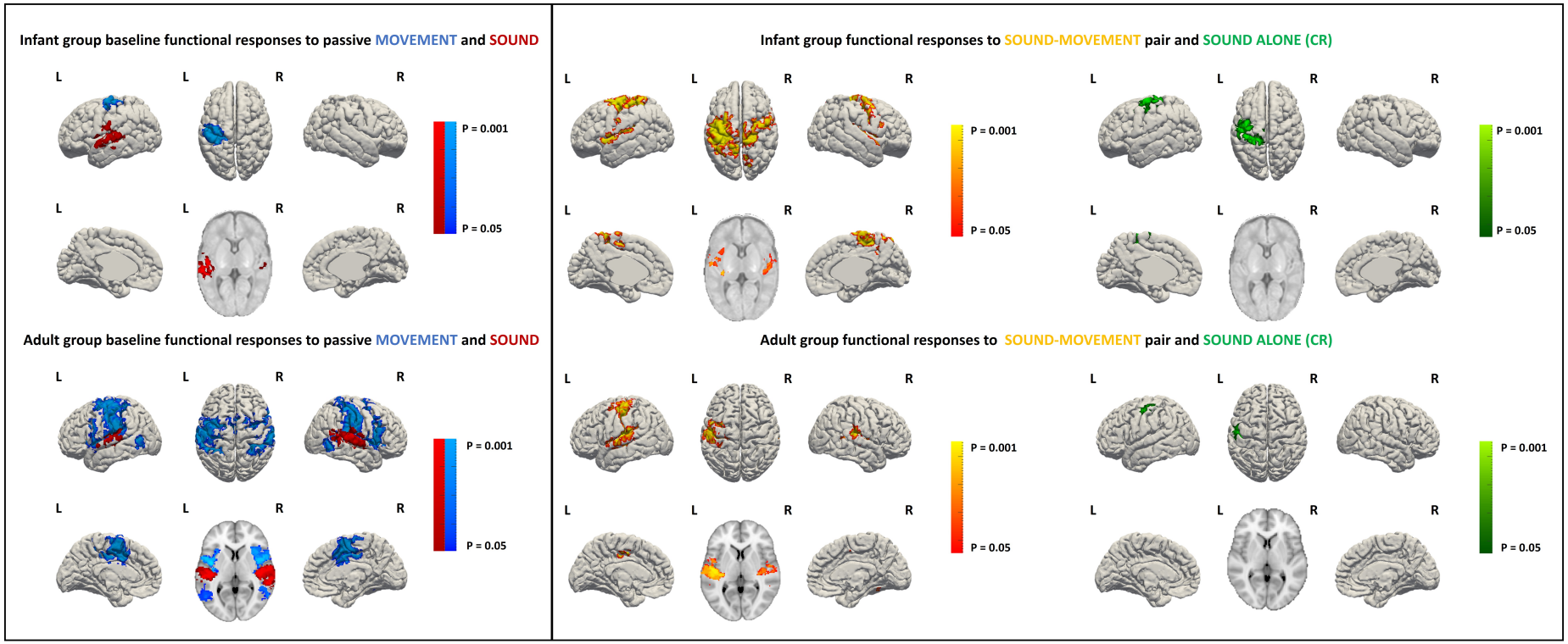

Figure 5.2: FMRI group results of baseline (left) and learning (right) sequences. Significant cluster of functional responses are projected onto the surface of the 3D brain template, in the top row infants group maps (n=11 baseline sound, n=13 baseline movement and learning) and in the bottom row adults group maps (n=10 baselines and learning). In light-blue are shown the group maps of the functional response to passive hand/fingers movement localised in the contralateral SM1 for infants and also in the ipsilateral S1 and SMA for adults. In red the group maps of functional response to sound localised in the auditory cortex for both infants and adults. In red-yellow are shown the group maps of learning (coupled sound and movement), which cover the areas activated during the baseline. While in in green are the group maps of the conditioned response (sound alone trials), which are localised in the contralateral SM1 and ACC for infants, and in S1 only in adults.

As in the infant group, measured BOLD responses within the identified SM1-CR cluster in the adult group were also of significantly higher amplitude in the baseline passive movement and learning conditions (with and without passive movement), in comparison to a negligible response in the baseline auditory condition. Therefore the sensorimotor network was not engaged by auditory stimulation during the baseline condition, but was significantly evoked by the auditory alone test condition after learning (figure 5.3 bottom row).

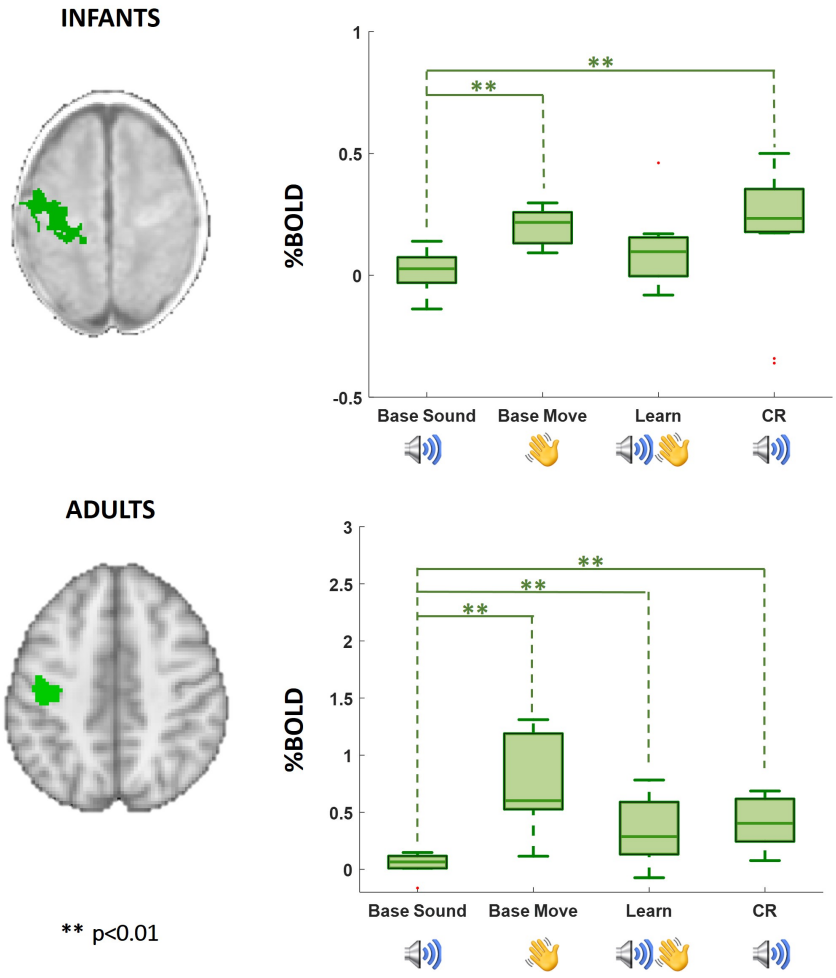

Figure 5.3: Measure of BOLD percentage signal change in the regions of interest relative to the overlapping area of responses to the passive movement and the conditioned response CR (green). Percent signal change was calculated for the sound and movement pre-learning (Base, n=11, n=13), and learning blocks (Learn, n=13) and sound alone (CR, n=13). On the top box-plot infants' data (top panels) show a significant difference of response between the sound pre-learning and both pre-learning hand movement and sound alone during learning. Row adults' data (bottom panels) show a significant difference between the Base sound and all the other events, including sound alone during learning, in both regions of interest.

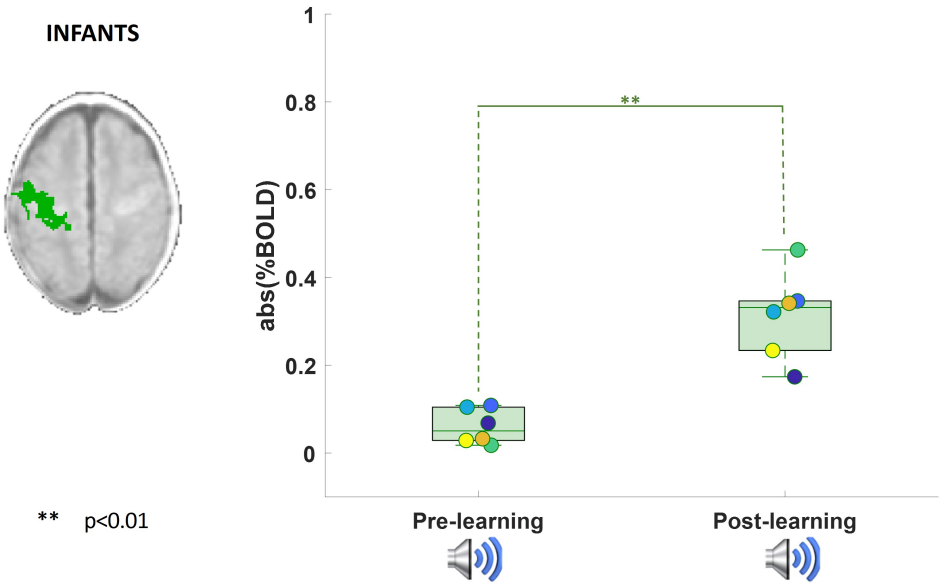

Figure 5.4: Measure of absolute BOLD change in SM1 in responses to the sound alone pre- and post-learning. Each subject is represented by a coloured dot in the two conditions.

A further analysis was carried out to investigate the features of the conditioned response. Single subject HRFs were characterised from the parameter estimates obtained from the fMRI data for each condition. Adult HRFs showed consistency across subjects with positive BOLD responses in S1 following passive movements (both during baseline and learning tasks), negligible responses following the sound during the baseline in contrast to negative BOLD responses following the sound during the learning paradigm (figure 5.5). However, there was great variability in the infant data due to the larger amount of data discard and therefore it was not possible to characterise a conditioned HRF across subjects (figure 5.6). The negative conditioned HRF identified in the adult group might reflect a mismatch between the expected somatosensory stimuli in contrast to its omission, while different patterns of conditioned HRFs were identified in the infant. In contrast to adults, the infant group showed highly variable responses: positive BOLD in 7/13 infants, of which 4/7 infants showed a similar shape seen in the adult group, and negative BOLD in the remaining 5/13 infants. More data would allow exploration of the source of this variability, and therefore could highlight important differences in the way learning is expressed at different developmental stages.

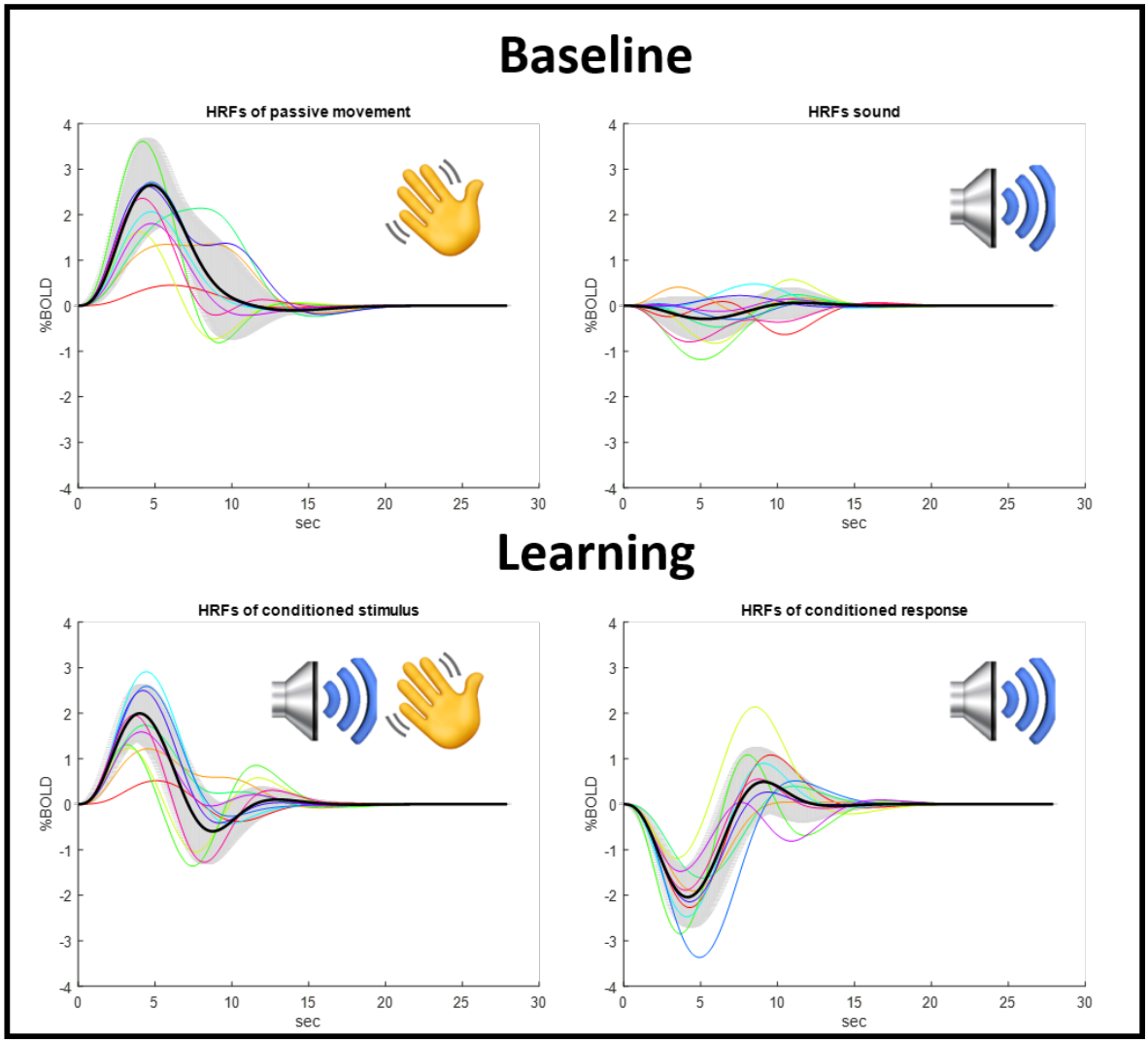

Figure 5.5: Adult HRFs corresponding to different conditions. Subject specific HRFs within S1 for each condition are represented in different colours, while the average trend is represented by the thick black and the standard deviation is represented in grey. Positive BOLD responses were identified following passive fingers movements during the baseline (top left) and learning (bottom left) paradigms. No response was identified in S1 following the sound during the baseline paradigm (top right), while negative BOLD responses were identified following the sound during the learning paradigm (bottom right).

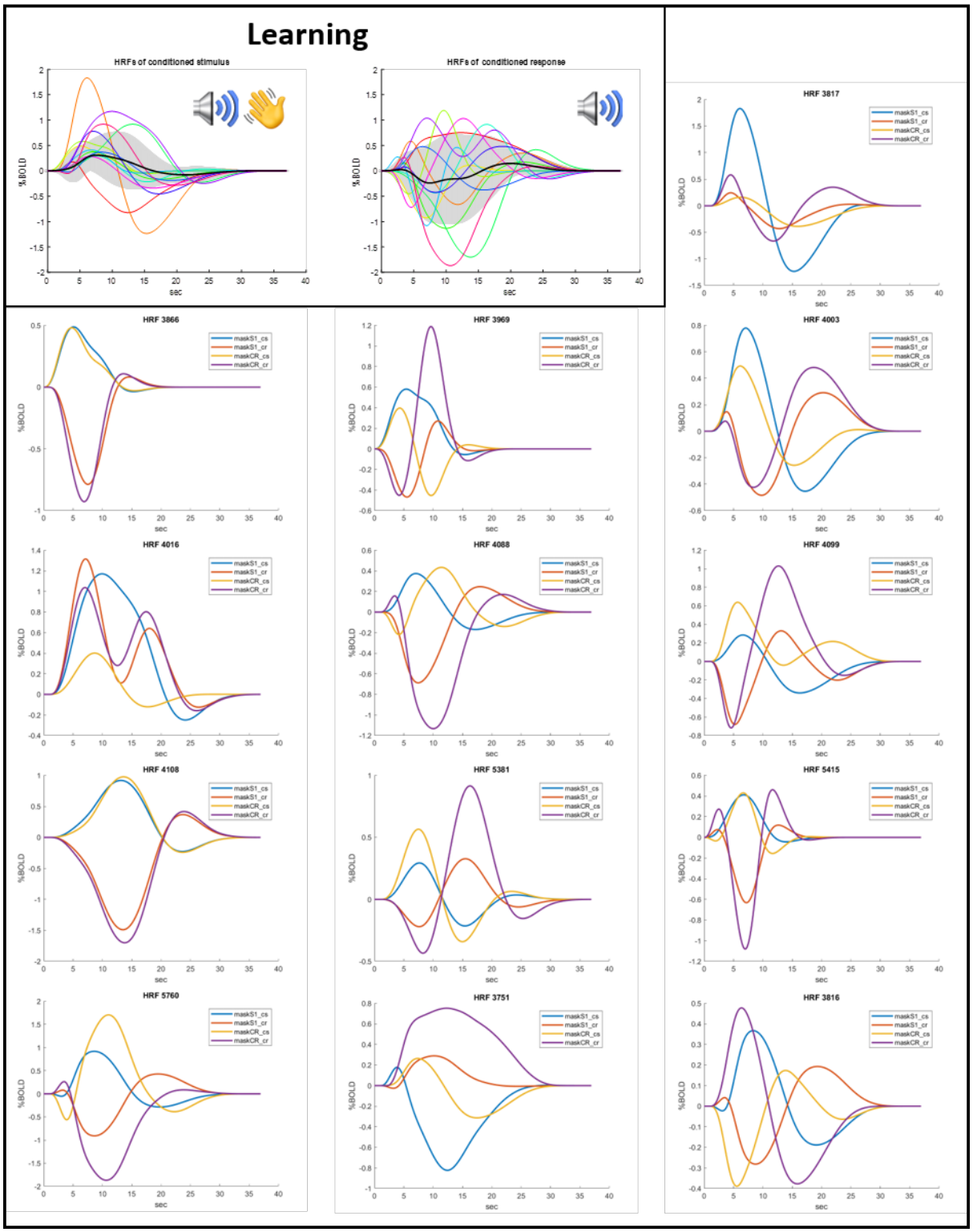

Figure 5.6: Infants' HRF corresponding to different conditions. Subject specific HRFs within S1 mask (blue and red) and CR mask (yellow and purple) clusters for conditioned stimulus (cs) and test trials (sound alone, cr) are represented for each subject. In the bottom left corner the subjects average (thick black line) of the HRF in S1 in response to conditioned stimulus (sound + passive movement) and in CR mask in response to conditioned response (sound alone) during the learning paradigm. Standard errors are represented in grey, and individual subject's responses in different colours.

5.4 Discussion

Across both subject groups, we identified a CR response within the primary sensory cortices as a result of our simple auditory-sensorimotor conditioning paradigm, as described in previous studies with adults where learning-related changes were observed in the motor/premotor cortex following implicit learning of a simple motor sequence or classical conditioning (Hazeltine *et al.,* 1997; Ramnani *et al.,* 2000). In keeping with the spatial representation of this activity, an increase of BOLD response was identified at the time of the test trials (sound alone) supporting associative learning having taken place. It is unclear what the identified increase in BOLD activity may actually reflect, as it could relate to a learning induced increase in neuronal excitability; an error signal due to violation of a sensory prediction; or finally to a predicted execution of movement (Hazeltine *et al.,* 1997). In favour of the latter explanation, the CR in our infant subjects included activity in the contralateral PMC, which is an area thought to play a key role in planning and preparing for movements (Halsband *et al.,* 1993). We also did not see activity in regions such as the anterior cingulate or prefrontal cortices as might be expected as a result of prediction error (Holroyd *et al.,* 2004; Garrison *et al.,* 2013).

In addition to a conditioned response in our infant subjects, the learning task induced a widespread pattern of activation across the entire sensorimotor network including the ipsilateral SM1 and the SMA (figure 5.2, top row middle). This is consistent with data from adults showing a spatial increase in motor cortical representation during the encoding phase of a motor learning task, suggesting that the entire motor network contributes to the learning process itself (Pascual-Leone *et al.,* 1994; Hardwick *et al.,* 2013). The involvement of the SMA during learning in our infant subjects is of particular interest, as it is commonly observed during implicit motor learning tasks in adults where it is thought to encode and coordinate temporal sequences of motor behaviour through generating an internal predictive model (Hazeltine *et al.,* 1997; Sanes, 2003). Increasing activity within the SMA in sensorimotor functional responses is seen with increasing postnatal and postmenstrual age across the human preterm period (Allievi *et al.,* 2016), which

further suggests that ex-utero sensorimotor experience may drive the establishment of SMA co-activation and connectivity in early life.

Activity across the sensorimotor network is of particular significance, as learning can result in sustained changes in resting functional connectivity between co-activated regions in a task, in keeping with network specific neuroplasticity (Pascual-Leone *et al.,* 1994; Büchel *et al.,* 1999; Sanes, 2003; Albert *et al.,* 2009). Both the timing and strength of learning-induced changes in connectivity significantly correlate with task performance, suggesting that increased interaction between involved brain regions is a crucial neural mechanism underlying associative learning (Büchel *et al.,* 1999; van den Bos *et al.,* 2012). In the developing human brain, long-range functional connectivity measures increase and associated network structure rapidly mature during the crucial perinatal period and through early infancy (Doria *et al.,* 2010; Thomason *et al.,* 2013; Gao *et al.,* 2015). Taken together, our results therefore suggest that associative learning may have an important role in overall network development and maturation through triggering and modulating ongoing patterns of network connectivity.

Although changes in cortical activity were seen in both of our subject groups, there were likely to have been significant differences in their behavioural state during the experiment; as the adults were studied during their typical awake state, while the infants were presumed to have been studied during natural sleep which also corresponds to their typical state (as they usually spend 16-18 hours per day asleep (So *et al.,* 2007)). This may suggest that cortical processing related to implicit learning is an intrinsic human property that occurs regardless of behavioural state. Alternatively, it may reflect a clear developmental difference in the need to extrapolate everyday sensory experiences during different age-typical behavioural states. In keeping with the latter, mismatch negativity (MMN) studies have found attenuated cortical responses to variation in stimulus pattern in sleeping adults, while a large amplitude MMN response is observed in both sleeping and awake infants (Sallinen *et al.,* 1994). Sleep generally is thought to play a key role in memory consolidation through mediating early neuroplasticity and overall brain development as it facilitates fundamental processes such as synapse formation and pruning, both of which

are impaired by early sleep deprivation (Shaffery *et al.,* 2006). These effects appear to be further modulated by sleep state, with more significant learning occurring during deeper sleep stages (Tarullo *et al.,* 2011; Tarullo *et al.,* 2016). In support to a developmental difference in the process of learning from the environment, infants' proportion of REM sleep much higher than in adults suggesting an important role of sleep for the brain plasticity (Peirano & Algarín, 2007). In our study, although our infant subjects were presumed to be asleep based on behavioural observations, it was not possible to extrapolate their sleep stage during the time of data collection. Our findings therefore endorse further studies to elucidate precisely how learning occurs in different behavioural states and sleep stages across human development.

5.5 Conclusions

Using a classical conditioning auditory-motor paradigm and fMRI, we aimed to study the underlying neural correlates of associative learning in the newborn human brain. This results demonstrate that infants can learn an association between two co-occurring but distinct non-aversive stimuli and that this is encoded through significant changes in neural activity in the corresponding primary sensory cortices, in addition to activity across the wider sensorimotor network during learning. This implies that even shortly after birth, activity and network connections across the developing human cortex are being constantly shaped by environmental experience. By replicating this finding in a group of adults, we further demonstrate that such learning induced changes in cortical activity are a fundamental process which continues across the lifespan. These results provide novel insight into how the newborn brain establishes its functional architecture and has wide-reaching implications both for understanding the alterations which may lead to later neurodevelopmental disorders and potentially how they could be treated.

"It's not enough what I did in the past - there is also the future."

– Rita Levi-Montalcini –

6

Conclusions

This chapter will first summarise the context that motivate this dissertation and the main objectives. Next, I will list the main outcomes of my research, then detail these contributions and draw possible future directions to extend this research.

6.1 Motivations and Objectives

The aim of this thesis was to advance our understanding of brain development around the time of birth with a particular focus on the sensorimotor system. Brain structure and function undergo drastic changes in perinatal period, as summarised by Pape & Wigglesworth (1979) "in many ways there are greater differences between the brain of a 28-weeks gestation infant and that of a 36 weeks infant, than there are between the brain

of a three month old baby and an adult". This developmental trajectory is guided by a sequence of events that must occur at the right time to ensure correct maturation, and thus when those fail to occur appropriately there might be severe sequelae. In keeping with this, preterm birth is often accompanied by neurodevelopmental disorders with long lasting negative consequences, suggesting that the last trimester of gestation is a critical period for development. Motor impairments (e.g. cerebral palsy (CP)) are among the most common in preterm born patients, in support of animal studies that suggest that sensory and motor systems develop during the last trimester of gestation in humans. Animal studies also suggest that experience-dependent activity plays a major role in the fine tuning of maturation in the brain, which has maximum plasticity during the period of rapid development coinciding with the perinatal period. Given that preterm infants are exposed to an abnormal environment compared to their peers born at full term, it is likely that early sensory experiences might alter the normal trajectory of maturation. While neonatal care has improved the rate of survival in the very young population, the ongoing lack of understanding about the pathophysiology of neurodevelopmental disorders may explain why the incidence rate of negative outcome engendered by premature birth has not reduced. Currently accurate diagnosis is not possible until symptoms are evident, and at this point the potential for recovery may be reduced. Gaining a better understanding of brain development in this critical period is therefore an important need as well as a challenge, which may open new possibilities for early diagnosis. Thereupon further research should examine how this trajectory can be influenced by experience in order to prevent and readjust aberrant developmental paths.

Expanding state-of-the-art tools for early diagnosis and targeted intervention thus is a gradual, challenging, yet important mission. In this framework, the work described in this thesis aimed to advance our knowledge on the **normal trajectory of human sensori-motor development** and the **effect of experience-dependent activity on cortical circuitry during early brain development**.

6.2 Outputs and Outcomes

The results of the experiments I carried out during my thesis revealed that:

- The fundamental organisation of the somatosensory cortex is already present in the brain of preterm infants.
- The functional somatotopic organisation of preterm infants is similar to that seen in the classical "homunculus" of the mature brain.
- I developed a classical conditioning paradigm that can be used to study the underlying neural processes supporting associative learning in human newborn infants.
- Newborn infants can learn an association between two distinct neutral sensory stimuli and the conditional response is mediated by cortical processing.
- During associative learning areas across the stimuli-related wide cortical networks are involved.
- Classical conditioning leads to changes of cortical activity in infants similar to those seen in adults.

6.2.1 Somatotopic mapping of the developing sensorimotor cortex in the preterm human brain

I studied a cohort of 35 healthy preterm infants using a combination of functional MRI and a set of custom-made automated devices, which provided precise and safe stimulation of their wrists, ankles and mouth. I found that the somatosensory functional responses of the preterm brain are already spatially localised in a somatotopic manner like the one described by the classical adult "homunculus". The functional responses resulting from ankle stimulation were located superiorly and medially to those of the wrist, which in turn were located superior to those of the mouth. Additionally, functional responses following wrist stimulation were significantly larger in comparison to those induced by

ankle stimulation. The findings of this study are in line with the radial unit hypothesis as they suggest that before the time of normal human birth, the initial development of the primary sensorimotor cortices (S1 and M1) and their somatotopic map are determined early in gestation by intrinsic genetic factors before later refinement by the establishment of activity-dependent connectivity.

These results have important applications for society and clinical care in light of the increasing rates of preterm birth, as they may explain why these fragile infants frequently suffer from life-long sensory and motor impairment which are largely not amenable to intervention later in childhood. The preterm functional maps I characterised have been made publicly available for download from `brain-development.org` as a reference of the normal somatosensory responses at the preterm time and to facilitate future studies.

6.2.2 Classical conditioning paradigm for the investigation of learning in neonates

I developed a classical conditioning paradigm to study the underlying neural processes of associative learning in newborn infants. Whilst in the literature there are behavioural or EEG classical conditioning studies on newborn infants, and fMRI classical conditioning studies on adults and older children, there are no fMRI classical conditioning studies on newborn infants due to the inherent challenges. Therefore, I carried out a pilot study where I tested 3 different classical conditioning paradigms in which an auditory cue was followed by the passive flexion/extension of the right wrist.

A final paradigm design was identified to investigate associative learning in combination with fMRI even in the young population, which was then used to perform a study in a larger group on neonates, of which the results are presented next.

6.2.3 Cortical processing of auditory-motor associative learning in newborn infants

I used the developed classical conditioning paradigm for newborn infants in combination with fMRI to study a cohort of 24 infants. The analysis of fMRI activity in response to the auditory-motor learning task revealed that newborn infants could learn the association between the two distinct sensory stimuli. Consistent with having learnt the association between the auditory and somatosensory stimuli, I found activation in the contralateral SM1 and anteriorly in the pre-motor cortex in response to the auditory stimuli alone. Additionally, associative learning engaged a wider cortical network compared to the stimuli presented individually. However, it is not clear whether this is due to learning, memory encoding or the integration of different sensory modalities.

These results suggest that learning can shape cortical circuitry and can influence early brain development. Furthermore, by replicating the experiment in a group of adult subjects, I further demonstrated that associative learning induced changes in cortical activity are a fundamental process which continues into adulthood. This work represents the first description of the underlying neural processes supporting associative learning in human newborn infants. It provides an entirely new insight into how the infant brain prepares itself for its role across the lifespan.

6.3 Future directions

The work and results here presented highlight the importance of task-based fMRI as a tool to investigate hypothesis-driven questions that other techniques have no power to address. Nevertheless, these studies included only a small number of subjects due to the great challenge of performing task-fMRI in infants, thus limiting definitive conclusions. Future work could therefore expand those studies to include a larger cohort of infants (including different developmental stages to complete the developmental trajectory), and integrate these findings with results from other complementary techniques.

6.3.1 General challenges

In developmental studies, researchers are constrained by the trade-off between a larger group of subjects and a smaller but more homogeneous group, often resulting in the investigation of small size cohorts. The recruitment of newborn subjects is challenging in itself as asking a family to volunteer in a research study during such a stressful moment (soon after the birth of their child) is understandably often rejected. Moreover, there is still a surprising misconception regarding the safety of MRI amongst the public. Fortunately, there are families that do volunteer to take part in research studies and we are very grateful to them.

Data quality remains one of the greatest challenges of neonatal fMRI studies. While structural images can be reconstructed post-acquisition, head motion may disrupt the timecourse of the signal in irreversible ways when it occurs in between volumes of a functional scan. Although all of the subject preparation and data collection were done carefully, head motion remains unavoidable, thus a substantial proportion of the data, and in some cases the entire data set, have to be discarded. This is accentuated in the specific case of task fMRI as infants are constantly stimulated as part of the experiment. For these reasons, data collection may take a long time even if the final data set is eventually extrapolated only from a small group of subjects.

Performing experiments involving a task with newborn infants requires use of technological tools to provide a precise and consistent stimulus. Over the years, the Human Robotics Group in collaboration with Prof. David Edwards and in particular Dr. Tomoki Arichi (Perinatal Imaging & Health department, King's College London) have developed a set of customised automated devices that overcome this challenge in neonatal research, although there is a widespread preference in resting-state fMRI (rs-fMRI) due to the experimental simplicity. While rs-fMRI data provides a great source for exploratory studies, task-fMRI data provides more specific answers and understanding about realistic situations such as the process of sensory experiences early in life. The two approaches should go hand-in-hand to complement each other, thus there is still the need for more task-fMRI studies

with young subjects.

6.3.2 Normal trajectory of human sensorimotor development

In chapter 3 I demonstrated that the foundation of functional topographical organisation is already established in the developing sensorimotor cortex at 34 weeks PMA. Given the dynamic nature of development in the preterm period, it would however be important to further characterise its dynamic evolution by means of longitudinal studies. These would clarify when the somatotopy achieves mature features such as the recruitment of the SMA and of the ipsilateral side. In view of experience as an important player for the shaping of cortical development, it would also be interesting to investigate the effect of postnatal days on the maturation stage by studying a larger cohort.

Although infants included in the study (Dall'Orso *et al.,* 2018) were considered healthy, there is still a chance that preterm birth altered their normal neurodevelopment and might lead to sensory impairments later in life. For this reason, it is important to have follow-up neurodevelopmental assessment of those infants, so as to compare their neuroimaging results with clinical outcome measures (with standard assessment tools later in childhood). Additionally, collecting similar data from infants at higher risk of negative outcomes, such as the presence of white matter abnormalities, would add value to the findings of the mapping of preterm somatosensory cortex by demonstrating altered functional responses associated to altered brain appearance.

Combining the functional maps with other MRI techniques would provide further insight into the pathophysiology of neurodevelopmental disorders. For instance, diffusion MRI images would complement our findings given the tight relationship between white matter pathology and later adverse developmental outcome such as CP (Arichi *et al.,* 2014; Peyton *et al.,* 2017). As well as structural connectivity, functional connectivity is also maturing with the establishment of cortical networks. It would be therefore interesting to compare the maturation of the spatial extent of functional responses with the underlying functional connectivity of the sensorimotor network.

Finally, future work should explore the tight relationship between cortical maturation and motor behaviour. It is acknowledged that the evolution of general movements which are characteristic during development from 7 weeks (in the foetal period) to 3-5 months corrected age is reflective of underlying brain development, and atypical general movements are predictive of CP (Hadders-Algra, 2018). While most studies have focused either on behaviour or brain development, a crucial next step will be to merge those two approaches and better understand their relationship. It is thought that the wax and wane of specific features of general movement are driven by the transition of specific neuronal activity, hence it will be important to quantitatively measure and characterise the progressive appearance of general movements in parallel with the changes in cortical connectivity and identify possible similar patterns.

6.3.3 Effect of experience-dependent activity on cortical circuitry during early brain development

The study in chapter 5 represents the first description of the underlying neural processes supporting associative learning in human newborn infants, and opens a new perspective into how the infant brain can learn. As data from the fMRI learning study consisted of fragments of the full paradigm due to data exclusion, it was not possible to have sufficient information to compare the initial and final part of the experiment. It would be interesting to reproduce the same conditioning experiment in a larger cohort to identify the dynamic emergence of the conditioned response as well as the possible interplay between cortical and subcortical areas. Additional brain regions such as the anterior cingulate cortex may be engaged during specific phases of learning (e.g. encoding or expression) which could not be identified due to insufficient statistical power resulting from the data fragmentation. More data could potentially reveal more details about the learning process.

Brain injuries that affect the motor and/or sensory pathways disrupt the essential integration between the two systems, which is essential for optimal motor learning and is crucial during the first period after birth. In keeping with this, CP is significantly related to the

integrity of the cortico-spinal tracts (efferent movement pathway) and thalamo-cortical tracts (afferent sensory feedback pathway). Descending cortico-spinal projections initially develop bilaterally from each hemisphere, then activity-dependent mechanisms produce a gradual weakening of ipsilateral and strengthening of contralateral axonal projections leading to a predominately contralateral system (Eyre *et al.,* 2001; Staudt, 2010). Thanks to this transient co-existence of bilateral axonal projections, if a brain injury occurs early in development the cortico-spinal tract can re-organise such that the healthy hemisphere takes control over both sides of the body (Staudt, 2010). Conversely, thalamo-cortical axons project almost entirely to the contralateral hemisphere and reorganise within the affected hemisphere leading to a weaker possibility of readaptation. Although it has been shown that thalamo-cortical projections can bypass even large unilateral periventricular brain lesions to reach their target in S1 (Staudt *et al.,* 2006), somatosensory adaptation is less robust and function restoration is poor (Guzzetta *et al.,* 2007). Targeted somatosensory stimulation could be an important strategy for recovery in children with CP given that somatosensory connectivity strongly influences motor function, even more than motor connectivity (Carmel *et al.,* 2017).

In this view, further experiments should investigate the effect of sensorimotor learning on functional connectivity, for instance by measuring the strengthening of functional connectivity between the somatosensory and auditory network following the auditory-motor associative learning task. This would give us a better understanding of how network activity can be manipulated by external stimulation, hence would provide new insight into how we could train impaired functions, for example using neurofeedback techniques. Neurofeedback is a promising approach to neurorehabilitation as it measures brain activity of the individual while performing a task in real-time and returns it in the form of perceivable feedback. Neurofeedback experiments have the potential to reinforce brain activity (hence behaviour) based on brain activity itself rather than behavioural performance, and it has already been used in stroke patients to improve their motor performance by enhancing the lateralisation of brain activity (Neyedli *et al.,* 2018), to induce visual perceptual learning (Shibata *et al.,* 2011), to train under-connected networks in patients

with ASD (Ramot *et al.,* 2017), and to facilitate implicit motor learning in adults with CP (Alves-Pinto *et al.,* 2017). A deeper understanding of experience-dependent mechanisms would enable exploitation of the enhanced plasticity in the neonatal period for compensating early brain injuries. Although many preliminary studies are needed in these areas of research before it can be applied in clinical practice, a promising future direction would be to use neurofeedback in order to train underdeveloped sensory networks in infants at high risk of developing CP.

In **Conclusion**, the work presented in this thesis showed that fMRI can be used to gather important insights into newborn brain development, which has implications for much needed novel diagnostic approaches and targeted treatments. This dissertation provided the foundations on early characterisation of the maturation of the sensorimotor cortex in the preterm period, which represents the ground truth from which future studies can advance to develop diagnostic tools. Moreover, I describe the first fMRI classical conditioning experiment in newborn infants strengthening the assumption of enhanced plasticity in the immature brain in humans, which is essential for learning and for developing adaptive behaviours. While these findings are only initial steps towards the understanding of newborn brain development, I hope that future work will be carried out to deepen our understanding on how brain activity can be optimally influenced by external sensory stimulation and generate invaluable tools for treatment of children at high risk of cerebral palsy or other neurodevelopmental disorders.

Bibliography

1. Akhmetshina, D., Nasretdinov, A., Zakharov, A., Valeeva, G. & Khazipov, R. The Nature of the Sensory Input to the Neonatal Rat Barrel Cortex. *Journal of Neuroscience* **36,** 9922–9932 (2016).

2. Albert, N. B., Robertson, E. M. & Miall, R. C. The Resting Human Brain and Motor Learning. *Current Biology* **19,** 1023–1027 (2009).

3. Allen, M. C. Neurodevelopmental outcomes of preterm infants. *Current Opinion in Neurology* **21,** 123–128 (2008).

4. Allievi, A. G., Arichi, T., Gordon, A. L. & Burdet, E. Technology-aided assessment of sensorimotor function in early infancy. *Frontiers in Neurology* **5,** 1–10 (2014).

5. Allievi, A. G., Arichi, T., Tusor, N., Kimpton, J., Arulkumaran, S., Counsell, S. J., Edwards, A. D. & Burdet, E. Maturation of Sensori-Motor Functional Responses in the Preterm Brain. *Cerebral Cortex* **26,** 402–413 (2016).

6. Allievi, A. G., Melendez-Calderon, A., Arichi, T., Edwards, A. D. & Burdet, E. An fMRI compatible wrist robotic interface to study brain development in neonates. *Annals of Biomedical Engineering* **41,** 1181–1192 (2013).

7. Altman, N. R. & Bernal, B. Brain Activation in Sedated Children: Auditory and Visual Functional MR Imaging. *Radiology* **221,** 56–63 (2001).

8. Alves-Pinto, A., Turova, V., Blumenstein, T., Hantuschke, C. & Lampe, R. Implicit Learning of a Finger Motor Sequence by Patients with Cerebral Palsy After Neurofeedback. *Applied Psychophysiology and Biofeedback* **42,** 27–37 (2017).

9. An, S., Kilb, W. & Luhmann, H. J. Sensory-evoked and spontaneous gamma and spindle bursts in neonatal rat motor cortex. *The Journal of neuroscience : the official journal of the Society for Neuroscience* **34,** 10870–83 (2014).

10. Anderson, A. W., Marois, R., Colson, E. R., Peterson, B. S., Duncan, C. C., Ehrenkranz, R. A., Schneider, K. C., Gore, J. C. & Ment, L. R. Neonatal auditory activation detected by functional magnetic resonance imaging. *Magnetic Resonance Imaging* **19,** 1–5 (2001).

11. Andiman, S. E., Haynes, R. L., Trachtenberg, F. L., Billiards, S. S., Folkerth, R. D., Volpe, J. J. & Kinney, H. C. The Cerebral Cortex Overlying Periventricular Leukomalacia: Analysis of Pyramidal Neurons. *Brain Pathology* **20,** 803–814 (2010).

12. Arichi, T., Gordon-Williams, R., Allievi, A. G., Groves, A., Burdet, E. & Edwards, A. Computer-controlled stimulation for functional magnetic resonance imaging studies of the neonatal olfactory system. *Acta Paediatrica* **102,** 868–875 (2013).

13. Arichi, T., Counsell, S. J., Allievi, A. G., Chew, A. T., Martinez-Biarge, M., Mondi, V., Tusor, N., Merchant, N., Burdet, E., Cowan, F. M. & Edwards, A. D. The effects of hemorrhagic parenchymal infarction on the establishment of sensori-motor structural and functional connectivity in early infancy. *Neuroradiology* **56,** 985–994 (2014).

14. Arichi, T., Fagiolo, G., Varela, M., Melendez-Calderon, A., Allievi, A. G., Merchant, N., Tusor, N., Counsell, S. J., Burdet, E., Beckmann, C. F. & Edwards, A. D. Development of BOLD signal hemodynamic responses in the human brain. *NeuroImage* **63,** 663–673 (2012).

15. Arichi, T., Moraux, A., Melendez, A., Doria, V., Groppo, M., Merchant, N., Combs, S., Burdet, E., Larkman, D., Counsell, S., Beckmann, C. & Edwards, A. Somatosensory cortical activation identified by functional MRI in preterm and term infants. *NeuroImage* **49,** 2063–2071 (2010).

16. Arichi, T., Whitehead, K., Barone, G., Pressler, R., Padormo, F., Edwards, A. D. & Fabrizi, L. Localization of spontaneous bursting neuronal activity in the preterm human brain with simultaneous EEG-fMRI. *eLife* **6** (2017).

17. Baldoli, C., Scola, E., Della Rosa, P. A., Pontesilli, S., Longaretti, R., Poloniato, A., Scotti, R., Blasi, V., Cirillo, S., Iadanza, A., Rovelli, R., Barera, G. & Scifo, P. Maturation of preterm newborn brains: a fMRI–DTI study of auditory processing of linguistic stimuli and white matter development. *Brain Structure and Function* **220,** 3733–3751 (2015).

18. Balsam, P. D. & Gallistel, C. R. Temporal maps and informativeness in associative learning. *Trends in Neurosciences* **32,** 73–78 (2009).

19. Balsam, P., Drew, M. & Gallistel, C. Time and Associative Learning. *Comparative Cognition & Behavior Reviews* **5,** 1–22 (2010).

20. Bartoletti, A., Medini, P., Berardi, N. & Maffei, L. Environmental enrichment prevents effects of dark-rearing in the rat visual cortex. *Nature Neuroscience* **7,** 215–216 (2004).

21. Batalle, D., Edwards, A. D. & O'Muircheartaigh, J. Annual Research Review: Not just a small adult brain: understanding later neurodevelopment through imaging the neonatal brain. *Journal of Child Psychology and Psychiatry* **59,** 350–371 (2018).

22. Bauer, P. J. Toward a neuro-developmental account of the development of declarative memory. *Developmental Psychobiology* **50,** 19–31 (2008).

23. Beckmann, C. F. & Smith, S. M. Probabilistic independent component analysis for functional magnetic resonance imaging. *IEEE Trans.Med Imaging* **23,** 137–152 (2004).

24. Beckmann, C. F., DeLuca, M., Devlin, J. T. & Smith, S. M. Investigations into resting-state connectivity using independent component analysis. *Philosophical Transactions of the Royal Society B: Biological Sciences* **360,** 1001–1013 (2005).

25. Ben-Ari, Y., Khazipov, R., Leinekugel, X., Caillard, O. & Gaiarsa, J.-L. GABAA, NMDA and AMPA receptors: a developmentally regulated 'ménage à trois'. *Trends in Neurosciences* **20,** 523–529 (1997).

26. Bennet, L., Van Den Heuij, L., M Dean, J., Drury, P., Wassink, G. & Jan Gunn, A. Neural plasticity and the Kennard principle: Does it work for the preterm brain? *Clinical and Experimental Pharmacology and Physiology* **40,** 774–784 (2013).

27. Berardi, N., Pizzorusso, T. & Maffei, L. Critical periods during sensory development. *Current Opinion in Neurobiology* **10,** 138–145 (2000).

28. Biswal, B., Yetkin, F. Z., Haughton, V. M. & Hyde, J. S. Functional connectivity in the motor cortex of resting human brain using echo-planar MRI. *Magnetic resonance in medicine : official journal of the Society of Magnetic Resonance in Medicine / Society of Magnetic Resonance in Medicine* **34,** 537–41 (1995).

29. Blankenburg, F., Ruben, J., Meyer, R., Schwiemann, J. & Villringer, A. Evidence for a Rostral-to-Caudal Somatotopic Organization in Human Primary Somatosensory Cortex with Mirror-reversal in Areas 3b and 1. *Cerebral Cortex* **13,** 987–993 (2003).

30. Blass, E. M., Ganchrow, J. R. & Steiner, J. E. Classical conditioning in newborn humans 2-48 hours of age. *Infant Behavior and Development* **7,** 223–235 (1984).

31. Blatow, M., Nennig, E., Durst, A., Sartor, K. & Stippich, C. fMRI reflects functional connectivity of human somatosensory cortex. *NeuroImage* **37,** 927–936 (2007).

32. Born, A. P., Miranda, M. J., Rostrup, E., Toft, P. B., Peitersen, B., Larsson, H. B. & Lou, H. C. Functional Magnetic Resonance Imaging of the Normal and Abnormal Visual System in Early Life. *Neuropediatrics* **31,** 24–32 (2000).

33. Brew, N., Walker, D. & Wong, F. Y. Cerebral vascular regulation and brain injury in preterm infants. *American Journal of Physiology-Regulatory, Integrative and Comparative Physiology* **306,** R773–R786 (2014).

34. Bright, M. G. & Murphy, K. Is fMRI "noise" really noise? Resting state nuisance regressors remove variance with network structure. *NeuroImage* **114,** 158–169 (2015).

35. Brillouin, L. *Science and Information Theory* (Academic, 1962).

36. Brodmann, K. K. Vergleichende Lokalisationslehre der Großhirnrinde: in ihren Prinzipien dargestellt auf Grund des Zellenbaues. *Johann Ambrosius Barth, Leipzig,* 324 (1909).

37. Büchel, C., Dolan, R. J., Armony, J. L. & Friston, K. J. Amygdala–Hippocampal Involvement in Human Aversive Trace Conditioning Revealed through Event-Related Functional Magnetic Resonance Imaging. *Journal of Neuroscience* **19,** 10869–10876 (1999).

38. Büchel, C., Morris, J., Dolan, R. J. & Friston, K. J. Brain systems mediating aversive conditioning: An event-related fMRI study. *Neuron* (1998).

39. Buxton, R. B. *Introduction to functional magnetic resonance imaging: Principles and techniques* (2009).

40. Buxton, R. B. & Frank, L. R. A Model for the Coupling between Cerebral Blood Flow and Oxygen Metabolism during Neural Stimulation. *Journal of Cerebral Blood Flow & Metabolism* **17,** 64–72 (1997).

41. Buxton, R. B., Uludağ, K., Dubowitz, D. J. & Liu, T. T. Modeling the hemodynamic response to brain activation. *NeuroImage* **23,** S220–S233 (2004).

42. Buxton, R. B., Wong, E. C. & Frank, L. R. Dynamics of blood flow and oxygenation changes during brain activation: The balloon model. *Magnetic Resonance in Medicine* **39,** 855–864 (1998).

43. Carmel, J. B., Gordon, A. M., Friel, K. M., Barachant, A., Kuo, H.-C., Ferre, C. & Gupta, D. Effect of sensory and motor connectivity on hand function in pediatric hemiplegia. *Annals of Neurology* **82,** 766–780 (2017).

44. Chen, J. J. & Pike, G. B. BOLD-specific cerebral blood volume and blood flow changes during neuronal activation in humans. *NMR in Biomedicine* **22** (2009).

45. Chen, J. J. & Pike, G. B. Origins of the BOLD post-stimulus undershoot. *NeuroImage* **46,** 559–568 (2009).

46. Cheng, D. T., Disterhoft, J. F., Power, J. M., Ellis, D. A. & Desmond, J. E. Neural substrates underlying human delay and trace eyeblink conditioning. *Proceedings of the National Academy of Sciences of the United States of America* **105,** 8108–13 (2008).

47. Chipaux, M., Colonnese, M. T., Mauguen, A., Fellous, L., Mokhtari, M., Lezcano, O., Milh, M., Dulac, O., Chiron, C., Khazipov, R. & Kaminska, A. Auditory Stimuli Mimicking Ambient Sounds Drive Temporal "Delta-Brushes" in Premature Infants. *PLoS ONE* **8** (ed de Castro, F.) e79028 (2013).

48. Christian, K. M. & Thompson, R. F. Neural Substrates of Eyeblink Conditioning: Acquisition and Retention. *Learning & Memory* **10,** 427–455 (2003).

49. Clark, R. E. & Squire, L. R. Classical conditioning and brain systems: the role of awareness. *Science (New York, N.Y.)* **280,** 77–81 (1998).

50. Clause, A., Kim, G., Sonntag, M., Weisz, C. J., Vetter, D. E., Rűbsamen, R. & Kandler, K. The Precise Temporal Pattern of Prehearing Spontaneous Activity Is Necessary for Tonotopic Map Refinement. *Neuron* **82,** 822–835 (2014).

51. Colonnese, M. T., Kaminska, A., Minlebaev, M., Milh, M., Bloem, B., Lescure, S., Moriette, G., Chiron, C., Ben-Ari, Y. & Khazipov, R. A Conserved Switch in Sensory Processing Prepares Developing Neocortex for Vision. *Neuron* **67,** 480–498 (2010).

52. Colonnese, M. T., Phillips, M. A., Constantine-Paton, M., Kaila, K. & Jasanoff, A. Development of hemodynamic responses and functional connectivity in rat somatosensory cortex. *Nature Neuroscience* **11,** 72–79 (2008).

53. Committee on Fetus and Newborn. Age Terminology During the Perinatal Period. *PEDIATRICS* **114,** 1362–1364 (2004).

54. Connor, D. A. & Gould, T. J. The role of working memory and declarative memory in trace conditioning. *Neurobiology of Learning and Memory* **134,** 193–209 (2016).

55. Dall'Orso, S., Steinweg, J., Allievi, A. G., Edwards, A. D., Burdet, E. & Arichi, T. Somatotopic Mapping of the Developing Sensorimotor Cortex in the Preterm Human Brain. *Cerebral Cortex* **28,** 2507–2515 (2018).

56. De Luca, M., Beckmann, C. F., De Stefano, N., Matthews, P. M. & Smith, S. M. fMRI resting state networks define distinct modes of long-distance interactions in the human brain. *NeuroImage* **29,** 1359–1367 (2006).

57. De Graaf-Peters, V. B. & Hadders-Algra, M. Ontogeny of the human central nervous system: What is happening when? *Early Human Development* **82,** 257–266 (2006).

58. De Villers-Sidani, E., Chang, E. F., Bao, S. & Merzenich, M. M. Critical Period Window for Spectral Tuning Defined in the Primary Auditory Cortex (A1) in the Rat. *Journal of Neuroscience* **27,** 180–189 (2007).

59. Dean, D. C., Dirks, H., O'Muircheartaigh, J., Walker, L., Jerskey, B. A., Lehman, K., Han, M., Waskiewicz, N. & Deoni, S. C. L. Pediatric neuroimaging using magnetic resonance imaging during non-sedated sleep. *Pediatric Radiology* **44,** 64–72 (2014).

60. DeCasper, A. & Fifer, W. Of human bonding: newborns prefer their mothers' voices. *Science* **208,** 1174–1176 (1980).

61. Dehaene-Lambertz, G., Dehaene, S. & Hertz-Pannier, L. Functional neuroimaging of speech perception in infants. *Science (New York, N.Y.)* **298,** 2013–5 (2002).

62. Del Rio-Bermudez, C., Sokoloff, G. & Blumberg, M. S. Sensorimotor Processing in the Newborn Rat Red Nucleus during Active Sleep. *Journal of Neuroscience* **35,** 8322–8332 (2015).

63. Diamond, M. E. & Arabzadeh, E. Whisker sensory system – From receptor to decision. *Progress in Neurobiology* **103,** 28–40 (2013).

64. Doria, V., Beckmann, C. F., Arichi, T., Merchant, N., Groppo, M., Turkheimer, F. E., Counsell, S. J., Murgasova, M., Aljabar, P., Nunes, R. G., Larkman, D. J., Rees, G. & Edwards, A. D. Emergence of resting state networks in the preterm human brain. *Proceedings of the National Academy of Sciences of the United States of America* **107,** 20015–20 (2010).

65. Drew, M. R., Zupan, B., Cooke, A., Couvillon, P. A. & Balsam, P. D. Temporal control of conditioned responding in goldfish. *Journal of experimental psychology. Animal behavior processes* **31,** 31–9 (2005).

66. Dunsmoor, J. E., Bandettini, P. A. & Knight, D. C. Impact of continuous versus intermittent CS-UCS pairing on human brain activation during Pavlovian fear conditioning. *Behavioral Neuroscience* **121,** 635–642 (2007).

67. Dunsmoor, J. E., Bandettini, P. A. & Knight, D. C. Neural correlates of unconditioned response diminution during Pavlovian conditioning. *NeuroImage* **40,** 811–817 (2008).

68. Edwards, A. D. & Arthurs, O. J. Paediatric MRI under sedation: is it necessary? What is the evidence for the alternatives? *Pediatric Radiology* **41,** 1353–1364 (2011).

69. Eichenbaum, H. Time (and space) in the hippocampus. *Current opinion in behavioral sciences* **17,** 65–70 (2017).

70. Eisenberg, R. B. *Auditory competence in early life: The roots of communicative behavior. - PsycNET* (U Park Press, 1976).

71. Ejaz, N., Hamada, M. & Diedrichsen, J. Hand use predicts the structure of representations in sensorimotor cortex. *Nature Neuroscience* **18,** 1034–1040 (2015).

72. Emberson, L. L., Richards, J. E. & Aslin, R. N. Top-down modulation in the infant brain: Learning-induced expectations rapidly affect the sensory cortex at 6 months. *Proceedings of the National Academy of Sciences* **112,** 9585–9590 (2015).

73. Eyre, J. A., Miller, S., Clowry, G. J., Conway, E. A. & Watts, C. Functional corticospinal projections are established prenatally in the human foetus permitting involvement in the development of spinal motor centres. *Brain* **123,** 51–64 (2000).

74. Eyre, J. A., Taylor, J. P., Villagra, F., Smith, M. & Miller, S. Evidence of activity-dependent withdrawal of corticospinal projections during human development. *Neurology* **57,** 1543–1554 (2001).

75. Eyre, J. Developmental aspects of corticospinal projections. *Handbook of Clinical Neurophysiology* **4,** 27–57 (2004).

76. Fabrizi, L., Slater, R., Worley, A., Meek, J., Boyd, S., Olhede, S. & Fitzgerald, M. A Shift in Sensory Processing that Enables the Developing Human Brain to Discriminate Touch from Pain. *Current Biology* **21,** 1552–1558 (2011).

77. Farkas, T., Kis, Z., Toldi, J. & Wolff, J.-R. Activation of the primary motor cortex by somatosensory stimulation in adult rats is mediated mainly by associational connections from the somatosensory cortex. *Neuroscience* **90,** 353–361 (1999).

78. Fawke, J. Neurological outcomes following preterm birth. *Seminars in Fetal and Neonatal Medicine* **12,** 374–382 (2007).

79. Feldman, D. E. & Brecht, M. Map Plasticity in Somatosensory Cortex. *Science* **310,** 810–815 (2005).

80. Fifer, W. P., Byrd, D. L., Kaku, M., Eigsti, I.-M., Isler, J. R., Grose-Fifer, J., Tarullo, A. R. & Balsam, P. D. Newborn infants learn during sleep. *Proceedings of the National Academy of Sciences* **107,** 10320–10323 (2010).

81. Fitzgerald, H. E. & Brackbill, Y. Classical conditioning in infancy: development and constraints. *Psychological Bulletin* **83,** 353–376 (1976).

82. Florence, S. L., Jain, N., Pospichal, M. W., Beck, P. D., Sly, D. L. & Kaas, J. H. Central reorganization of sensory pathways following peripheral nerve regeneration in fetal monkeys. *Nature* **381,** 69–71 (1996).

83. Fox, K. A critical period for experience-dependent synaptic plasticity in rat barrel cortex. *Journal of Neuroscience* **12,** 1826–1838 (1992).

84. Fox, K., Henley, J. & Isaac, J. Experience-dependent development of NMDA receptor transmission. *Nature Neuroscience* **2,** 297–299 (1999).

85. Fransson, P., Åden, U., Blennow, M. & Lagercrantz, H. The Functional Architecture of the Infant Brain as Revealed by Resting-State fMRI. *Cerebral Cortex* **21,** 145–154 (2011).

86. Friston, K. J., Holmes, A. P., Worsley, K. J., Poline, J.-P., Frith, C. D. & Frackowiak, R. S. J. Statistical parametric maps in functional imaging: A general linear approach. *Human Brain Mapping* **2,** 189–210 (1994).

87. Friston, K. J., Williams, S., Howard, R., Frackowiak, R. S. J. & Turner, R. Movement-Related effects in fMRI time-series. *Magnetic Resonance in Medicine* **35,** 346–355 (1996).

88. Friston, K., Frith, C., Turner, R. & Frackowiak, R. Characterizing Evoked Hemodynamics with fMRI. *NeuroImage* **2,** 157–165 (1995).

89. Fukuchi-Shimogori, T. & Grove, E. A. Neocortex Patterning by the Secreted Signaling Molecule FGF8. *Science* **294,** 1071–1074 (2001).

90. Gallistel, C. R. & Gibbon, J. Time, rate, and conditioning. *Psychological review* **107,** 289–344 (2000).

91. Ganguly, K., Schinder, A. F., Wong, S. T. & Poo, M.-m. GABA Itself Promotes the Developmental Switch of Neuronal GABAergic Responses from Excitation to Inhibition. *Cell* **105,** 521–532 (2001).

92. Gao, W., Alcauter, S., Smith, J. K., Gilmore, J. H. & Lin, W. Development of human brain cortical network architecture during infancy. *Brain Structure and Function* **220,** 1173–1186 (2015).

93. Garrison, J., Erdeniz, B. & Done, J. Prediction error in reinforcement learning: A meta-analysis of neuroimaging studies. *Neuroscience & Biobehavioral Reviews* **37,** 1297–1310 (2013).

94. Gassert, R., Burdet, E. & Chinzei, K. Opportunities and Challenges in MR-Compatible Robotics. *IEEE Engineering in Medicine and Biology Magazine* **27,** 15–22 (2008).

95. Ghosh, A., Haiss, F., Sydekum, E., Schneider, R., Gullo, M., Wyss, M. T., Mueggler, T., Baltes, C., Rudin, M., Weber, B. & Schwab, M. E. Rewiring of hindlimb corticospinal neurons after spinal cord injury. *Nature Neuroscience* **13,** 97–104 (2010).

96. Gibbon, J. Scalar expectancy theory and Weber's law in animal timing. *Psychological Review* **84,** 279–325 (1977).

97. Glover, G. H. Deconvolution of Impulse Response in Event-Related BOLD fMRI1. *NeuroImage* **9,** 416–429 (1999).

98. Griffanti, L., Douaud, G., Bijsterbosch, J., Evangelisti, S., Alfaro-Almagro, F., Glasser, M. F., Duff, E. P., Fitzgibbon, S., Westphal, R., Carone, D., Beckmann, C. F. & Smith, S. M. Hand classification of fMRI ICA noise components. *NeuroImage* **154,** 188–205 (2017).

99. Guzzetta, A., Bonanni, P., Biagi, L., Tosetti, M., Montanaro, D., Guerrini, R. & Cioni, G. Reorganisation of the somatosensory system after early brain damage. *Clinical Neurophysiology* **118,** 1110–1121 (2007).

100. Hadders-Algra, M. Neural substrate and clinical significance of general movements: an update. *Developmental Medicine & Child Neurology* **60,** 39–46 (2018).

101. Háden, G. P., Honing, H. & Winkler, I. *Newborn infants are sensitive to sound timing* tech. rep. (2012), 378–379.

102. Hajnal, J. V., Myers, R., Oatridge, A., Schwieso, J. E., Young, I. R. & Bydder, G. M. Artifacts due to stimulus correlated motion in functional imaging of the brain. *Magnetic Resonance in Medicine* **31,** 283–291 (1994).

103. Halsband, U., Ito, N., Tanji, J. & Freund, H.-J. The role of premotor cortex and the supplementary motor area in the temporal control of movement in man. *Brain* **116,** 243–266 (1993).

104. Handwerker, D. A., Ollinger, J. M. & D'Esposito, M. Variation of BOLD hemodynamic responses across subjects and brain regions and their effects on statistical analyses. *NeuroImage* **21,** 1639–1651 (2004).

105. Hanganu, I. L., Ben-Ari, Y. & Khazipov, R. Retinal waves trigger spindle bursts in the neonatal rat visual cortex. *The Journal of neuroscience : the official journal of the Society for Neuroscience* **26,** 6728–36 (2006).

106. Hanson, L. G. Is quantum mechanics necessary for understanding magnetic resonance? *Concepts in Magnetic Resonance Part A* **32A,** 329–349 (2008).

107. Hardiman, M. J. & Yeo, C. H. The Effect of Kainic Acid Lesions of the Cerebellar Cortex on the Conditioned Nictitating Membrane Response in the Rabbit. *European Journal of Neuroscience* **4,** 966–980 (1992).

108. Hardwick, R. M., Rottschy, C., Miall, R. C. & Eickhoff, S. B. A quantitative meta-analysis and review of motor learning in the human brain. *NeuroImage* **67,** 283–297 (2013).

109. Hazeltine, E., Grafton, S. T. & Ivry, R. Attention and stimulus characteristics determine the locus of motor- sequence encoding. A PET study. *Brain* **120,** 123–140 (1997).

110. Hebb, D. O. *The Organization of Behavior: A Neuropsychological Approach* (1949).

111. Heed, T. & Röder, B. Common Anatomical and External Coding for Hands and Feet in Tactile Attention: Evidence from Event-related Potentials. *Journal of Cognitive Neuroscience* **22,** 184–202 (2010).

112. Henson, R. in *Statistical Parametric Mapping: The analysis of functional brain images.* 193–210 (Elsevier, 2006).

113. Henson, R. in *Statistical Parametric Mapping* 193–210 (Academic Press, 2007).

114. Herbert, J. S., Eckerman, C. O., Goldstein, R. F. & Stanton, M. E. Contrasts in Infant Classical Eyeblink Conditioning as a Function of Premature Birth. *Infancy* **5,** 367–383 (2004).

115. Herbert, J. S., Eckerman, C. O. & Stanton, M. E. The Ontogeny of Human Learning in Delay, Long-Delay, and Trace Eyeblink Conditioning. *Behavioral Neuroscience* **117,** 1196–1210 (2003).

116. Herlenius, E. & Lagercrantz, H. Neurotransmitters and neuromodulators during early human development. *Early Human Development* **65,** 21–37 (2001).

117. Hlustik, P., Solodkin, A., Gullapalli, R. P., Noll, D. C. & Small, S. L. Somatotopy in Human Primary Motor and Somatosensory Hand Representations Revisited. *Cerebral Cortex* **11,** 312–321 (2001).

118. Hoerder-Suabedissen, A. & Molnár, Z. Development, evolution and pathology of neocortical subplate neurons. *Nature Reviews Neuroscience* **16,** 133–146 (2015).

119. Holroyd, C. B., Nieuwenhuis, S., Yeung, N., Nystrom, L., Mars, R. B., Coles, M. G. H. & Cohen, J. D. Dorsal anterior cingulate cortex shows fMRI response to internal and external error signals. *Nature Neuroscience* **7,** 497–498 (2004).

120. Hooks, B. M. & Chen, C. Critical Periods in the Visual System: Changing Views for a Model of Experience-Dependent Plasticity. *Neuron* **56,** 312–326 (2007).

121. Huang, R. S. & Sereno, M. I. Dodecapus: An MR-compatible system for somatosensory stimulation. *NeuroImage* **34,** 1060–1073 (2007).

122. Hughes, E. J., Winchman, T., Padormo, F., Teixeira, R., Wurie, J., Sharma, M., Fox, M., Hutter, J., Cordero-Grande, L., Price, A. N., Allsop, J., Bueno-Conde, J., Tusor, N., Arichi, T., Edwards, A. D., Rutherford, M. A., Counsell, S. J. & Hajnal, J. V. A dedicated neonatal brain imaging system. *Magnetic Resonance in Medicine* **78,** 794–804 (2017).

123. Hüppi, P. S., Warfield, S., Kikinis, R., Barnes, P. D., Zientara, G. P., Jolesz, F. A., Tsuji, M. K. & Volpe, J. J. Quantitative magnetic resonance imaging of brain development in premature and mature newborns. *Annals of Neurology* **43,** 224–235 (1998).

124. Huttenlocher, P. R. Morphometric study of human cerebral cortex development. *Neuropsychologia* **28,** 517–527 (1990).

125. Inácio, A. R., Nasretdinov, A., Lebedeva, J. & Khazipov, R. Sensory feedback synchronizes motor and sensory neuronal networks in the neonatal rat spinal cord. *Nature Communications* **7,** 13060 (2016).

126. Ivkovich, D. & Stanton, M. E. Effects of Early Hippocampal Lesions on Trace, Delay, and Long-Delay Eyeblink Conditioning in Developing Rats. *Neurobiology of Learning and Memory* **76,** 426–446 (2001).

127. Jenkinson, M., Bannister, P., Brady, M. & Smith, S. Improved Optimization for the Robust and Accurate Linear Registration and Motion Correction of Brain Images. *NeuroImage* **17,** 825–841 (2002).

128. Jenkinson, M., Beckmann, C. F., Behrens, T. E., Woolrich, M. W. & Smith, S. M. FSL. *NeuroImage* **62,** 782–790 (2012).

129. Juenger, H., de Haan, B., Krageloh-Mann, I., Staudt, M. & Karnath, H.-O. Early Determination of Somatosensory Cortex in the Human Brain. *Cerebral Cortex* **21,** 1827–1831 (2011).

130. Kaminska, A., Delattre, V., Laschet, J., Dubois, J., Labidurie, M., Duval, A., Manresa, A., Magny, J. .-.-F., Hovhannisyan, S., Mokhtari, M., Ouss, L., Boissel, A., Hertz-Pannier, L., Sintsov, M., Minlebaev, M., Khazipov, R. & Chiron, C. Cortical Auditory-Evoked Responses in Preterm Neonates: Revisited by Spectral and Temporal Analyses. *Cerebral Cortex* **28,** 3429–3444 (2018).

131. Kanold, P. O. & Luhmann, H. J. The Subplate and Early Cortical Circuits. *Annual Review of Neuroscience* **33,** 23–48 (2010).

132. Kattoor, J., Gizewski, E. R., Kotsis, V., Benson, S., Gramsch, C., Theysohn, N., Maderwald, S., Forsting, M., Schedlowski, M. & Elsenbruch, S. Fear Conditioning in an Abdominal Pain Model: Neural Responses during Associative Learning and Extinction in Healthy Subjects. *PLoS ONE* **8** (ed Sakakibara, M.) e51149 (2013).

133. Khazipov, R. & Luhmann, H. J. Early patterns of electrical activity in the developing cerebral cortex of humans and rodents. *Trends in Neurosciences* **29,** 414–418 (2006).

134. Khazipov, R., Sirota, A., Leinekugel, X., Holmes, G. L., Ben-Ari, Y. & Buzsáki, G. Early motor activity drives spindle bursts in the developing somatosensory cortex. *Nature* **432,** 758–761 (2004).

135. Knight, D. C. Neural Substrates Mediating Human Delay and Trace Fear Conditioning. *Journal of Neuroscience* **24,** 218–228 (2004).

136. Kocak, M., Ulmer, J. L., Sahin Ugurel, M., Gaggl, W. & Prost, R. W. Motor Homunculus: Passive Mapping in Healthy Volunteers by Using Functional MR Imaging—Initial Results. *Radiology* **251,** 485–492 (2009).

137. Kostović, I. & Jovanov-Milošević, N. The development of cerebral connections during the first 20–45 weeks' gestation. *Seminars in Fetal and Neonatal Medicine* **11,** 415–422 (2006).

138. Kwong, K. K., Belliveau, J. W., Chesler, D. A., Goldberg, I. E., Weisskoff, R. M., Poncelet, B. P., Kennedy, D. N., Hoppel, B. E., Cohen, M. S. & Turner, R. Dynamic magnetic resonance imaging of human brain activity during primary sensory stimulation. *Proceedings of the National Academy of Sciences of the United States of America* **89,** 5675–9 (1992).

139. Ladher, R. & Schoenwolf, G. C. in *Developmental Neurobiology* 1–20 (Kluwer Academic Publishers-Plenum Publishers, New York, 2005).

140. Lagercrantz, H. *The newborn brain : neuroscience and clinical applications* 412 (Cambridge University Press, 2010).

141. Larroque, B., Ancel, P.-Y., Marret, S., Marchand, L., André, M., Arnaud, C., Pierrat, V., Rozé, J.-C., Messer, J., Thiriez, G., Burguet, A., Picaud, J.-C., Bréart, G. & Kaminski, M. Neurodevelopmental disabilities and special care of 5-year-old children born before 33 weeks of gestation (the EPIPAGE study): a longitudinal cohort study. *The Lancet* **371,** 813–820 (2008).

142. Lau, C., Alagugurusamy, R., Schanler, R., Smith, E. & Shulman, R. Characterization of the developmental stages of sucking in preterm infants during bottle feeding. *Acta Paediatrica* **89,** 846–852 (2000).

143. Laughlin, S. B. Communication in Neuronal Networks. *Science* **301,** 1870–1874 (2003).

144. Li, L., Weiss, C., Disterhoft, J. F. & Wyrwicz, A. M. Functional magnetic resonance imaging in the awake rabbit: a system for stimulus presentation and response detection during eyeblink conditioning. *Journal of Neuroscience Methods* **130,** 45–52 (2003).

145. Lindner, K., Neubert, J., Pfannmöller, J., Lotze, M., Hamm, A. O. & Wendt, J. Fear-potentiated startle processing in humans: Parallel fMRI and orbicularis EMG assessment during cue conditioning and extinction. *International Journal of Psychophysiology* **98,** 535–545 (2015).

146. Lindquist, M. A. The Statistical Analysis of fMRI Data. *Statistical Science* **23,** 439–464 (2008).

147. Linnman, C., Rougemont-Bücking, A., Beucke, J. C., Zeffiro, T. A. & Milad, M. R. Unconditioned responses and functional fear networks in human classical conditioning. *Behavioural Brain Research* **221,** 237–245 (2011).

148. Lipsitt, L. P. Learning and emotion in infants. *Pediatrics* **102,** 1262–1267 (1998).

149. Lipton, S. A. & Nakanishi, N. Shakespeare in love—with NMDA receptors? *Nature Medicine* **5,** 270–271 (1999).

150. Little, A. H., Lipsitt, L. P. & Rovee-Collier, C. Classical conditioning and retention of the infant's eyelid response: Effects of age and interstimulus interval. *Journal of Experimental Child Psychology* **37,** 512–524 (1984).

151. Lømo, T. The discovery of long-term potentiation. *Philosophical Transactions of the Royal Society of London. Series B: Biological Sciences* **358** (eds Bliss, T. V. P., Collingridge, G. L. & Morris, R. G. M.) 617–620 (2003).

152. Lonsdorf, T. B., Menz, M. M., Andreatta, M., Fullana, M. A., Golkar, A., Haaker, J., Heitland, I., Hermann, A., Kuhn, M., Kruse, O., Meir Drexler, S., Meulders, A., Nees, F., Pittig, A., Richter, J., Römer, S., Shiban, Y., Schmitz, A., Straube, B., Vervliet, B., Wendt, J., Baas, J. M. & Merz, C. J. *Don't fear 'fear conditioning': Methodological considerations for the design and analysis of studies on human fear acquisition, extinction, and return of fear* 2017.

153. López-Bendito, G. & Molnár, Z. Thalamocortical development: how are we going to get there? *Nature Reviews Neuroscience* **4,** 276–289 (2003).

154. MacDonald, A. W., Cohen, J. D., Stenger, A. V. & Carter, C. S. Anterior Cingulate Cortex, Error Detection, and the Online Monitoring of Performance. *Science* **288,** 1835–1837 (2000).

155. Marshall, P. J. & Meltzoff, A. N. Body maps in the infant brain. *Trends in Cognitive Sciences* **19,** 499–505 (2015).

156. Marstaller, L., Burianová, H. & Reutens, D. C. Dynamic competition between large-scale functional networks differentiates fear conditioning and extinction in humans. *NeuroImage* **134,** 314–319 (2016).

157. Martin, J. H. The Corticospinal System: From Development to Motor Control. *The Neuroscientist* **11,** 161–173 (2005).

158. Martuzzi, R., van der Zwaag, W., Farthouat, J., Gruetter, R. & Blanke, O. Human finger somatotopy in areas 3b, 1, and 2: A 7T fMRI study using a natural stimulus. *Human Brain Mapping* **35,** 213–226 (2014).

159. McCormick, D. A., Clark, G. A., Lavond, D. G. & Thompson, R. F. Initial localization of the memory trace for a basic form of learning. *Proceedings of the National Academy of Sciences of the United States of America* **79,** 2731–5 (1982).

160. Ment, L. R., Hirtz, D. & Hüppi, P. S. Imaging biomarkers of outcome in the developing preterm brain. *The Lancet Neurology* **8,** 1042–1055 (2009).

161. Miles, R. A homeostatic switch. *Nature* **397,** 215–216 (1999).

162. Milh, M., Kaminska, A., Huon, C., Lapillonne, A., Ben-Ari, Y. & Khazipov, R. Rapid Cortical Oscillations and Early Motor Activity in Premature Human Neonate. *Cerebral Cortex* **17,** 1582–1594 (2007).

163. Miller, M. J., Chen, N.-K., Li, L., Tom, B., Weiss, C., Disterhoft, J. F. & Wyrwicz, A. M. fMRI of the Conscious Rabbit during Unilateral Classical Eyeblink Conditioning Reveals Bilateral Cerebellar Activation. *The Journal of Neuroscience* **23,** 11753–11758 (2003).

164. Mitrukhina, O., Suchkov, D., Khazipov, R. & Minlebaev, M. Imprecise Whisker Map in the Neonatal Rat Barrel Cortex. *Cerebral Cortex* **25,** 3458–3467 (2015).

165. Miyamoto, J. J., Honda, M., Saito, D. N., Okada, T., Ono, T., Ohyama, K. & Sadato, N. The Representation of the Human Oral Area in the Somatosensory Cortex: a Functional MRI Study. *Cerebral Cortex* **16,** 669–675 (2005).

166. Molchan, S. E., Sunderland, T., McIntosh, A. R., Herscovitch, P. & Schreurs, B. G. A functional anatomical study of associative learning in humans. *Proceedings of the National Academy of Sciences* **91,** 8122–8126 (1994).

167. Monti, M. Statistical Analysis of fMRI Time-Series: A Critical Review of the GLM Approach. *Frontiers in Human Neuroscience* **5,** 28 (2011).

168. Moon, C., Bever, T. G. & Fifer, W. P. Canonical and non-canonical syllable discrimination by two-day-old infants. *J Child Lang* **19,** 1–17 (1992).

169. Moore, C. I., Stern, C. E., Corkin, S., Fischl, B., Gray, a. C., Rosen, B. R. & Dale, a. M. Segregation of somatosensory activation in the human rolandic cortex using fMRI. *Journal of Neurophysiology* **84,** 558–569 (2000).

170. Moore, R., Vadeyar, S., Fulford, J., Tyler, D., Gribben, C., Baker, P., James, D. & Gowland, P. Antenatal determination of fetal brain activity in response to an acoustic stimulus using functional magnetic resonance imaging. *Human Brain Mapping* **12,** 94–99 (2001).

171. Mumford, J. *A Guide to Calculating Percent Change with Featquery* tech. rep. ().

172. Mumford, J. A., Poline, J.-B. & Poldrack, R. A. Orthogonalization of Regressors in fMRI Models. *PLOS ONE* **10** (ed Ben Hamed, S.) e0126255 (2015).

173. Nakamura, A., Yamada, T., Goto, A., Kato, T., Ito, K., Abe, Y., Kachi, T. & Kakigi, R. Somatosensory homunculus as drawn by MEG. *NeuroImage* **7,** 377–386 (1998).

174. Neyedli, H. F., Sampaio-Baptista, C., Kirkman, M. A., Havard, D., Lührs, M., Ramsden, K., Flitney, D. D., Clare, S., Goebel, R. & Johansen-Berg, H. Increasing Lateralized Motor Activity in Younger and Older Adults using Real-time fMRI during Executed Movements. *Neuroscience* **378,** 165–174 (2018).

175. Nguyen, L., Rigo, J.-M., Rocher, V., Belachew, S., Malgrange, B., Rogister, B., Leprince, P. & Moonen, G. Neurotransmitters as early signals for central nervous system development. *Cell and Tissue Research* **305,** 187–202 (2001).

176. Nichols, T. & Hayasaka, S. Controlling the familywise error rate in functional neuroimaging: a comparative review. *Statistical Methods in Medical Research* **12,** 419–446 (2003).

177. O'Doherty, J. P., Dayan, P., Friston, K., Critchley, H. & Dolan, R. J. *Temporal Difference Models and Reward-Related Learning in the Human Brain* tech. rep. (2003), 329–337.

178. Ogawa, S., Lee, T. M., Kay, A. R. & Tank, D. W. *Brain magnetic resonance imaging with contrast dependent on blood oxygenation (cerebral blood flow/brain metabolism/oxygenation)* tech. rep. (1990), 9868–9872.

179. Ogawa, S., Tank, D. W., Menon, R., Ellermann, J. M., Kim, S. G., Merkle, H. & Ugurbil, K. Intrinsic signal changes accompanying sensory stimulation: functional brain mapping with magnetic resonance imaging. *Proceedings of the National Academy of Sciences of the United States of America* **89,** 5951–5 (1992).

180. Ohyama, T. & Mauk, M. Latent acquisition of timed responses in cerebellar cortex. *The Journal of neuroscience : the official journal of the Society for Neuroscience* **21,** 682–90 (2001).

181. Ohyama, T., Nores, W. L., Murphy, M. & Mauk, M. D. What the cerebellum computes. *Trends in Neurosciences* **26,** 222–227 (2003).

182. OpenStax. in *Anatomy and Physiology* online (OpenStax, 2016).

183. Pallas, S. L. Intrinsic and extrinsic factors that shape neocortical specification. *Trends in Neurosciences* **24,** 417–423 (2001).

184. Paluszynska, D. A., Harris, K. A. & Thach, B. T. Influence of Sleep Position Experience on Ability of Prone-Sleeping Infants to Escape From Asphyxiating Microenvironments by Changing Head Position. *PEDIATRICS* **114,** 1634–1639 (2004).

185. Pape, K. E. & Wigglesworth, J. S. *Haemorrhage, ischaemia and the perinatal brain* (JB Lippincott Co, 1979).

186. Papoušek, H. Conditioned Head Rotation Reflexes in Infants in the First: Months of Life. *Acta Paediatrica* **50,** 565–576 (1961).

187. Parpia, P. Reappraisal of the Somatosensory Homunculus and Its Discontinuities. *Neural Computation* **23,** 3001–3015 (2011).

188. Pascual-Leone, A., Grafman, J. & Hallett, M. Modulation of cortical motor output maps during development of implicit and explicit knowledge. *Science* **263,** 1287–1289 (1994).

189. Pascual-Leone, A., Wassermann, E. M., Grafman, J. & Hallett, M. *The role of the dorsolateral prefrontal cortex in implicit procedural learning* tech. rep. (1996), 479–485.

190. Passingham, R., Toni, I. & Rushworth, M. Specialisation within the prefrontal cortex: the ventral prefrontal cortex and associative learning. *Experimental Brain Research* **133,** 103–113 (2000).

191. Passingham, R. E., Stephan, K. E. & Kötter, R. The anatomical basis of functional localization in the cortex. *Nature Reviews Neuroscience* **3,** 606–616 (2002).

192. Paus, T. Primate anterior cingulate cortex: Where motor control, drive and cognition interface. *Nature Reviews Neuroscience* **2,** 417–424 (2001).

193. Peirano, P. D. & Algarín, C. R. Sleep in brain development. *Biological Research* **40,** 471–478 (2007).

194. Penfield, W. & Faulk, M. E. THE INSULA. *Brain* **78,** 445–470 (1955).

195. Penfield, W. & Boldrey, E. Somatic motor and sensory representation in the cerebral cortex of man as studied by electrical stimulation. *Brain* **60,** 389–443 (1937).

196. Perani, D., Saccuman, M. C., Scifo, P., Anwander, A., Awander, A., Spada, D., Baldoli, C., Poloniato, A., Lohmann, G. & Friederici, A. D. Neural language networks at birth. *Proceedings of the National Academy of Sciences of the United States of America* **108,** 16056–61 (2011).

197. Perani, D., Saccuman, M. C., Scifo, P., Spada, D., Andreolli, G., Rovelli, R., Baldoli, C. & Koelsch, S. Functional specializations for music processing in the human newborn brain. *Proceedings of the National Academy of Sciences of the United States of America* **107,** 4758–4763 (2010).

198. Perkins, L., Hughes, E., Srinivasan, L., Allsop, J., Glover, A., Kumar, S., Fisk, N. & Rutherford, M. Exploring Cortical Subplate Evolution Using Magnetic Resonance Imaging of the Fetal Brain. *Developmental Neuroscience* **30,** 211–220 (2008).

199. Peyton, C., Yang, E., Msall, M. E., Adde, L., Støen, R., Fjørtoft, T., Bos, A. F., Einspieler, C., Zhou, Y., Schreiber, M. D., Marks, J. D. & Drobyshevsky, A. White Matter Injury and General Movements in High-Risk Preterm Infants. *AJNR. American journal of neuroradiology* **38,** 162–169 (2017).

200. Poline, J.-B. & Brett, M. The general linear model and fMRI: Does love last forever? *NeuroImage* **62,** 871–880 (2012).

201. Power, J. D., Barnes, K. A., Snyder, A. Z., Schlaggar, B. L. & Petersen, S. E. Spurious but systematic correlations in functional connectivity MRI networks arise from subject motion. *NeuroImage* **59,** 2142–2154 (2012).

202. Ragsdale, C. W. & Grove, E. A. Patterning the mammalian cerebral cortex. *Current opinion in neurobiology* **11,** 50–8 (2001).

203. Rakic, P. Specification of cerebral cortical areas. *Science (New York, N.Y.)* **241,** 170–6 (1988).

204. Rakic, P. The radial edifice of cortical architecture: From neuronal silhouettes to genetic engineering. *Brain Research Reviews* **55,** 204–219 (2007).

205. Rakic, P. Evolution of the neocortex: a perspective from developmental biology. *Nature Reviews Neuroscience* **10,** 724–735 (2009).

206. Ramnani, N., Toni, I., Josephs, O., Ashburner, J. & Passingham, R. E. Learning- and Expectation-Related Changes in the Human Brain During Motor Learning. *Journal of Neurophysiology* **84,** 3026–3035 (2000).

207. Ramot, M., Kimmich, S., Gonzalez-Castillo, J., Roopchansingh, V., Popal, H., White, E., Gotts, S. J. & Martin, A. Direct modulation of aberrant brain network connectivity through real-time NeuroFeedback. *eLife* **6,** e28974 (2017).

208. Reeb-Sutherland, B. C., Fifer, W. P., Byrd, D. L., Hammock, E. A., Levitt, P. & Fox, N. A. One-month-old human infants learn about the social world while they sleep. *Developmental Science* **14,** 1134–1141 (2011).

209. Reeb-Sutherland, B. C. & Fox, N. A. Eyeblink Conditioning: A Non-invasive Biomarker for Neurodevelopmental Disorders. *Journal of Autism and Developmental Disorders* **45,** 376–394 (2015).

210. Rescorla, R. A. Probability of shock in the presence and absence of cs in fear conditioning. *Journal of Comparative and Physiological Psychology* **66,** 1–5 (1968).

211. Rescorla, R. A. Pavlovian conditioning. It's not what you think it is. *The American psychologist* **43,** 151–60 (1988).

212. Rosazza, C., Aquino, D., D'Incerti, L., Cordella, R., Andronache, A., Zacà, D., Bruzzone, M. G., Tringali, G. & Minati, L. Preoperative Mapping of the Sensorimotor Cortex: Comparative Assessment of Task-Based and Resting-State fMRI. *PLoS ONE* **9** (ed Margulies, D.) e98860 (2014).

213. Rovee-Collier, C. & Cuevas, K. Multiple Memory Systems Are Unnecessary to Account for Infant Memory Development: An Ecological Model. *Developmental Psychology* **45,** 160–174 (2009).

214. Rutherford, M., Srinivasan, L., Dyet, L., Ward, P., Allsop, J., Counsell, S. & Cowan, F. Magnetic resonance imaging in perinatal brain injury: clinical presentation, lesions and outcome. *Pediatric Radiology* **36,** 582–592 (2006).

215. Rutishauser, U. Polysialic acid in the plasticity of the developing and adult vertebrate nervous system. *Nature Reviews Neuroscience* **9,** 26–35 (2008).

216. Sale, A., Maya Vetencourt, J. F., Medini, P., Cenni, M. C., Baroncelli, L., De Pasquale, R. & Maffei, L. Environmental enrichment in adulthood promotes amblyopia recovery through a reduction of intracortical inhibition. *Nature Neuroscience* **10,** 679–681 (2007).

217. Sallinen, M., Kaartinen, J. & Lyytinen, H. Is the appearance of mismatch negativity during stage 2 sleep related to the elicitation of K-complex? *Electroencephalography and Clinical Neurophysiology* **91,** 140–148 (1994).

218. Sanes, J. N. Neocortical mechanisms in motor learning. *Current Opinion in Neurobiology* **13,** 225–231 (2003).

219. Sanes, J. N. & Donoghue, J. P. Plasticity and Primary Motor Cortex. *Annual Review of Neuroscience* **23,** 393–415 (2000).

220. Schulz, M., Chau, W., Graham, S. J., McIntosh, A. R., Ross, B., Ishii, R. & Pantev, C. An integrative MEG–fMRI study of the primary somatosensory cortex using cross-modal correspondence analysis. *NeuroImage* **22,** 120–133 (2004).

221. Schweizer, R. & Frahm, J. High-resolution mapping of finger representations in human primary somatosensory cortex using fMRI in 10 min. *NeuroImage* **47,** S131 (2009).

222. Seelke, A. M. H., Dooley, J. C. & Krubitzer, L. A. The Emergence of Somatotopic Maps of the Body in S1 in Rats: The Correspondence Between Functional and Anatomical Organization. *PLoS ONE* **7** (ed Arabzadeh, E.) e32322 (2012).

223. Seghier, M. L. & Hüppi, P. S. The Role of Functional Magnetic Resonance Imaging in the Study of Brain Development, Injury, and Recovery in the Newborn. *Seminars in Perinatology* **34,** 79–86 (2010).

224. Seidler, R. D., Purushotham, A., Kim, S.-G., Uğurbil, K., Willingham, D. & Ashe, J. Cerebellum activation associated with performance change but not motor learning. *Science (New York, N.Y.)* **296,** 2043–6 (2002).

225. Serag, A., Aljabar, P., Ball, G., Counsell, S. J., Boardman, J. P., Rutherford, M. A., Edwards, A. D., Hajnal, J. V. & Rueckert, D. Construction of a consistent high-definition spatio-temporal atlas of the developing brain using adaptive kernel regression. *NeuroImage* **59,** 2255–2265 (2012).

226. Setänen, S., Lehtonen, L., Parkkola, R., Aho, K., Haataja, L., Ahtola, A., Ekblad, M., Ekblad, S., Ekholm, E., Eurola, A., Huhtala, M., Kero, P., Kiiski-Mäki, H., Korja, R., Lahti, K., Lapinleimu, H., Lehtonen, T., Leppänen, M., Lind, A., Manninen, H., Matomäki, J., Maunu, J., Munck, P., Määttänen, L., Niemi, P., Nyman, A., Palo, P., Rautava, L., Rautava, P., Saarinen, K., Saunavaara, V., Sillanpää, M., Stolt, S., Sutinen, S., Tuomikoski-Koiranen, P., Tuovinen, T., Väliaho, A. & Ylijoki, M. Prediction of neuromotor outcome in infants born preterm at 11 years of age using volumetric neonatal magnetic resonance imaging and neurological examinations. *Developmental Medicine and Child Neurology* **58,** 721–727 (2016).

227. Shaffery, J. P., Lopez, J., Bissette, G. & Roffwarg, H. P. Rapid eye movement sleep deprivation revives a form of developmentally regulated synaptic plasticity in the visual cortex of post-critical period rats. *Neuroscience Letters* **391,** 96–101 (2006).

228. Shannon, C. E. *A Mathematical Theory of Communication* tech. rep. (1948), 623–656.

229. Shibata, K., Watanabe, T., Sasaki, Y. & Kawato, M. Perceptual learning incepted by decoded fMRI neurofeedback without stimulus presentation. *Science (New York, N.Y.)* **334,** 1413–5 (2011).

230. Siqueland, E. R. & Lipsitt, L. P. Conditioned head-turning in human newborns. *Journal of Experimental Child Psychology* **3,** 356–376 (1966).

231. Smith, S. M. & Nichols, T. Threshold-free cluster enhancement: Addressing problems of smoothing, threshold dependence and localisation in cluster inference. *NeuroImage* **44,** 83–98 (2009).

232. Smith, S. M. Fast robust automated brain extraction. *Human Brain Mapping* **17,** 143–155 (2002).

233. Smith, S. M., Jenkinson, M., Woolrich, M. W., Beckmann, C. F., Behrens, T. E., Johansen-Berg, H., Bannister, P. R., De Luca, M., Drobnjak, I., Flitney, D. E., Niazy, R. K., Saunders, J., Vickers, J., Zhang, Y., De Stefano, N., Brady, J. M. & Matthews, P. M. Advances in functional and structural MR image analysis and implementation as FSL. *NeuroImage* **23,** S208–S219 (2004).

234. Smith-Collins, A. P., Luyt, K., Heep, A. & Kauppinen, R. A. High frequency functional brain networks in neonates revealed by rapid acquisition resting state fMRI. *Human Brain Mapping* **36,** 2483–2494 (2015).

235. So, K., Adamson, T. M. & Horne, R. S. The use of actigraphy for assessment of the development of sleep/wake patterns in infants during the first 12 months of life. *Journal of Sleep Research* **16,** 181–187 (2007).

236. Solana, A. B., Menini, A., Sacolick, L. I., Hehn, N. & Wiesinger, F. Quiet and distortion-free, whole brain BOLD fMRI using T ¡sub¿2¡/sub¿ -prepared RUFIS. *Magnetic Resonance in Medicine* **75,** 1402–1412 (2016).

237. Spolidoro, M., Sale, A., Berardi, N. & Mavei, L. Plasticity in the adult brain: lessons from the visual system. *Exp Brain Res* **192,** 335–341 (2009).

238. Stanton, M. E. Multiple memory systems, development and conditioning. *Behavioural Brain Research* **110,** 25–37 (2000).

239. Staudt, M., Braun, C., Gerloff, C., Erb, M., Grodd, W. & Krägeloh-Mann, I. Developing somatosensory projections bypass periventricular brain lesions. *Neurology* **67,** 522–5 (2006).

240. Staudt, M. Reorganization after pre- and perinatal brain lesions. *Journal of Anatomy* **217,** 469–474 (2010).

241. Staudt, M., Gerloff, C., Grodd, W., Holthausen, H., Niemann, G. & Krägeloh-Mann, I. Reorganization in congenital hemiparesis acquired at different gestational ages. *Annals of Neurology* **56,** 854–863 (2004).

242. Stippich, C., Hofmann, R., Kapfer, D., Hempel, E., Heiland, S., Jansen, O. & Sartor, K. Somatotopic mapping of the human primary somatosensory cortex by fully automated tactile stimulation using functional magnetic resonance imaging. *Neuroscience Letters* **277,** 25–28 (1999).

243. Su, H., Iordachita, I. I., Tokuda, J., Hata, N., Liu, X., Seifabadi, R., Xu, S., Wood, B. & Fischer, G. S. Fiber-Optic Force Sensors for MRI-Guided Interventions and Rehabilitation: A Review. *IEEE Sensors Journal* **17,** 1952–1963 (2017).

244. Sullivan, R. M., Taborsky-Barba, S., Mendoza, R., Itano, A., Leon, M., Cotman, C. W., Payne, T. F. & Lott, I. Olfactory Conditioning in Neonates. *Pediatrics* **87,** 511–518 (1991).

245. Sun, H., Takesian, A. E., Wang, T. T., Lippman-Bell, J. J., Hensch, T. K. & Jensen, F. E. Early Seizures Prematurely Unsilence Auditory Synapses to Disrupt Thalamocortical Critical Period Plasticity. *Cell Reports* **23,** 2533–2540 (2018).

246. Sur, M. & Rubenstein, J. L. R. Patterning and Plasticity of the Cerebral Cortex. *Science* **310,** 805–810 (2005).

247. Tarullo, A. R., Balsam, P. D. & Fifer, W. P. Sleep and infant learning. *Infant and Child Development* **20,** 35–46 (2011).

248. Tarullo, A. R., Isler, J. R., Condon, C., Violaris, K., Balsam, P. D. & Fifer, W. P. Neonatal eyelid conditioning during sleep. *Developmental Psychobiology* **58,** 875–882 (2016).

249. Tharpe, A. M. & Ashmead, D. H. A Longitudinal Investigation of Infant Auditory Sensitivity. *American Journal of Audiology* **10,** 104–112 (2001).

250. Thomason, M. E., Dassanayake, M. T., Shen, S., Katkuri, Y., Alexis, M., Anderson, A. L., Yeo, L., Mody, S., Hernandez-Andrade, E., Hassan, S. S., Studholme, C., Jeong, J.-W. & Romero, R. Cross-hemispheric functional connectivity in the human fetal brain. *Science translational medicine* **5,** 173ra24 (2013).

251. Tiriac, A., Del Rio-Bermudez, C. & Blumberg, M. S. Self-Generated Movements with "Unexpected" Sensory Consequences. *Current Biology* **24,** 2136–2141 (2014).

252. Van den Bos, W., Cohen, M. X., Kahnt, T. & Crone, E. A. Striatum–Medial Prefrontal Cortex Connectivity Predicts Developmental Changes in Reinforcement Learning. *Cerebral Cortex* **22,** 1247–1255 (2012).

253. Van Kooij, B., Hendrikse, J., Benders, M., de Vries, L. & Groenendaal, F. Anatomy of the Circle of Willis and Blood Flow in the Brain-Feeding Vasculature in Prematurely Born Infants. *Neonatology* **97,** 235–241 (2010).

254. Virgintino, D., Errede, M., Robertson, D., Girolamo, F., Masciandaro, A. & Bertossi, M. VEGF expression is developmentally regulated during human brain angiogenesis. *Histochemistry and cell biology* **119,** 227–32 (2003).

255. Volpe, J. J. *Neurology of the newborn* 1094 (Saunders/Elsevier, 2008).

256. Volpe, J. J. Brain injury in premature infants: a complex amalgam of destructive and developmental disturbances. *The Lancet Neurology* **8,** 110–124 (2009).

257. Volpe, J. J. The Encephalopathy of Prematurity—Brain Injury and Impaired Brain Development Inextricably Intertwined. *Seminars in Pediatric Neurology* **16,** 167–178 (2009).

258. Wandell, B. A., Dumoulin, S. O. & Brewer, A. A. Visual field maps in human cortex. *Neuron* **56,** 366–83 (2007).

259. Wang, C.-L., Zhang, L., Zhou, Y., Zhou, J., Yang, X.-J., Duan, S.-m., Xiong, Z.-Q. & Ding, Y.-Q. Activity-Dependent Development of Callosal Projections in the Somatosensory Cortex. *Journal of Neuroscience* **27,** 11334–11342 (2007).

260. Wang, H. C. & Bergles, D. E. Spontaneous activity in the developing auditory system. *Cell and Tissue Research* **361,** 65–75 (2015).

261. Wasserman, E. A. & Miller, R. R. WHAT'S ELEMENTARY ABOUT ASSOCIATIVE LEARNING? *Annual Review of Psychology* **48,** 573–607 (1997).

262. Werner, L. A. Issues in human auditory development. *Journal of Communication Disorders* **40,** 275–283 (2007).

263. Wess, J. M., Isaiah, A., Watkins, P. V. & Kanold, P. O. Subplate neurons are the first cortical neurons to respond to sensory stimuli. *Proceedings of the National Academy of Sciences* **114,** 12602–12607 (2017).

264. Westbrook, C., Roth, C. K. & Talbot, J. *MRI in Practice* 4th. arXiv: arXiv:1011.1669v3 (Wiley-Blackwell, Oxford, 2005).

265. Whitehead, K., Pressler, R. & Fabrizi, L. Characteristics and clinical significance of delta brushes in the EEG of premature infants. *Clinical Neurophysiology Practice* **2,** 12–18 (2017).

266. Williams, J., Lee, K. J. & Anderson, P. J. Prevalence of motor-skill impairment in preterm children who do not develop cerebral palsy: a systematic review. *Developmental Medicine & Child Neurology* **52,** 232–237 (2010).

267. Wilson, M. A., Johnston, M. V., Goldstein, G. W. & Blue, M. E. Neonatal lead exposure impairs development of rodent barrel field cortex. *Proceedings of the National Academy of Sciences of the United States of America* **97,** 5540–5 (2000).

268. Winkler, A. M., Ridgway, G. R., Webster, M. A., Smith, S. M. & Nichols, T. E. Permutation inference for the general linear model. *NeuroImage* **92,** 381–397 (2014).

269. Woolrich, M. W., Jbabdi, S., Patenaude, B., Chappell, M., Makni, S., Behrens, T., Beckmann, C., Jenkinson, M. & Smith, S. M. Bayesian analysis of neuroimaging data in FSL. *NeuroImage* **45,** S173–S186 (2009).

270. Woolrich, M. W., Ripley, B. D., Brady, M. & Smith, S. M. Temporal Autocorrelation in Univariate Linear Modeling of FMRI Data. *NeuroImage* **14,** 1370–1386 (2001).

271. Worsley, K. J. in *Functional MRI: An Introduction to Methods* (eds Jezzard, P., Matthews, P. M. & Smith, S. M.) 251–270 (2001).

272. Worsley, K. J., Taylor, J. E., Tomaiuolo, F. & Lerch, J. Unified univariate and multivariate random field theory. *NeuroImage* **23,** S189–S195 (2004).

273. Wu, G., Luo, F., Li, Z., Zhao, X. & Li, S.-J. Transient relationships among BOLD, CBV, and CBF changes in rat brain as detected by functional MRI. *Magnetic Resonance in Medicine* **48,** 987–993 (2002).

274. Yang, J.-W., Hanganu-Opatz, I. L., Sun, J.-J. & Luhmann, H. J. Three Patterns of Oscillatory Activity Differentially Synchronize Developing Neocortical Networks In Vivo. *Journal of Neuroscience* **29,** 9011–9025 (2009).

275. Yeo, C. H. & Hesslow, G. Cerebellum and conditioned reflexes. *Trends in Cognitive Sciences* **2,** 322–330 (1998).

276. Yousry, T., Schmid, U. D., Alkadhi, H., Schmidt, D., Peraud, A., Buettner, A. & Winkler, P. Localization of the motor hand area to a knob on the precentral gyrus. A new landmark. *Brain* **120,** 141–157 (1997).

277. Zald, D. H. & Pardo, J. V. Cortical Activation Induced by Intraoral Stimulation with Water in Humans. *Chemical Senses* **25,** 267–275 (2000).

278. Zaramella, P., Freato, F., Amigoni, A., Salvadori, S., Marangoni, P., Suppjei, A., Schiavo, B. & Chiandetti, L. Brain Auditory Activation Measured by Near-Infrared Spectroscopy (NIRS) in Neonates. *Pediatric Research* **49,** 213–219 (2001).

279. Zecevic, N. Synaptogenesis in layer I of the human cerebral cortex in the first half of gestation. *Cerebral Cortex* **8,** 245–252 (1998).

280. Zhang, J., Ackman, J. B., Xu, H.-P. & Crair, M. C. Visual map development depends on the temporal pattern of binocular activity in mice. *Nature Neuroscience* **15,** 298–307 (2012).

281. Zhao, C., Kao, J. P. Y. & Kanold, P. O. Functional Excitatory Microcircuits in Neonatal Cortex Connect Thalamus and Layer 4. *Journal of Neuroscience* **29,** 15479–15488 (2009).

Appendix

Basic principles of Nuclear Magnetic Resonance

Nuclear spin and precession

To understand NMR one should comprehend two fundamental properties of particle physics: *Spin* and *Precession*.

Subatomic particles possess a "spin", a discrete value that although cannot directly represent as a physical property it can be imagined as the rotation of a particle around its axis (from which the name). Spins are naturally distributed in pairs and therefore they cancel each other in most of the atoms. However, nuclei with odd mass number have a non-zero net spin. In the view of spinning charged particles, nuclei possessing a net spin generate a magnetic field defined as magnetisation (M). Importantly, the spin of nuclei are generally randomly oriented, but in the presence of an external magnetic field (B_0) they align to it either in a parallel (spin-up) or anti-parallel (spin-down) fashion, and the distribution of directions depends on a fine energetic equilibrium. Given that spin-up orientation requires less energy than the spin-down, the resulting net magnetisation vector (NMV) is always parallel to the external magnetic field. At a higher field strength, the energy gap between spin-up and spin-down states becomes greater and fewer nuclei would align anti-parallel, thus the NMV strength is directly proportional to the strength of B_0. On the other hand, at a higher temperature the thermal energy of the nuclei increases,

allowing them to align anti-parallel, thus the NMV strength is inversely proportional to the temperature. MRI relies on MR active elements present in biological tissues, among which the hydrogen atom is the most important. H atoms are particularly important for MRI because they are an abundant element in the human body (for example in the form of water and fat) and they are characterised by a relatively large magnetic momentum.

It is possible to neglect the quantum mechanics of individual nuclei spins and consider the NMV in a more classical physics approach (Hanson, 2008). According to classical electrodynamics laws, a moving electrical charge produces a magnetic field and conversely a varying magnetic field induce a current. In this view, a charged particle with a net spin, like ^1H, produces a magnetic field and can be described as a magnet (magnetic dipole). When a magnetic dipole is under the influence of another magnetic field, B_0, it is subject to a torque that tends to align the dipole to the stronger field. Nevertheless, due to the intrinsic angular momentum of the particle (the spin), the dipole does not simply align to B_0 but it follows instead a circular path around it. This spinning movement is called "precession", and the frequency of rotation (known as Larmor frequency) is also proportional to the strength of the magnetic field as described by Larmor formula: $\omega = B_0\lambda$. In this equation, λ is the gyromagnetic ratio characteristic of each MR active nucleus. Being λ a constant, different active nuclei would have a different Larmor frequency while exposed to the same magnetic field. The processional frequency of hydrogen corresponds to the radio frequency (RF) band, more specifically at 3T ω_H it is 127.71 MHz.

MR signal

It is possible to excite the processing nuclei through the phenomenon of resonance by applying an energy wave at the exact precessional frequency. Given that each nuclei type precesses at a specific frequency, the excitation can be selective. Therefore, H nuclei can be targeted by applying a RF pulse that matches the hydrogen's Larmor frequency. The resonance effect produces two concurrent but independent phenomenons. On one hand, the nuclei gain energy and they align anti-parallel to B_0, reducing the magnitude of the

overall NMV. On the other hand, the magnetic moments of the resonant element become coherent and they precess at the Larmor frequency now all in phase. Being coherent, the perpendicular component of the individual magnetic moments sums up resulting in a NMV perpendicular to B_0. Considering the B_0 on the longitudinal plane, the NMV tilts to the transverse plane as a result of the exciting pulse. This in-phase transverse magnetisation generates a moving magnetic field that produces an alternate voltage, which in turn induces a current in a receiver coil placed in proximity. The induced current is the resulting MR signal.

Imaging contrasts

When the RF pulse is then switched off, the two phenomenons that lead to the MR signal occur in the opposite direction, resulting in the realignment of the NMV with B_0. The hydrogen nuclei lose the previously gained energy as a result of spin-lattice interaction (interaction with the environment), recovering the longitudinal magnetisation. And the nuclei lose coherence due to the spin-spin interaction (interaction between nuclei) reducing the transverse magnetisation. The two processes are exponential and have a characteristic time constant named $T1$ *relaxation time* and $T2$ *relaxation time* respectively. The loss of phase coherence occurring after the RF pulse is switched off is accelerated by the inhomogeneity within B_0. Slightly different variations in magnetic field strength give rise to variation in the Larmor frequencies at different locations causing additional dephasing. Taking together the dephasing due to spin-spin interaction and field inhomogeneity, the relaxation time constant is described by the T2*. Because the transverse magnetisation vector decays while rotating, the resulting MR signal is a sine wave in a decaying envelop that takes the name of free induction decay FID. Measuring the FID signal alone is rather inefficient for most clinical images because it is particularly susceptible to field inhomogeneity, decays very quickly and potentially causes artefactual signal dropout. In certain cases, the sensibility to local inhomogeneity is particularly advantageous as in the case of functional MRI which indeed relies on the T2* contrast. However, structural images acquisition are better when using the T2 contrast. This is possible using spin-

echo sequences that reverse the dephasing caused by the B_0 inhomogeneity and make the transverse magnetisation decay depending solely on the spin-spin interaction.

The time necessary for the longitudinal magnetisation to recovery and transverse magnetisation to decay differs for different tissue types, so does the MR signal. Therefore the MR signal is tissue-specific and by repeating the RF pulse in a sequence it is possible to generate the contrasts in MRI. The time between RF pulse applications is termed *repetition time* (TR) and affects the amount of T1 relaxation allowed. On the other hand, the *echo time* (TE) is the time lag between the RF pulse and the induced signal, thus regulates the amount of T2 relaxation that has occurred when the signal is read. The tuning of those two parameters, among other factors, affect the image contrast. The image contrast is also affected by intrinsic factors such as those related to tissue properties. Fortunately, MRI has excellent tissue discrimination. For instance, hydrogen atoms in fat and water have different behaviour (spin-spin and spin-lattice interactions), therefore appear differently in MR images. Given that the brain is composed in great amount by fat and water, it is convenient to explain some of the image contrast property using those two extremes. In keeping with the signal in the coil being proportional to the transverse magnetisation vector, a large component of coherent magnetisation produce a high signal (bright in the image) and vice versa. In the table below (1) there is a summary of tissue property and how they impact the T1 recovery time and T2 decay time.

	Fat		**Water**
short T1 (bright)	low inherent energy → efficient energy exchange in spin-lattice interaction	long T1 (dark)	high inherent energy → cannot easily absorb energy in spin-lattice interaction
short T2 (dark)	molecules closely packed → more spin-spin interaction, thus fast dephasing	long T2 (bright)	molecules spaced apart → less spin-spin interaction, thus slow dephasing

Table 1: Properties of fat and and water in relation with T1 and T2 time.

Image construction

The MR signal would be meaningless without knowing where it comes from in space. To achieve the spatial localisation of the MR signal, additional magnetic field are superimposed to the main magnetic field to create a gradient in the field strength, and in turns different Larmor frequencies at different locations. Those secondary magnetic fields are

generated by the gradient coils which are allocated within the MRI scanner bore. There are three gradient coils which are arranged to act along each directional axis (x,y,z), thus provide a 3D spatial localisation of the MR signal. The image is constructed over three steps, each achieved by using a gradient coil. The first step is *slice selection*. At the same time of the RF pulse, a slice-selecting gradient is applied parallel to B_0 (along the z-axis) so that the nuclei will precess at different Larmor frequencies depending on their position along the z-axis. A selected RF pulse bandwidth will excite specific nuclei with matching Larmor frequency and determine the slice location and thickness. After the slice has been selected with the slice-specific RF pulse, the *phase encoding* aim to spatially localise the signal along the y-axis. The phase-encoding gradient modulates the precession frequency along its axis but once the gradient is switched off the nuclei are exposed to the same field strength and precess at the same frequency but now at different phases along the y-axis. The effect is similar to provide the same RF pulse but at different times. Finally, the *frequency encoding*. The x-axis localisation is achieved during the readout by using an additional gradient perpendicular to the phase-encoding gradient. The in-phase direction is now subject to the frequency-encoding gradient that alters the precession frequency. The frequency encoding gradient is switched on when the signal is received and determine the field of view.

Different slice orientations can be achieved by allocating the gradients to a different task. Within each slice excitation, the MR signal for one phase-encoding step is digitised and stored as a line in a matrix that contains the frequency information. To acquire sufficient phase-encoding information for a signal to be assigned to each location within the slice, the pulse sequence (comprising slice selection, frequency encoding and phase encoding) must be repeated many times. Data of each slice is then stored as the resulting k-space matrix of phases and frequencies. Thanks to the Fast Fourier Transform, the data can be transformed from the spatial frequency domain (k-space) into a grayscale 2D image. Having all the slices stack together we obtain the 3D digital image where the brightness of each voxel (unit volume) represents the strength of the MRI signal generated by the tissue volume.